JOHN H. WILLIAMS LABORATORY OF NUCLEAR PHYSICS

COO-1265-83

MASTER

RECEIVED BY DTIE OCT 1 4 1969

ANNUAL REPORT 1969

United States Atomic Energy Commission Contract number AT(11-1) 1265

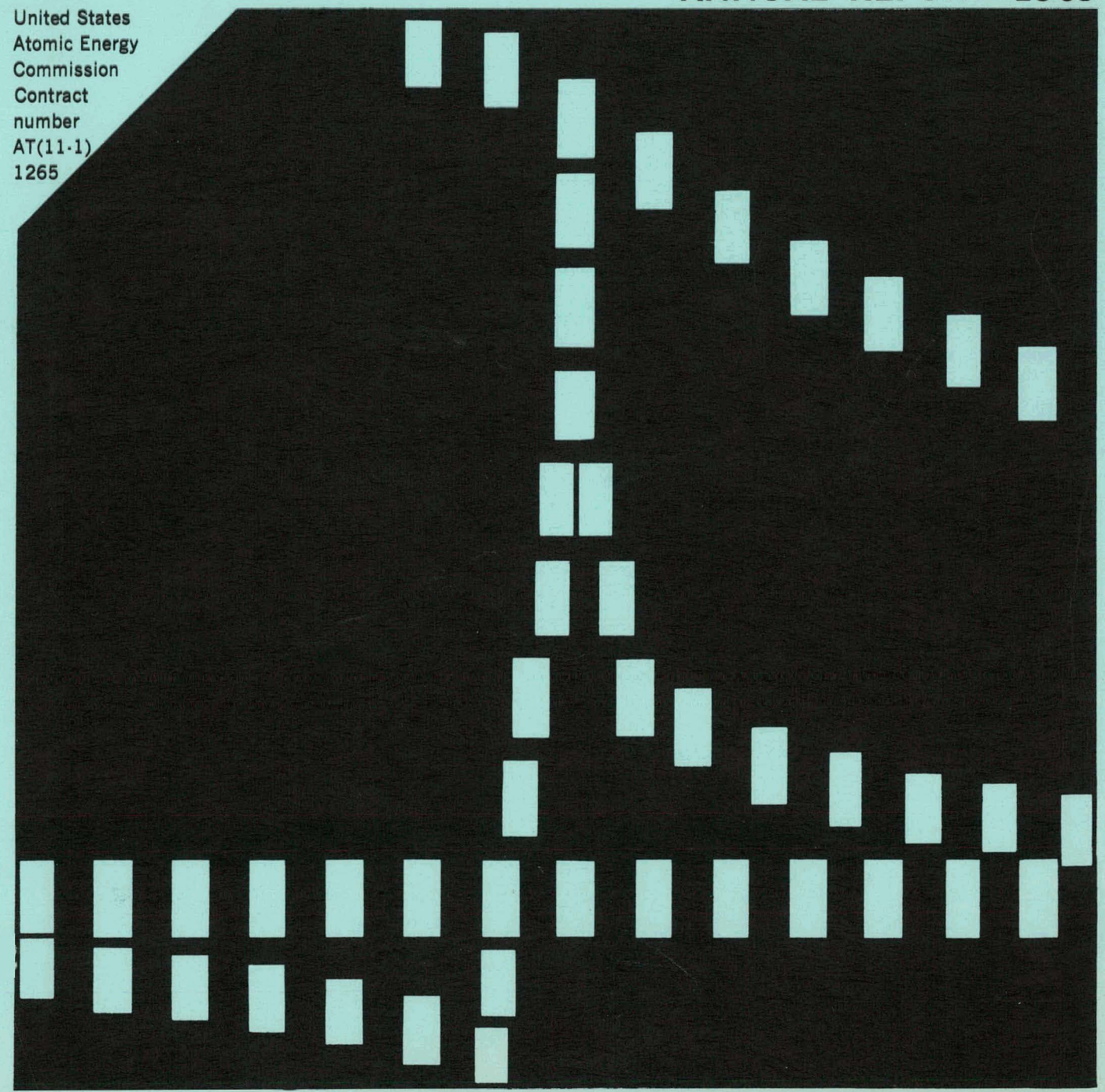

DISTRIBUTION OF THIS DOCUMENT IS UNLIMITED

UNIVERSITY OF MINNESOTA

DISCLAIMER

This report was prepared as an account of work sponsored by an agency of the United States Government. Neither the United States Government nor any agency Thereof, nor any of their employees, makes any warranty, express or implied, or assumes any legal liability or responsibility for the accuracy, completeness, or usefulness of any information, apparatus, product, or process disclosed, or represents that its use would not infringe privately owned rights. Reference herein to any specific commercial product, process, or service by trade name, trademark, manufacturer, or otherwise does not necessarily constitute or imply its endorsement, recommendation, or favoring by the United States Government or any agency thereof. The views and opinions of authors expressed herein do not necessarily state or reflect those of the United States Government or any agency thereof.

DISCLAIMER

Portions of this document may be illegible in electronic image products. Images are produced from the best available original document.

COO-1265-83

ANNUAL REPORT 1969

JOHN H. WILLIAMS LABORATORY

OF

NUCLEAR PHYSICS

UNIVERSITY OF MINNESOTA

August, 1969

LEGAL NOTICE

This report was prepared as an account of Government sponsored work. Neither the United States, nor the Commission, nor any person acting on behalf of the Commission:

A. Makes any warranty or representation, expressed or implied, with respect to the accuracy, completeness, or usefulness of the information contained in this report, or that the use of any information, apparatus, method, or process disclosed in this report may not infringe privately owned rights; or

B. Assumes any liabilities with respect to the use of, or for damages resulting from the use of any information, apparatus, method, or process disclosed in this report.

As used in the above, "person acting on behalf of the Commission" includes any employee or contractor of the Commission, or employee of such contractor, to the extent that such employee or contractor of the Commission, or employee of such contractor prepares, disseminates, or provides access to, any information pursuant to his employment or contract with the Commission, or his employment with such contractor.

U.S. Atomic Energy Commission

Contract AT(11-1)-1265

DISTRIBUTION OF THIS DOCUMENT IS UNLIMITED

THIS PAGE

WAS INTENTIONALLY

LEFT BLANK

CONTENTS

C. ACCELERATOR PERFORMANCE AND DEVELOPMENT

APPENDIX

INTRODUCTION

This report summarizes the work done at the John H. Williams Laboratory of Nuclear Physics at the University of Minnesota during the year ending in August 1969. The work was supported by the United States Atomic Energy Commission under Contract AT(11-1)-1265.

Part A of this report describes the research conducted by the faculty, research associates and students of the University of Minnesota. Although the reactions studied involved elements ranging throughout the periodic table, a large fraction of the work dealt with the spectroscopy of nuclei in the groups from fluorine through nickel. Attention was devoted to some of the rare-earth elements and also to lead and bismuth. The nuclear spectroscopy of these elements was investigated by elastic and inelastic scattering of charged particles and a number of nucleon transfer reactions. The analysis of several of these experiments contributed to a better understanding of the optical model of the nucleus.

The proton linear accelerator was in operation until January 7, 1969 and the model MP tandem Van de Graaff was in operation throughout the year. Polarized protons were produced by the linear accelerator during a large fraction of its operation.

The CDC 3100 computer was used extensively for accumulation of data with arrays of charged particle detectors, both in the ORTEC target chamber and in the split-pole magnetic spectrometer. Some computer programs developed for aid in data taking are described briefly.

Part B includes improvements to equipment and facilities.

Part C summarizes the year's operation of the two accelerators, the computer, and the magnetic spectrometer. The linear accelerator performed at high efficiency until it was shut down and the tandem Van de Graaff provided more time for experimental work than in the previous year.

There is included a summary of experience with the polarized proton source used on the linear accelerator and a description of the development and test work now under way on the polarized ion source soon to be installed on the tandem Van de Graaff.

The Appendix gives a list of laboratory personnel, of the advanced degrees granted, and of reports and publications since last year's report.

J. M. Blair

A. RESEARCH PROGRAM

I. ELASTIC AND INELASTIC SCATTERING

1. Search for $Be^{6*}(2.08)$

D. K. Olsen, W. S. Chien, and R. E. Brown

In the previous annual report[1] was described a search for states in Be^6 by means of the $Li^6(He^3,t)$ reaction at 28-MeV bombarding energy. A ΔE-E detection system was used to identify tritons. Only the well known ground state and broad 1.67-MeV state of Be^6 were clearly observed. However, at 25° and 30° a slight structure was observed on the high-excitation-energy side of the $Be^{6*}(1.67)$ structure, which would correspond to a state in Be^6 at about 2.08 MeV. About 800 counts were recorded in this region of the triton spectrum.

In order to investigate further the possibility of a state in Be^6 at 2.08 MeV, tritons from the above described reaction were observed with position-sensitive detectors[2] in the focal plane of the split-pole spectrometer.[3] Data were obtained at 25° and 30°, and no indication of any additional state in Be^6 between 1.89 and 2.33 MeV was observed. Figure 1-1 shows the triton spectrum obtained at 25° in a single detector. Had the structure indicated in the above mentioned ΔE-E experiment been due to a state in Be^6, a peak about 5-channels wide would have been present in Fig. 1-1 near an excitation energy of 2.08 MeV. The counting statistics here are much better than previously, there being about 2000 triton counts near 2.08-MeV excitation.

The conclusion drawn from this and the previous experiment is that Be^6(g.s.) and $Be^{6*}(1.67)$ are the only two states in Be^6 observed in the $Li^6(He^3,t)$ reaction up to a Be^6 excitation energy of about 11 MeV.

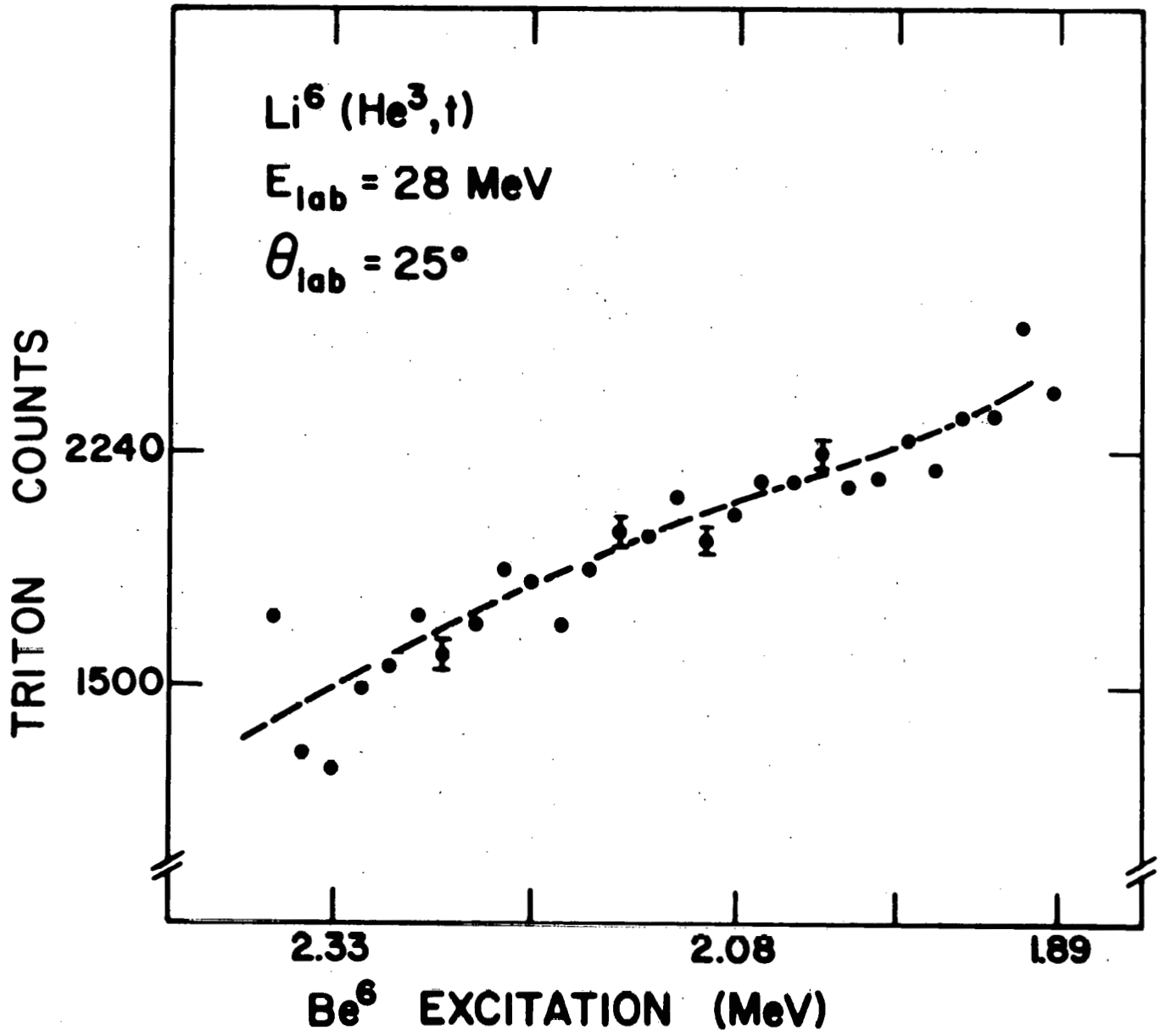
Li⁶ (He³,t)
E_lab = 28 MeV
θ_lab = 25°
TRITON COUNTS
2240
1500
2.33
2.08
1.89
Be⁶ EXCITATION (MeV)

Fig. 1-1

References

1. J. G. Jenkin, D. C. Weisser, and R. E. Brown, John H. Williams Laboratory of Nuclear Physics Annual Report, 1968, p. 131.

2. P. H. Debenham, D. Dehnhard, and R. W. Goodwin, John H. Williams Laboratory of Nuclear Physics Annual Report, 1968, p. 154.

3. J. M. Blair, P. H. Debenham, D. Dehnhard, N. M. Hintz, and M. A. Oothoudt, John H. Williams Laboratory of Nuclear Physics Annual Report, 1968, p. 150.

---

2. Elastic and Inelastic Scattering of Alphas from N^{14}

D. H. Fitzgerald and R. K. Hobbie

Recently, several experimenters have investigated nuclear reactions with the exit channel $\alpha + N^{14}$. All of these workers have placed particular emphasis on examining the intensity of the reaction leading to the T=1, 2.31 MeV level in N^{14}. This reaction is forbidden by conservation of both charge parity and isospin, since in all cases the incident particles and the outgoing alpha-particles have T=0. The present work was initially undertaken to extend to higher excitation energies in F^{18} the study of the isospin non-conserving reaction to $\alpha + N^{14*}(T=1)$. Later it became apparent that excitation functions from the α_0 and α_2 T-allowed reaction channels lent themselves to a study of compound nucleus cross section fluctuations. These data were examined in the spirit of Ericson fluctuation theory[1] and a "coherence width" was established for the fluctuations.

Excitation function data were taken at four angles corresponding to zeros of Legendre polynomials with the following ℓ-values: 24.3° (ℓ=4), 74° (odd ℓ), 127.7° (ℓ=3), and 157.6° (ℓ=8). Nitrogen targets for the

experiment were obtained by evaporating roughly 70 $\mu g/cm^2$ of adenine ($C_5H_3N_4 \cdot NH_2$) onto 10 $\mu g/cm^2$ thick, commercially obtained carbon foils. Cross section normalization was accomplished by comparison to gas cell scattering data obtained using gas cell detector systems developed by R. E. Brown and C. G. Jacobs.[2]

The most apparent feature of the excitation functions is the strong fluctuation of the cross section with energy. The fluctuations appear uncorrelated at large angles and between different reaction channels. Accordingly, the excitation functions were subjected to an Ericson fluctuation analysis in an effort to determine if the structure is due to preferential formation of wide, partially overlapping levels in the compound nucleus or due to statistical processes. Unfortunately, the results of the analysis are somewhat ambiguous due to finite range of data effects and energy dependence of average quantities, such as structure width and cross section magnitude, which must be assumed constant for the analysis. However, the results, taken with the qualitatively observed lack of fluctuation correlation mentioned above, make it seem likely that the cross section fluctuations are due to statistical processes. Assuming this to be the case, the analysis yields an average coherence width of about 250 keV. This is in good agreement with the results of Dzubay,[3] who studied $C^{12}(Li^6,\alpha_1)N^{14*}$ (T=1) at somewhat lower excitation energies in F^{18}. (Dzubay's range was 15.5-17.2 MeV of excitation, compared with 15.3-21.6 MeV for the present experiment.)

The investigation of the T-forbidden reaction to the 2.31 MeV state in N^{14} also yielded results which are difficult to interpret. The α_1 cross section at 32° (CM) ranged typically from .05% to .4% of the α_0 cross section. (This investigation was severely limited by the presence

of several target contaminants whose reaction groups interfered at the other detector angles with the α_1-group from N^{14}.) In addition to the T-forbiddeness of the α_1 reaction, it is inhibited by angular momentum and parity conservation. Thus it is invalid to interpret the α_1/α_0 yield ratio as an indication of the true degree of isospin conservation in $N^{14}(\alpha,\alpha_1)N^{14*}$. The results may be compared with the predictions of Wilkinson,[4] who indicates that for nuclei with $A = 4n + 2$ ($A \approx 20$) a transition to effective high isospin purity occurs in the excitation region 14-18 MeV. The basis for this transition is that states this high in excitation decay too fast for isospin mixing to occur. Indeed, the relative α_1 yield for the present work is considerably smaller than that for other experiments done at lower energies[3,5,6] where the α_1/α_0 yield ratio ranged up to 30%. However, the α_1 cross section in the present case shows no measurable overall decrease with increasing energy in the excitation region 15.3-21.6 MeV. In addition, fairly sharp structure appears in the excitation function throughout the energy range studied, instead of washing out at higher energies as one would expect on the basis of Wilkinson's predictions.

References

1. T. Ericson, Adv. in Phys. 9, 425 (1960).
2. C.G. Jacobs, M.S. Thesis, University of Minnesota (1968).
3. T. Dzubay, Phys. Rev. 158, 977 (1967).
4. D.H. Wilkinson, Phil. Mag. 1, 379 (1958).
5. J.E. Jobst, Phys. Rev. 168, 1156 (1968).
6. P. Tollefsrud, University of Wisconsin, private communication.

3. ^{16}O States Via the $^{14}N(^{3}He,p)^{16}O$ Reaction

A. R. Barnett and D. Dehnhard

An investigation of the highly excited states of ^{16}O in the energy region between 15 MeV and 25 MeV is under way using the $^{14}N(^{3}He,p)^{16}O$ reaction at a bombarding energy of 24 MeV. Surprising little is known[1] about spin-parity values of states in this region and almost all the information has come from resonance reactions. The excitation of the T=1 states in the spectrum can be directly compared with the analogous reaction $^{14}N(t,p)^{16}O$ for which angular distributions up to 8 MeV excitation in ^{16}N (21 MeV in ^{16}O) are known.[2] In the $(^{3}He,p)$ reaction the T=0 states of ^{16}O are excited, in addition to the T=1 states. This tends to produce a general background since most of the T=0 states seem to be broad.[1] Also three-body-break-up contributes to the "background" in this energy region.

We used a gas target system at a pressure of 203 mm of pure $^{14}N_2$ gas and an E-ΔE particle identification system for the initial runs. This eliminated the considerable difficulties arising from strong $(^{3}He,p)$ peaks from the carbon present in many solid targets (e.g. adenine[3]) and it has the great advantage that absolute cross sections can be obtained to high accuracy. A 700 μ surface barrier Si transmission detector was used for ΔE and a 3 mm Si-Li stopping detector for E; pulses were analyzed with the power-law routine in the on-line 3100 computer.[4] Protons with energies between 10 and 25 MeV were stopped by the detector telescope,

corresponding to the excitation region 13-27 MeV in ^{16}O; deuterons from the $^{14}N(^{3}He,d)^{15}O$ reaction were also analyzed; ^{3}He and α particles were completely stopped in the ΔE detector. Fig. 3-1 shows a spectrum taken at 30^{o} and covering the energy range 18-27 MeV; the peaks are labelled with their excitation energies in ^{16}O.

A resolution of 180 keV was obtained for the proton group, due mainly to the entrance foil thickness (1 mil H-film) and to kinematic spread, and partially due to detector noise. Calibration runs with a solid ^{12}C target of 100 $\mu g/cm^{2}$ showed 100 keV resolution. An angular distribution was taken at a bombarding energy of 24 MeV ^{3}He at five angles between $\theta_{lab} = 15^{o}$ and 30^{o}. The states seen by Comfort et al[3] were at 15.8, 16.2, 17.1, 17.8, 18.0, 19.0, 19.4, 19.9, and 20.4 MeV and we find general agreement. More detailed angular distributions are being taken and will be analyzed with a two particle transfer code to determine L values and to test wave functions in ^{16}O.

The $^{14}N(^{3}He,d)^{15}O$ Reaction.

As a byproduct of this work we have measured the angular distribution of deuteron groups from the $^{14}N(^{3}He,d)^{15}O$ reaction leading to ^{15}O states below 9 MeV in excitation. The overall deuteron resolution of 130 keV (FWHM) was adequate to resolve all the ^{15}O states except the 5.188 MeV, 5.240 MeV and the 6.789 MeV, 6.857 MeV doublets. A distribution between $\theta_{lab} = 15^{o}$ and 30^{o} has been taken and a more detailed study is planned. The data can be compared with the recent Rochester study[5] of the same reaction at a ^{3}He energy of 14 MeV. An energy spectrum of the $^{14}N(^{3}He,\alpha)^{15}O$ reaction at θ_{lab} 30^{o} is shown in Fig. 3-2.

$^{14}N(^{3}He,p)^{16}O$
24 MeV
30°
21.0 MeV
20.4 MeV
19.8 MeV
19.4 MeV
18.6 MeV
18.1 MeV
17.7 MeV
17.2 MeV
16.2 MeV
15.8 MeV
200
100
Counts per Channel
250
300
350
Channel Number

Fig. 3-1

$^{14}N(^{3}He,d)^{15}O$
E = 24 MeV
θ = 30°
Counts per Channel
800
400
Channel Number
50
100
150
200
8.915 MeV 3/2 +
8.283 MeV 3/2 +
7.550 MeV 1/2 +
7.284 MeV 7/2 +
6.857 MeV 5/2 +
(6.789 MeV 3/2 +)
6.180 MeV 3/2 -
5.240 MeV 5/2 +
(5.188 MeV 1/2 +)
g.s. 1/2 -

Fig. 3-2

References

1. A.R. Barnett, Nucl. Phys. A120, 342 (1968).

2. P.V. Hewka, C.H. Holbrow and R. Middleton, Nucl. Phys. 88, 561 (1966).

3. J.R. Comfort, et al, B.A.P.S. 13, 608 (1968).

4. D.C. Weisser, R.W. Goodwin and R.K. Hobbie, J.H. Williams Laboratory Annual Report 1968, p. 143.

5. W.P. Alford and K.H. Purser, Nucl. Phys. A132, 86 (1969).

II. SPECTROSCOPY OF NUCLEI FROM F THROUGH Ca

4. Octupole and Quadrupole Transition Rates in F^{19} from Scattering of 15 MeV Deuterons

D. Dehnhard and N. M. Hintz

Experimental results from 15.0 MeV deuterons scattered by F^{19} were reported previously.[1] Inelastic groups leaving F^{19} in its five lowest lying excited states had been observed using two position-sensitive detectors placed in the focal plane of a split-pole magnetic spectrometer. The elastic scattering cross section has now been analyzed using an optical model (see Fig. 4-1). $B(E2)\downarrow$ values for the transitions from the 5/2 + (0.197 MeV) and the 3/2 + (1.56 MeV) states to the g.s. were found to be 9 ± 3 and 10 ± 3 W.u. (single particle units). They were calculated from the β_2 deformation parameter extracted from a DWBA analysis (Figs. 4-2 and 4-3) using a complex form factor derived from the optical model analysis with a surface absorption term. These results are in good agreement with results obtained from inelastic proton scattering[2] and from Coulomb excitation experiments.[3]

However, the $B(E3)\downarrow$ value for the $5/2^- \rightarrow 1/2^+$ transition from the 1.35 MeV state was found to be 1.4 ± 0.6 W.u. as compared to 3.8 ± 0.6 W.u. from a (p,p') experiment[2] and to 12.0 ± 4.0 W.u.[3] and 6.5 ± 1.1 W.u.[4] from two different Coulomb excitation experiments. The results have been compared to various model predictions and will be published soon.

References

1. D. Dehnhard and N.M. Hintz, 1968 Annual Report.

2. G.M. Crawley and G.T. Harvey, Phys. Rev. 167, 1070 (1968).

3. A.E. Litherland, M.A. Clark and C. Bronde, Phys. Letters 3, 204 (1963).

4. T.K. Alexander, O. Hausser, K.W. Allen, and A.E. Litherland, B.A.P.S. 14, 123 (1969).

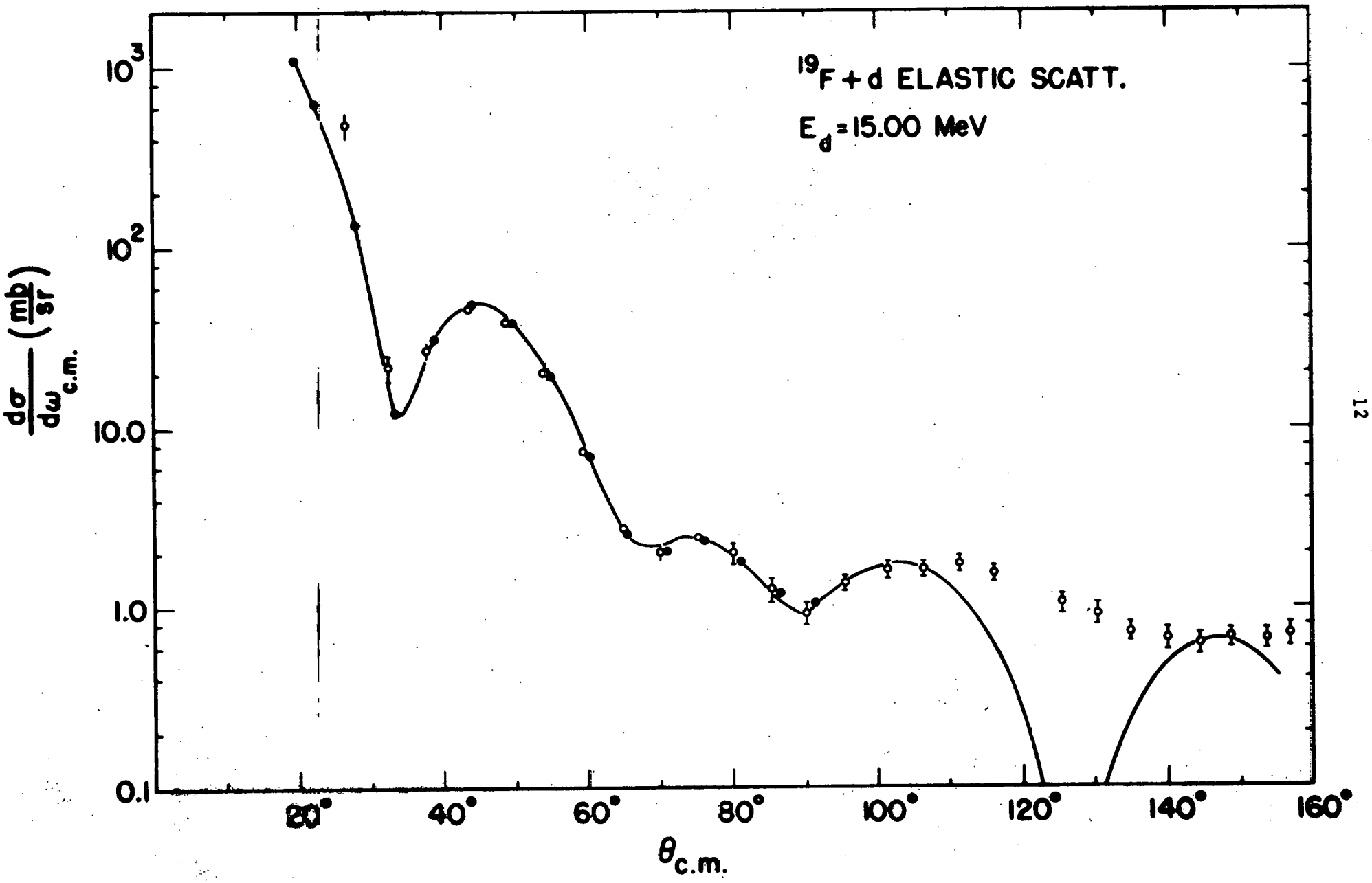
$^{19}F + d$ ELASTIC SCATT.
$E_d = 15.00$ MeV
$\frac{d\sigma}{d\omega_{c.m.}} \left(\frac{mb}{sr}\right)$
10^3
10^2
10.0
1.0
0.1
20°
40°
60°
80°
100°
120°
140°
160°
$\theta_{c.m.}$

Fig. 4-1

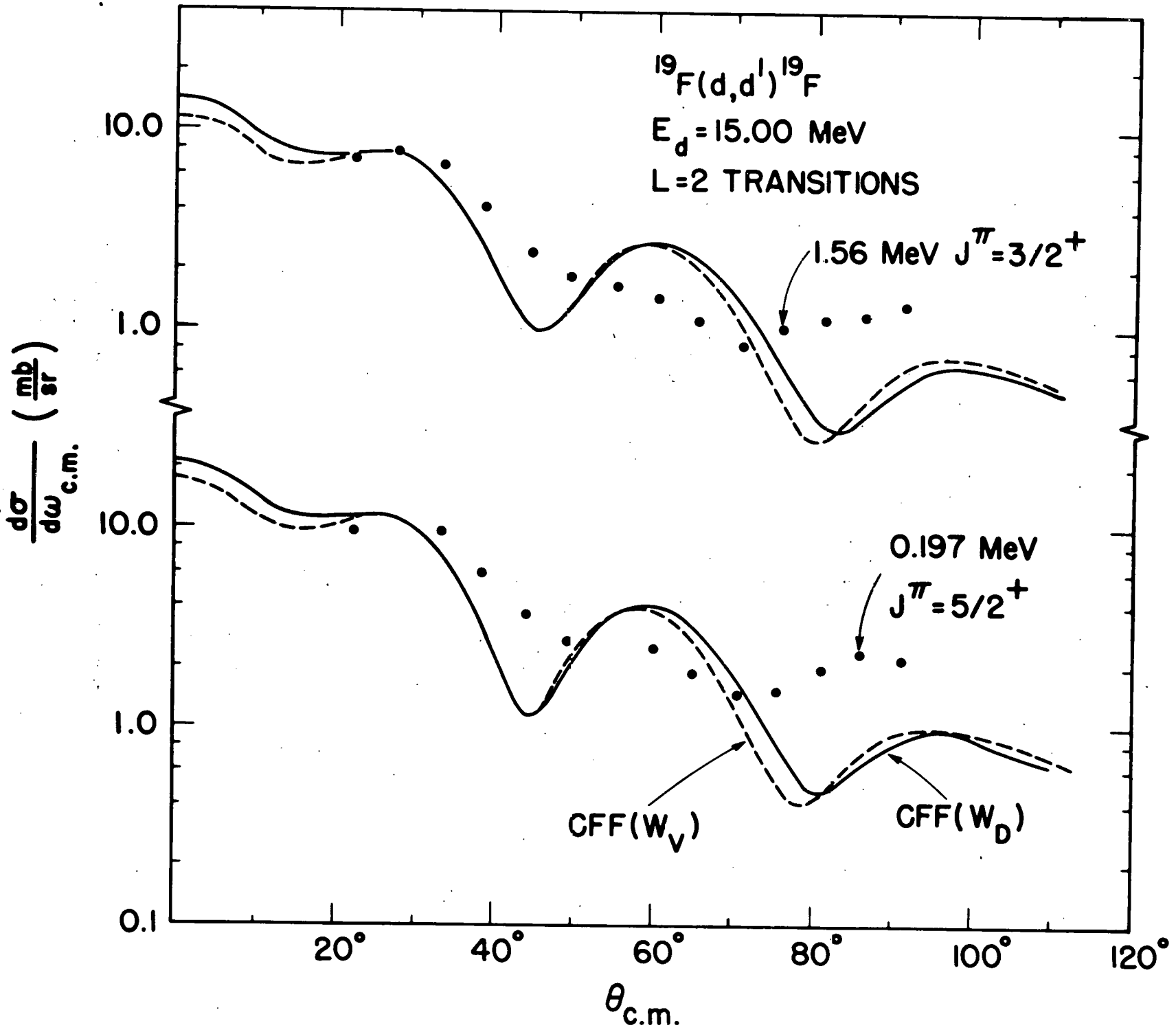
$^{19}F(d,d')^{19}F$
$E_d = 15.00$ MeV
L=2 TRANSITIONS
1.56 MeV $J^\pi = 3/2^+$
0.197 MeV
$J^\pi = 5/2^+$
CFF(W_V)
CFF(W_D)
$\frac{d\sigma}{d\omega}_{c.m.}$ $\left(\frac{mb}{sr}\right)$
10.0
1.0
10.0
1.0
0.1
20°
40°
60°
80°
100°
120°
$\theta_{c.m.}$

Fig. 4-2

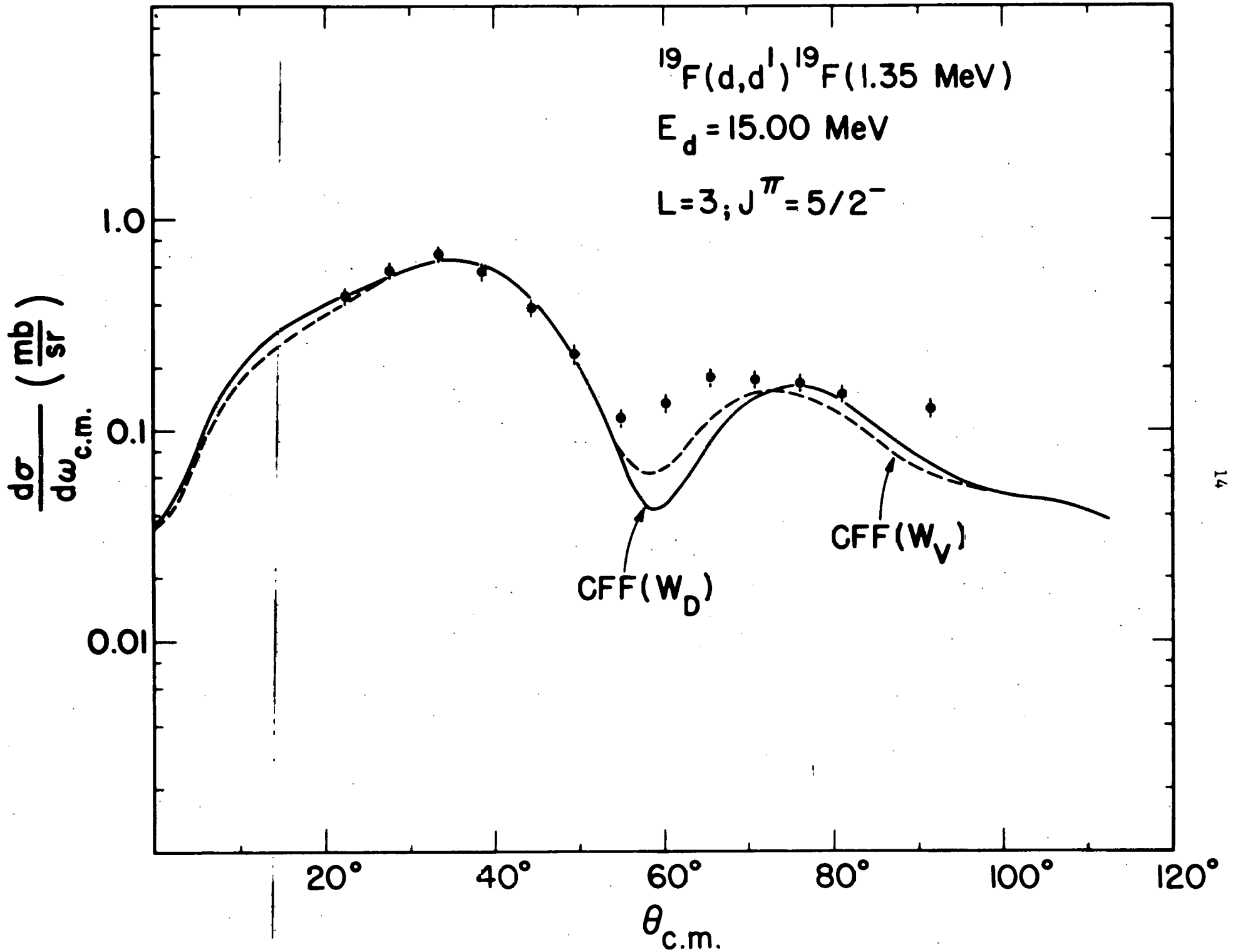
$^{19}F(d,d')^{19}F(1.35\ MeV)$
$E_d = 15.00\ MeV$
$L=3; J^{\pi}=5/2^-$
$\frac{d\sigma}{d\omega_{c.m.}}\ (\frac{mb}{sr})$
1.0
0.1
0.01
CFF(W_D)
CFF(W_V)
20°
40°
60°
80°
100°
120°
$\theta_{c.m.}$

Fig. 4-3

5. Energy Levels of Ne^{19} from $F^{19}(He^3,t)N^{19}$

D. Dehnhard and H. Ohnuma

The (He^3,t) reaction on F^{19} leading to states in the mirror nucleus Ne^{19} has been studied at an incident energy of 25 MeV. An array of three position-sensitive detectors placed in the focal plane of the split-pole magnetic spectrometer was used. Angular distributions of the transitions to the six lowest levels of Ne^{19} were measured between 7^o and 70^o(lab). Complete spectra between 0 and about 8 MeV excitation were taken at 8^o and 36^o(lab). Many excited states not previously known were identified. Several states were found in the region of the isobaric analog of the ground state doublet of O^{19}, and angular distributions to these states were taken between 8^o and 48^o(lab).

The first three states in Ne^{19} are known to be $1/2^+$, $5/2^+$, and $1/2^-$. Olness et al[1] made tentative assignments $5/2^-$, $3/2^+$, and $3/2^-$ for the 1.51, 1.54, and 1.61 MeV, respectively.

In inelastic scattering on F^{19} the negative parity states are very weak, while low-lying positive parity states, forming a K=1/2 rotational band based on Nilsson orbit number 6, are very strongly excited.[2,3] If the (He^3,t) reaction to excited states in Ne^{19} proceeds as "quasi-elastic" scattering[4] we would expect relative (He^3,t) cross sections to be similar to those of $(d,d')^2$ and $(p,p')^3$ on F^{19}.

The transitions to the 0.275-, 1.51-, and 1.61-MeV states are an order of magnitude weaker than those to the ground state and the 0.238- and 1.54- MeV states. Therefore, the former three states are most likely the negative parity states, while the latter three are positive parity states.

To extract L-values we performed distorted wave calculations assuming complex collective form factors derived from an optical model potential for He^3 scattering.[5] The angular distributions to the 0.238-- and 1.54-MeV states can be fitted by an L=2 calculated curve. This confirms that these states are $5/2^+$ and $3/2^+$ states. It is interesting to note that the (He^3,t) cross section ratio for these two states $d\sigma(0.22)/d\sigma(1.54)$ is close to 1.5 as expected for "quasi-inelastic" scattering to the $5/2^+$ and $3/2^+$ states of the rotational band. The transition to the 1.51-MeV state can be fitted by an L=3 angular distribution. The 1.61-MeV state angular distribution has a significantly different shape. If this state is $3/2^-$ it may be excited by L=1 (or a mixture of L=1 and L=3). No attempt was made to fit L=1 because it is not justified to use collective form factors for these transitions. We conclude that the 1.51-MeV state is the $5/2^-$ state and the 1.61-MeV state is $3/2^-$.

References

1. J.W. Olness, A.R. Poletti, and E.K. Warburton, Phys. Rev. 161, 1131 (1967).

2. D. Dehnhard and N.M. Hintz, Williams Laboratory 1968 Annual Report and to be published.

3. G.M. Crawley and G.T. Garvey, Phys. Rev. 167, 1070 (1968).

4. G.R. Satchler, R.M. Drisko, and R.H. Bassel, Phys. Rev. 136, B637 (1964).

5. D.J. Baugh, Nucl. Phys., A131, 417 (1969).

6. (p,p), (p,p'), and (p,d) Reactions on Neon at 40 MeV

D. G. Madland and N. M. Hintz

The experimental work on the (p,p), (p,p'), and (p,d) reactions on the neon isotopes has been completed. The elastic differential cross sections ^{22}Ne(p,p) and ^{20}Ne(p,p) were measured over an angular range of $15^{\circ} \leq \theta \leq 140^{\circ}$. The (p,p') work on ^{22}Ne and ^{20}Ne described in the last progress report[1] has been extended to backward angles while the (p,p') reaction on ^{21}Ne has yielded less data because the target was only available with 52% enrichment. The results of the (p,d) reaction studies include angular distributions on resolved states up to 6 MeV of excitation in ^{20}Ne and up to 3 MeV of excitation in ^{19}Ne and ^{21}Ne. Finally, the gas cell geometry was measured by comparing the H(p,p)H differential cross section with the 1% absolute experiment of Johnston.[2]

The optical model analysis of the elastic differential cross sections is in progress. The optical parameters obtained will be used in the DWBA analysis of the (p,p') and (p,d) data.

References

1. D.G. Madland and N.M. Hintz, John H. Williams Laboratory of Nuclear Physics Annual Report, 1968, p. 35.

2. L.H. Johnston and D.A. Swenson, Phys. Rev. 111, 212 (1958).

---

7. The (p,t) and (p,He^3) Reactions on Oxygen and Neon at 40 MeV

D. K. Olsen and R. E. Brown

The experimental work described in the 1968 Progress Report on the (p,t) and (p,He^3) reactions on the neon isotopes has been completed.

Table 7-1 summarizes the angular distributions obtained during the past year. Altogether cross sections for 25 transitions from the Ne^{20} and Ne^{22} isotopes have been measured.

TABLE 7-1

(p,t) and (p,He^3) Data Obtained on Ne^{20} and Ne^{22}

Reaction	J^π,T of Final-State	Angular Range
$Ne^{20}(p,He^3)F^{18}$(G.S.)	1^+,0	8°-80°
$Ne^{20}(p,t)Ne^{18}$(1.88)	2^+,1	10°-75°
(3.36)	?,1	10°-50°
(3.61)	?,1	10°-55°
(4.55)	1^-,1	10°-65°
$Ne^{22}(p,t)Ne^{20}$(10.27)	2^+,1	8°-75°

Fig. 7-1 shows the differential cross sections for the $O^{17}(p,t)O^{15}$(G.S.), $O^{17}(p,t)O^{15}$(6.16), $O^{17}(p,He^3)N^{15}$(G.S.), and $O^{17}(p,He^3)O^{15}$(6.33) reactions. The absolute cross section scale is arbitrary; however, the relative cross sections between the angular distributions are in correct proportion. The targets were made by oxidizing 0.9 mgm/cm^2 nickel foils in a pure oxygen atmosphere having the following isotopic composition: O^{16}:23.4%, O^{17}:36.6%, O^{18}:40.0%. The (p,He^3) differential cross sections have less structure and are considerably smaller in magnitude than the (p,t) differential cross sections. An attempt is being made to understand the experimental data in terms of a direct two-nucleon transfer process.

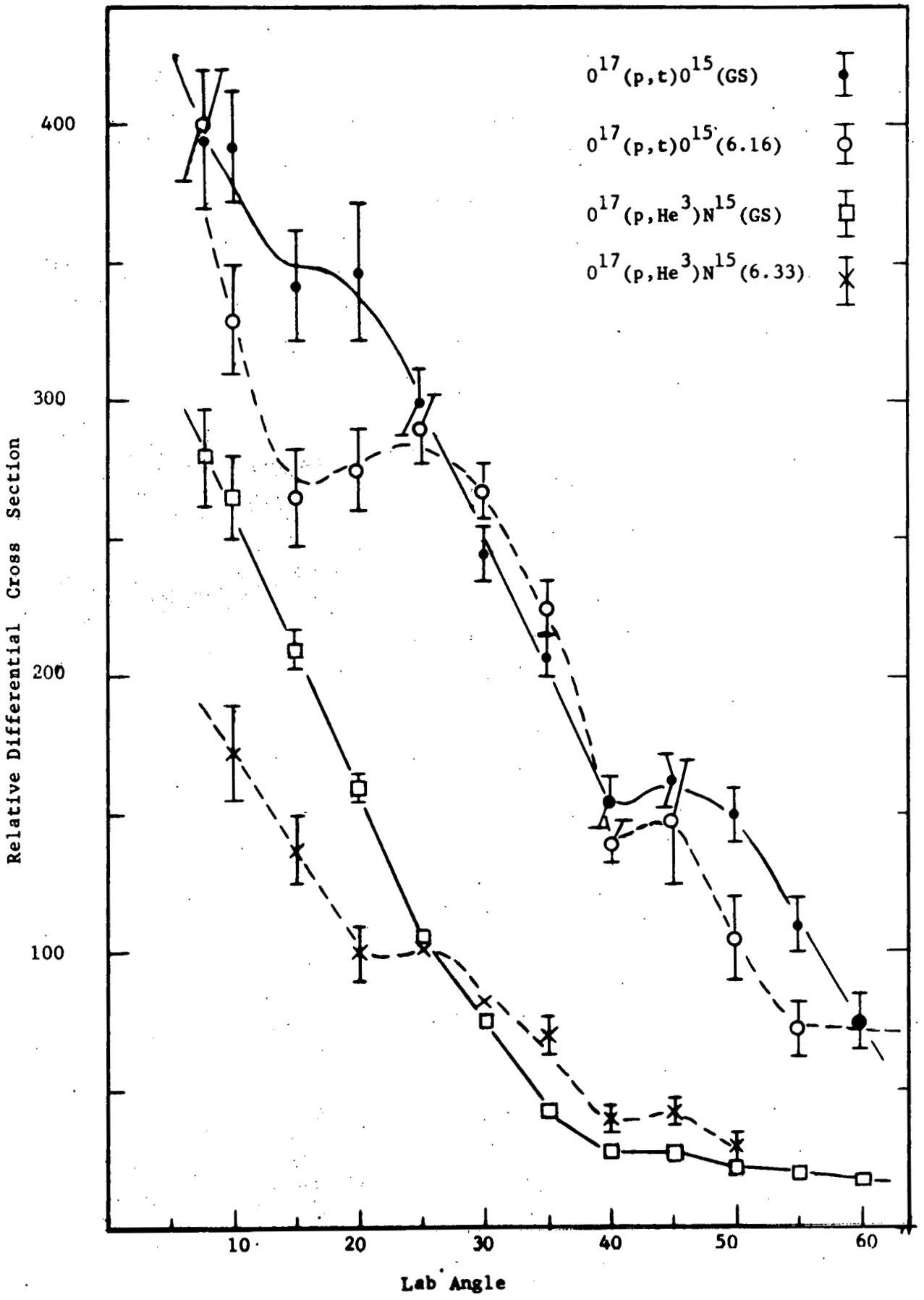
$O^{17}(p,t)O^{15}(GS)$
$O^{17}(p,t)O^{15}(6.16)$
$O^{17}(p,He^3)N^{15}(GS)$
$O^{17}(p,He^3)N^{15}(6.33)$
Relative Differential Cross Section
400
300
200
100
10
20
30
40
50
60
Lab Angle

Fig. 7-1

8. Proton Pickup From Al^{27}

R. DeLong and D. Dehnhard

Wildenthal and Newman[1] and G. J. Wagner et al[2] have observed a rather strong ℓ=2 transition in the $Al^{27}(d,He^3)Mg^{26}$ reaction to the unresolved 4.3 MeV triplet in Mg^{26}. The strength of this transition (C^2S=2.0-2.3) can be explained[1] by a shell model calculation assuming the transition goes mainly to a 4^+ state near 4 MeV. From (t,α) and (t,p) experiments[3] states at 4.32 MeV and 4.33 MeV were tentatively assigned to be 4^+. It is important to know what fraction of the total transition strength observed in Ref. 1 and 2 is contained in the 4^+ state proposed by theory.[1] Another triplet of states around 4.9 MeV was also not resolved in the latter two experiments.

We have studied the reaction $Al^{27}(d,He^3)$ at 19 MeV using the split-pole magnetic spectrometer[4] and two position-sensitive detectors located so as to detect the 4.3 MeV and the 4.9 MeV triplets simultaneously. Fig. 8-1 shows a position spectrum of the 4.3 MeV triplet from the (d,He^3) reaction with a target of 20 $\mu g/cm^2$ Al^{27} on a 10 $\mu g/cm^2$ carbon backing. The solid line was determined by using a Gaussian peak fitting program. The resolution at forward angles was about 13 keV (FWHM) and deteriorated at larger angles because of the larger energy loss in the target.

Angular distributions were taken from 10° to 70°. The 4.313 MeV and 4.330 MeV states are excited by ℓ=2 transitions. For the transition to the 4.350 MeV state an ℓ=0 assignment appears likely, in agreement

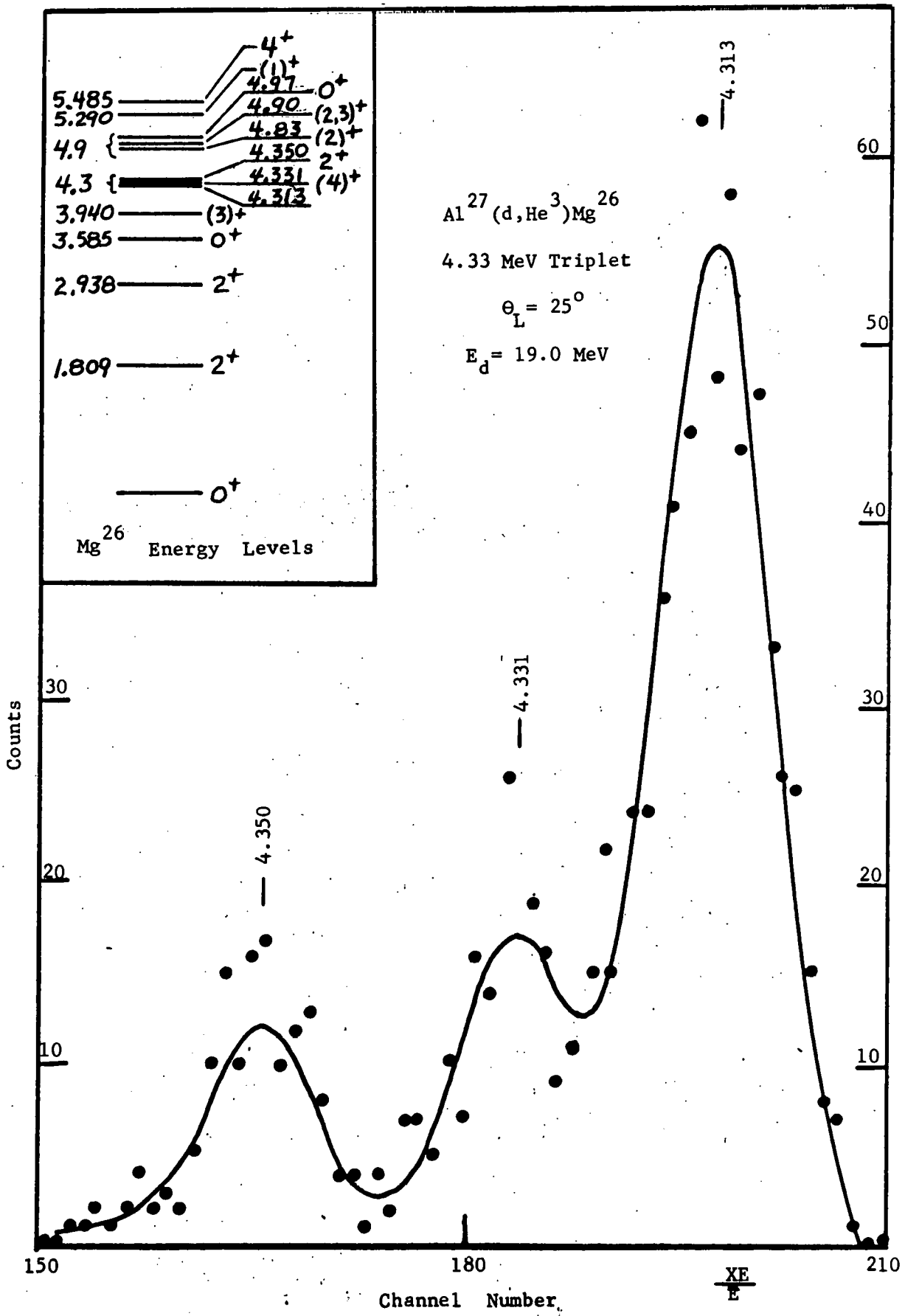
5.485
5.290
4.9
4.3
3.940
3.585
2.938
1.809
4+
(1)+
4.97
0+
4.90
(2,3)+
4.83
(2)+
4.350
2+
4.331
(4)+
4.313
(3)+
0+
2+
2+
0+
Mg26 Energy Levels
Al27(d,He3)Mg26
4.33 MeV Triplet
θL = 25°
Ed = 19.0 MeV
4.313
4.331
4.350
Counts
Channel Number
XE/E
150
180
210
10
20
30
40
50
60

Fig. 8-1

with the theoretical calculations,[1] which predict a predominately $\ell=0$ transition to a 2^+ state around that energy. Apparently, most of the strength of the transition to the triplet is contained in the 4.313 MeV state, which would then have to be the 4^+ state in the shell model calculations.[1]

The 4.9 MeV triplet was found to be only weakly excited, with most of the strength being in the 4.83 MeV state. Angular distributions on this triplet are incomplete.

References

1. B.H. Wildenthal and E. Newman, Phys. Rev. 175, 1431 (1968).
2. G.J. Wagner, G. Mairle, and U. Schmidt-Rohr, Nucl. Phys. A125, 80 (1969).
3. S. Hinds, H. Marchant, and R. Middleton, Nucl. Phys. 67, 257 (1965).
4. J.E. Spencer and H.A. Enge, Nucl. Instr. and Meth. 49, 181 (1967); John H. Williams Laboratory Annual Progress Report, University of Minnesota, 1968, p. 150.

---

9. The ^{26}Mg(d,^{3}He) ^{25}Na Reaction and the "Modified DWBA"

D. Dehnhard and R. DeLong

P. D. Kunz et al.[1] have shown that the effects of strong coupling in the initial and final state in a particle transfer reaction may be simulated by a modification of the optical model parameters for incoming and outgoing particles. We have applied their prescription to distorted wave calculations for the ^{26}Mg(d,^{3}He) ^{25}Na reaction at 20 MeV and at 34.4 MeV.[2]

The data at 20 MeV were taken with the split-pole magnetic spectrometer and position-sensitive detectors. Angular distributions of the g.s., the 90 keV state, and the 1.07 MeV state were obtained between 10^{o} and 55^{o} (lab)(Fig. 9-1). The 90 keV state, not resolved at E_d = 34 MeV[2], was easily resolved with the spectrometer and found to be only very weakly excited. "Regular" DWBA calculations with optical model parameters obtained by Wildenthal and Newman[3] from 34 MeV deuteron scattering on several nuclei and by Yntema and Dehnhard[4] from 33 MeV He^3 scattering on Mg^{26} gave only very poor fits to the experimental data at 20 MeV (Fig. 9-1, solid lines). Very good fits to the ℓ=0 transition to the 1.07 MeV state and the ℓ=2 transition to the 90 keV state (Fig. 9-1, broken lines) are obtained by increasing the radius of the optical model parameters in incoming and outgoing channel as suggested in Ref. 1 by a factor of $(1 + \chi\beta) = 1.2$ where β is the deformation parameter and χ (defined in Ref. 1) depends upon the Nilsson coefficients $C_{j\ell}$. The applicability of the Nilsson model to explain low-lying states in ^{25}Na is not quite clear, because the g.s. of ^{25}Na has $J^{\pi} = 5/2^{+}$ and not $3/2^{+}$ as expected from the rotational model and as observed in ^{23}Na. However, we performed preliminary Coriolis band mixing calculations using a code written by J. R. Erskine[5] and found that the $5/2^{+}$ rotational state based on the $K=3/2^{+}$ Nilsson orbit number 7 mixes strongly with the $5/2^{+}$ state of Nilsson orbit number 6 and can therefore be found below the $3/2^{+}$ state. It is not yet clear how the prescription given by Kunz et al.[1] should be modified to include band mixing. Nevertheless, the considerable improvement of the fits for the $1/2^{+}$ and $3/2^{+}$ states is interesting. (The regular DWBA fit for the $3/2^{+}$ state has the same shape as for the $5/2^{+}$ g.s.(solid line).)

If the $5/2^+$ g.s. state would be a pure rotational state based on orbit number 7 it would have to be above the $3/2^+$ state and χ would be very small (see Table III in Ref. 1), however, through band mixing with the $K=1/2^+$ band (orbit number 6) χ would probably increase as is suggested by the experimental points which are found just between the calculated curves for $\chi=0$ and for $\lambda(1+\chi\beta) = 1.2$. For the 34 MeV data (not shown) the effect of changing the radius was much less drastic than for the 20 MeV data.

At present it cannot be excluded that the good fits obtained by the increase in the radius of the optical model parameters may be due to otherwise poor optical model parameters at the lower energy. More examples of transfer reactions on strongly deformed nuclei should be investigated in the way suggested by Ref. 1.

References

1. P.D. Kunz, E. Rost, and R.R. Johnson, Phys. Rev. 177, 1737 (1969).
2. D. Dehnhard, E. Newman, J.C. Hiebert, and B.M. Preedom, unpublished.
3. E. Newman, L.C. Becker, P.M. Preedom and J.C. Hiebert, Nucl. Phys.
4. J.L. Yntema and D. Dehnhard, to be published.
5. We are grateful to Dr. J.R. Erskine for permitting us to use his code at Argonne National Laboratory.

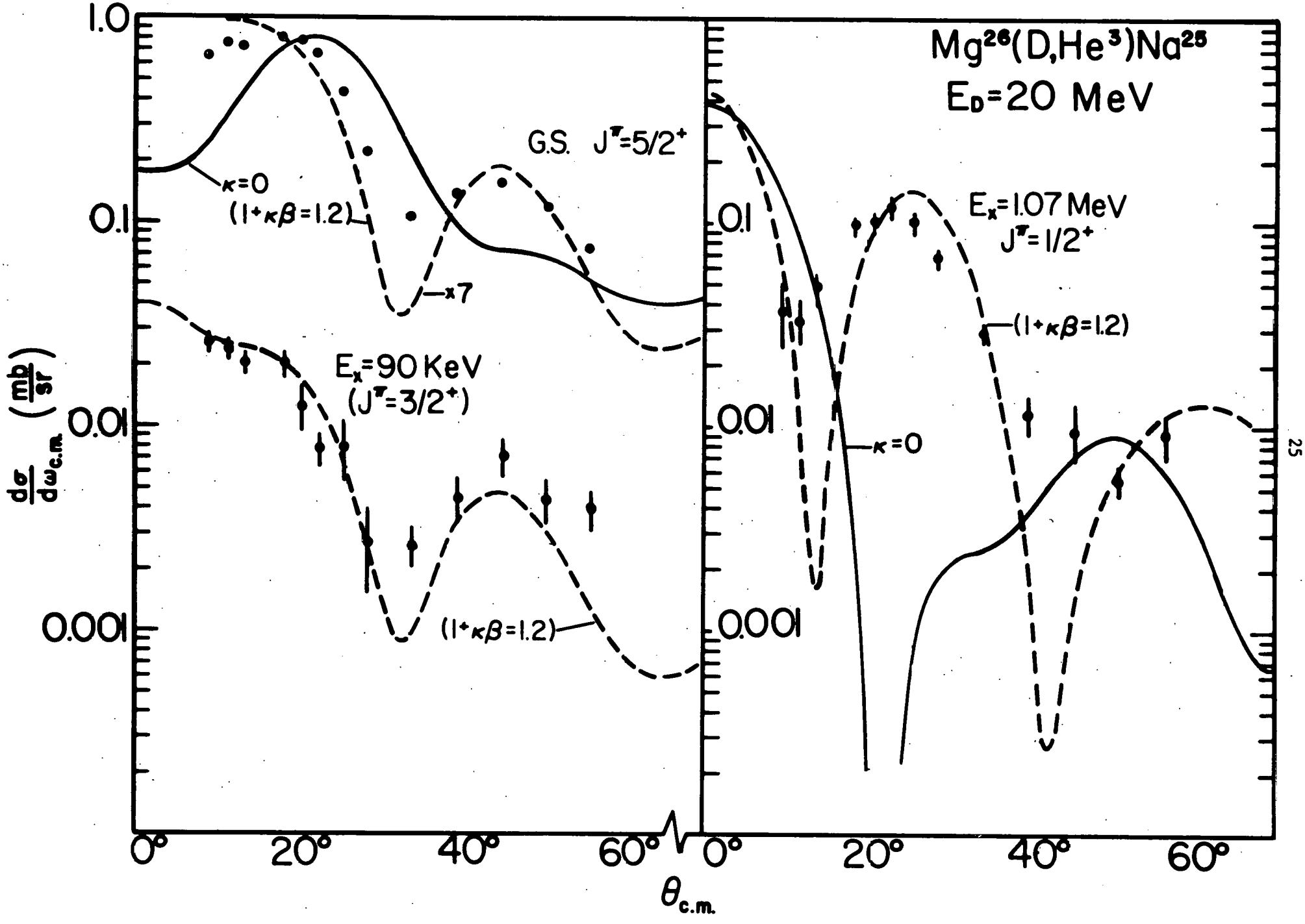
Mg²⁶(D,He³)Na²⁵
E_D=20 MeV
G.S. J^π=5/2⁺
κ=0
(1+κβ=1.2)
×7
E_x=90 KeV
(J^π=3/2⁺)
(1+κβ=1.2)
E_x=1.07 MeV
J^π=1/2⁺
(1+κβ=1.2)
κ=0
1.0
0.1
0.01
0.001
dσ/dω_c.m. (mb/sr)
0°
20°
40°
60°
θ_c.m.

Fig. 9-1

10. (^{3}He,d) Reactions on ^{29}Si

W. W. Dykoski and D. Dehnhard

It has been suggested[1] that the strength of transitions in particle transfer reactions may be reduced when target and final nucleus have significantly different shapes. Some evidence for this effect was seen in neutron pickup reactions on Si isotopes.[2] We are now studying proton stripping reactions on the Si isotopes using the (^{3}He,d) reaction.

So far, SiO_2 targets enriched in ^{29}Si to 92% were exposed to 25 MeV ^{3}He particles. The split-pole magnetic spectrometer together with nuclear emulsion plates was used to detect the deuterons. Broad range spectra at several angles between 8° and 29° were taken and have been scanned between 0 and 6 MeV excitation. A part of a typical spectrum is shown in the Fig. 10-1 . These data are now being analyzed. For comparison, we expect to study the (^{3}He,d) reaction on ^{28}Si and ^{30}Si.

References

1. G. R. Satchler, Ann. of Phys. 3, 275 (1958).
2. D. Dehnhard and C. G. Hoot, John H. Williams Laboratory of Nuclear Physics Annual Report, 1968, Sec. 24.

---

11. $Si^{29}(d,p)Si^{30}$ Reaction

H. Ohnuma and D. Dehnhard

The $Si^{29}(d,p)Si^{30}$ reaction has been studied at an incident energy of 20 MeV. The split-pole magnetic spectrometer and nuclear emulsion plates, covered with absorber foils, have been used to detect the pro-

$^{28}Si(^3He,d)^{30}P$
$E_{^3He}$ = 25 MeV
Θ_{LAB} = 26°
COUNTS PER 0.25 mm
DISTANCE ALONG FOCAL PLANE IN cm.
E_x(MeV), J$^\pi$; T
4.496
4.475
4.421
4.342
4.296
4.230
4.181, (2$^+$); 1
4.141, 2$^-$
3.926
3.836
3.734
3.018, (1)
2.937, (2$^+$); 1
2.839
2.725, (2)
2.539, 3$^+$
1.976, 3$^+$
1.455, 2$^+$
0.709, 1$^+$
0.678, 0; 1
3.446
3.102, ½$^+$
G.S., 1$^+$
4.340, ½$^-$
4.078, (½$^+$, ½$^+$)
5.738, ½$^-$
1.38, ½$^+$
G.S.
G.S.
½$^+$

FIG. 10-1

tons. A typical spectrum obtained at 25°(lab) is shown in Fig. 11-1. Angular distributions have been measured for states between 2 and 6 MeV excitation. The states at 2.23, 3.51, 4.81, 5.22, and 5.61 MeV are excited by ℓ=2. A recent assignment[1] ($J^{\pi}=2^{+}$) to the 4.808-MeV state is consistent with the present result. An ℓ=2 transition to the 5.22 MeV state confirms the recent assignment[2] of 3^{+} and contradicts the old assignment[3] of 3^{-}. An unresolved doublet at 3.78 MeV is probably a mixture of ℓ=0 and ℓ=2, in agreement with the 1^{+} and 0^{+} assignment[3,4] to the 3.767 and 3.786 MeV states, respectively. The 5.48 MeV state is seen strongly excited by ℓ=3, supporting the 3^{-} assignment[3] to this state. The strong excitation suggests that this state is not a purely collective octupole state as expected from neighboring nuclei, but a state formed mainly by the coupling of an f particle to the ground state of Si^{29}. The energy of this state is quite high compared to neighboring nuclei where the states with a large f component are around 3.5 MeV. The states at 4.83 MeV and 5.27 MeV were seen weakly excited; an ℓ assignment has not yet been made.

References

1. H. Ohnuma et al, to be published.

2. B.H. Wildenthal and E. Newman, Phys. Lett. 20B, 108 (1968).

3. P.M. Endt and C. Van der Leun, Nucl. Phys. A105, 1 (1967).

4. P.J.M. Smulders, Phys. Lett. 9, 155 (1964); C. Broude, P.J.M. Smulders, and T.K. Alexander, Nucl. Phys. A90, 321 (1967).

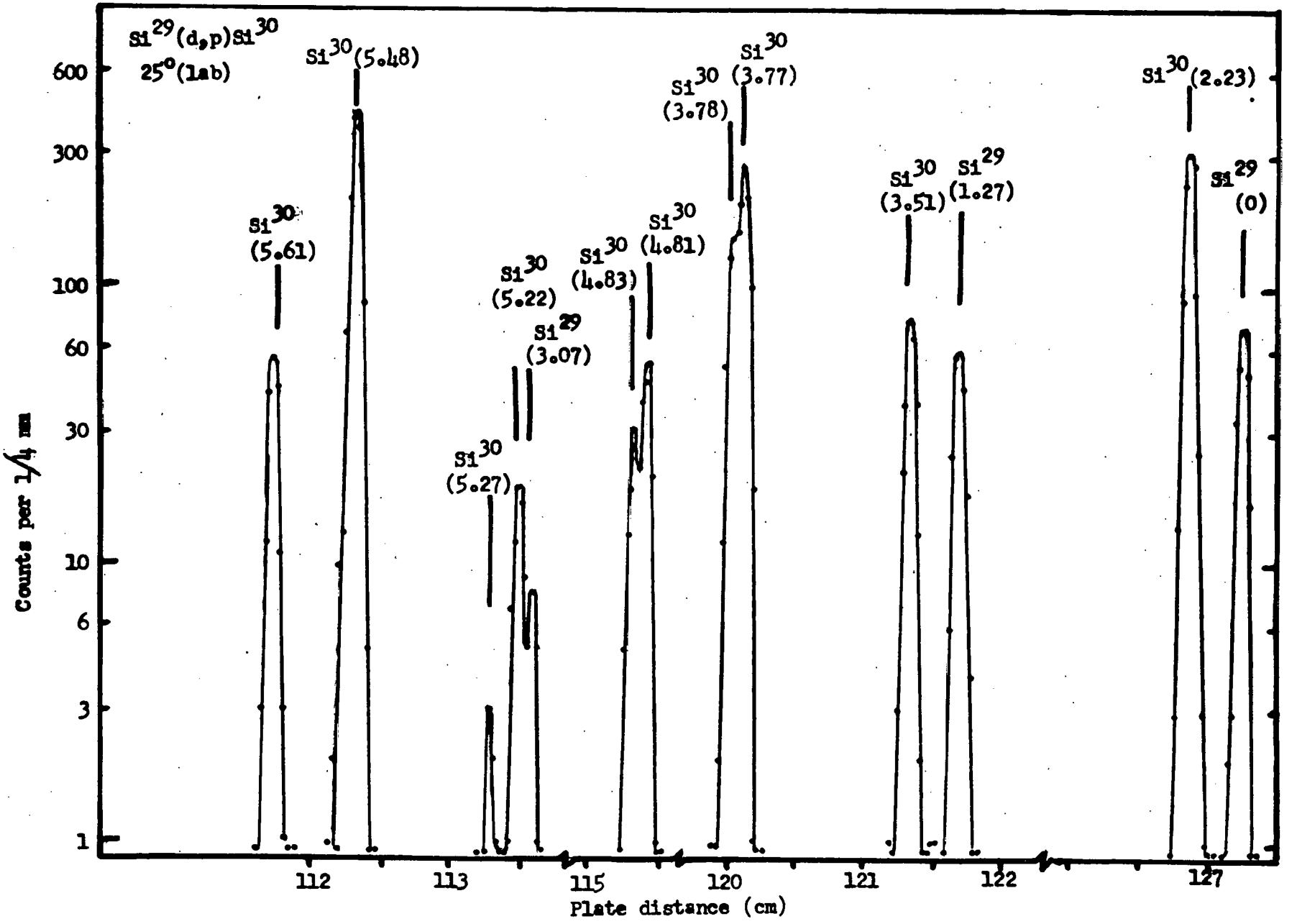
Si29(d,p)Si30
25°(lab)
Si30 (5.48)
Si30 (5.61)
Si30 (5.22)
Si29 (3.07)
Si30 (5.27)
Si30 (4.83)
Si30 (4.81)
Si30 (3.78)
Si30 (3.77)
Si30 (3.51)
Si29 (1.27)
Si30 (2.23)
Si29 (0)
Counts per 1/4 mm
600
300
100
60
30
10
6
3
1
112
113
115
120
121
122
127
Plate distance (cm)

Fig. 11-1

III. SPECTROSCOPY OF NUCLEI FROM Sc THROUGH Ni

12. Levels in Sc^{44} from the $Ca^{42}(\alpha,d)Sc^{44}$ Reaction

R. H. Cornett, H. Ohnuma, and N. M. Hintz

In an attempt to study the energy level structure of Sc^{44}, we are currently at work on the $Ca^{42}(\alpha,d)Sc^{44}$ reaction with the split-pole spectrometer, using 25 MeV α's from the tandem Van de Graaff accelerator. The (α,d) reaction will yield information complementary to that of other two-nucleon transfer experiments such as the $Ca^{42}(He^3,p)Sc^{44}$ work done at Heidelberg[1] and the $Ti^{46}(d,\alpha)Sc^{44}$ experiment done here by Wallen, Ohnuma and Hintz.[2] The contamination free calcium target used necessitated the development of the vacuum target transfer system described elsewhere.[3]

References

1. Jahresbericht 1968, Max-Planck Institut für Kernphysik, Heidelberg, p. 34.
2. This report, section 14 ,
3. This report, section 46

---

13. $Sc^{45}(d,t)Sc^{44}$ Reaction

H. Ohnuma, A. M. Sourkes and N. M. Hintz

The $Sc^{45}(d,t)Sc^{44}$ reaction has been studied with a 19.5 MeV deuteron beam from the Williams Laboratory tandem Van de Graaff. The reaction products have been analyzed by a split-pole magnetic spectrometer and position-sensitive detectors. The targets were metallic scandium

foils, some on carbon backings. A typical triton spectrum obtained at 20°(lab) is shown in Fig. 13-1 . Peaks between group 11 and 15 are due to pile-up from the out-of-focus deuteron elastic groups. Angular distributions for some low-lying states are shown in Fig. 13-2 . In Table 13-1 the results are summarized and compared with previous neutron pickup experiments.[1,2] Sums of the spectroscopic factors obtained here are also given in the Table. The ℓ=3 strength is exhausted by about 1.5 MeV, except for the analog state at 2.8 MeV; many states with d and s strength appear thereafter. A weak ℓ=1 component was observed indicating that there is a mixture of p-neutrons in the ground state of Sc^{45}. The first and second excited states, which are known[3] to be 1^{+}, are not excited in the present experiment.

References

1. E. Kashy, Phys. Rev. 134, B378 (1964).

2. D.E. Bainum, J. Rapaport, T.A. Belote, and W.E. Dorenbusch, Bull. Am. Phys. Soc. 13, 174 (1968), and private communications.

3. R.A. Ristinen and A.W. Sunyar, Phys. Rev. 153, 1209 (1967).

---

14. Levels in Odd-Odd Scandium Isotopes from Ti(d,α)

R. A. Wallen, H. Ohnuma, and N. M. Hintz

In order to obtain more information on energy levels, spins, and configuration mixing in the odd-odd isotopes, we have been studying the (d,α) reaction on the three even-even Ti isotopes at E_d=19 MeV. We have taken data at laboratory angles from 10° to 90°. The level of excitation in the Ti nuclei ranged from 0 to 5 MeV.

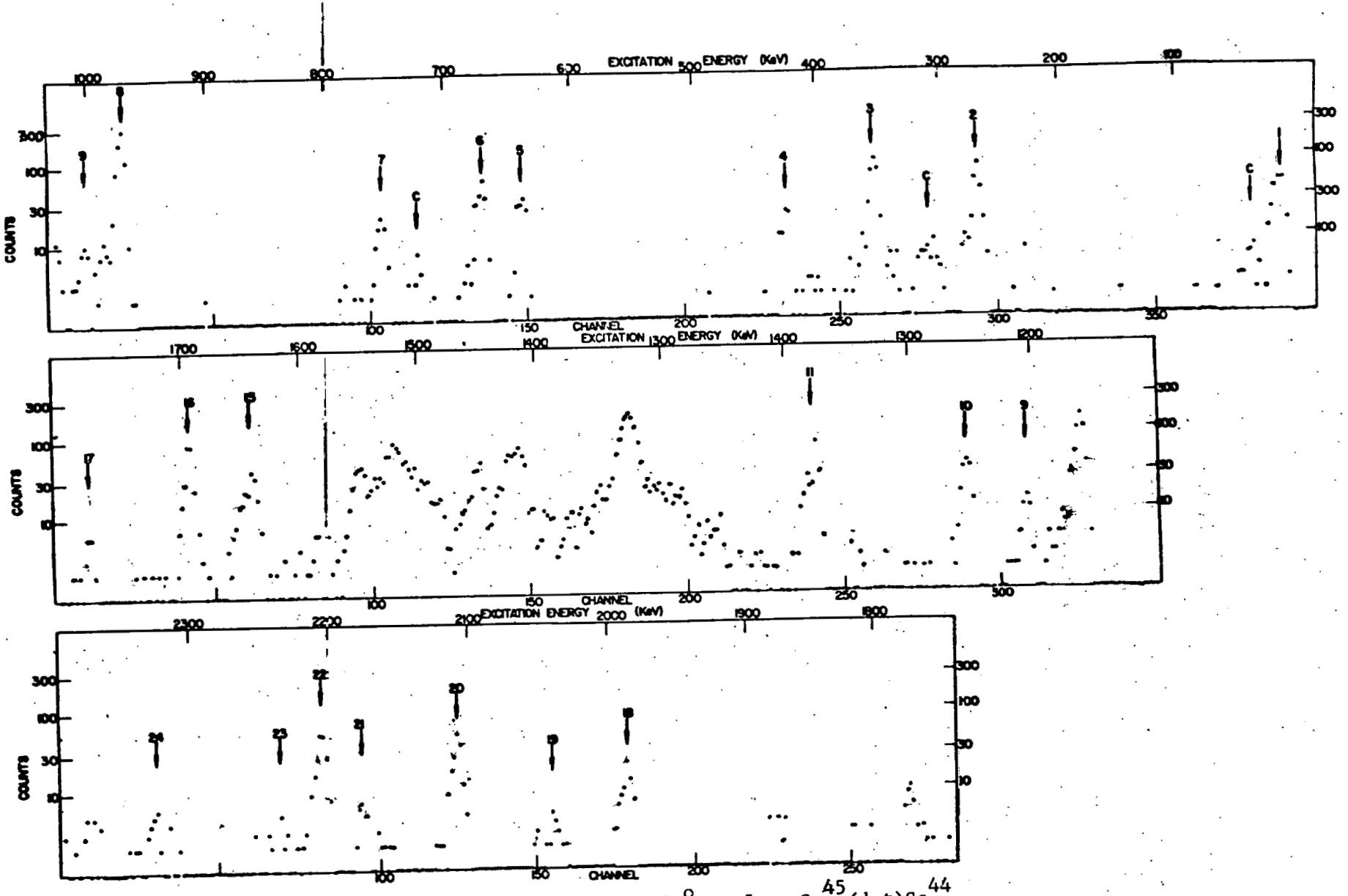

Triton Spectrum at 20°_{lab} from $Sc^{45}(d,t)Sc^{44}$

Fig. 13-1

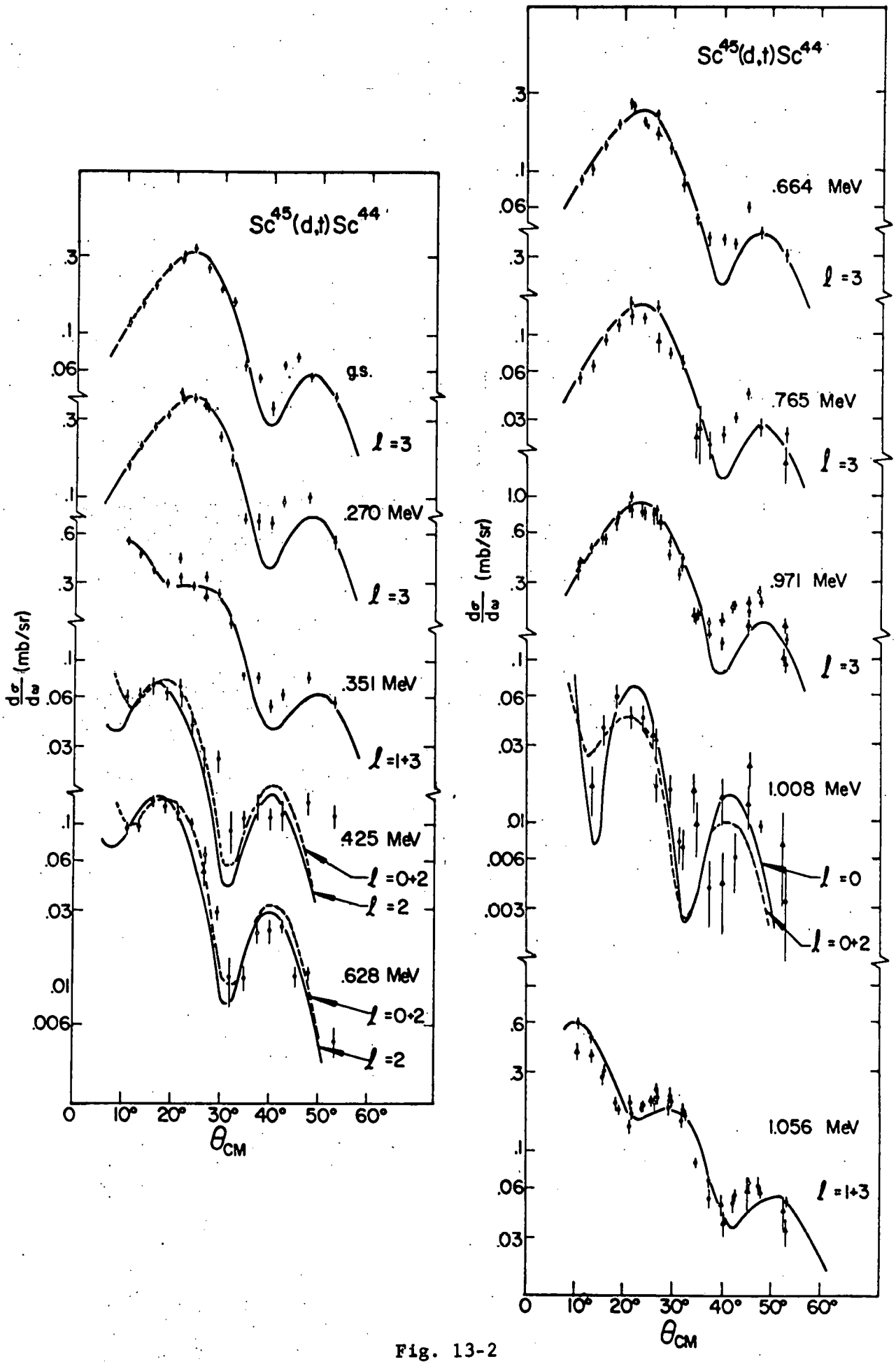
Sc45(d,t)Sc44
g.s.
l =3
.270 MeV
l =3
.351 MeV
l =1+3
.425 MeV
l =0+2
l =2
.628 MeV
l =0+2
l =2
dσ/dΩ (mb/sr)
θCM
0 10° 20° 30° 40° 50° 60°
Sc45(d,t)Sc44
.664 MeV
l =3
.765 MeV
l =3
.971 MeV
l =3
1.008 MeV
l =0
l =0+2
1.056 MeV
l =1+3
dσ/dΩ (mb/sr)
θCM
0 10° 20° 30° 40° 50° 60°

Fig. 13-2

TABLE 13-1. Comparison of Various Neutron Pick-Up Reactions on Sc^{45}.

Ref. 1 (p,d)			Ref. 2 (He^3,α)			Present work (d,t)		
E(MeV)	ℓ	c^2S	E(keV)	ℓ	c^2S	E(keV)	ℓ	c^2S
0	3	0.30	0	3	0.42	0	3	0.52
0.266±0.009	3	0.47	269±20	3	0.60	270±5	3	0.70
0.344±0.010	3	0.38	344	3	0.43	351	1,3	0.04, 0.28
						425	0,2	0.01, 0.07
						628	0,2	0.01, 0.15
0.646±0.012	3	0.32	654	3	0.38	668	3	0.39
0.748±0.015	3	0.22	756	3	0.17	765	3	0.26
0.952±0.015	3	1.36	976	3	1.66	971	3	1.50
						1008	0,2	0.01, 0.04
1.025±0.02			1043	3	0.28	1056	1,3	0.07, 0.36
1.165±0.017			1181	3	0.28	1183	1,3	0.04, 0.24
1.41±0.02	(2)		1424	(2)	0.24	1409	2	0.54
1.51±0.02								
			1531	(2)	0.54	1533	1,3	0.05, 0.15
				(3)	0.30			
						1559	0,2	0.05, 0.20
1.66±0.02	(2)		1682	2	0.39	1690	0,2	0.03, 0.40
						1767		
						1988±10	0	0.07
						2042	0,2	0.02,0.08
			2110	(3)	0.18	2111	0,2	0.04,0.46
			2210	(2)	0.24	2186	2	0.08
						2245		
						2336	2	0.13
						2498	0	0.15
						2526	(2)	(0.17)
			2584			2589	0	0.20
						2625	0,2	0.04, 0.14
			2696					
			2763	3	0.12			
			2907					
			3004	(2)	0.25			

$$\sum_{\ell=3} c^2S = 4.41$$

$$\sum_{\ell=1} c^2S = 0.20$$

$$\sum_{\ell=2} c^2S = 2.47$$

$$\sum_{\ell=0} c^2S = 0.84$$

Because the level density is rather high in odd-odd nuclei, especially away from closed shells, and because particle identification was required, we used position-sensitive detectors and the split-pole magnetic spectrometer. Using enriched self-supporting metallic targets of approximately 100 $\mu g/cm^2$ we obtained an overall resolution of 10 keV, FWHM.

The system was calibrated by moving strong alpha particle peaks across our detectors, in 3 mm steps, by changing the magnetic field of the spectrometer. We then compared our calibrations with the G.S. and with excited states in Sc^{46} that have been measured accurately in gamma work using bent crystal spectrometers. In this way we were able to obtain excitation energies to an accuracy of one or two keV for strong states and two to four keV for weak or highly excited states. A number of previously unknown states have been identified. A spectrum for $Ti^{50}(d,\alpha)Si^{48}$ at 25^o up to 2.6 MeV excitation is shown in Fig. 14-1.

We are in the process of comparing our angular distributions with those obtained from Bayman's two-nucleon transfer code, TWOPAR, and with DWUCK by making use of the cluster approximation as discussed by Daehnick and Park.[1] Preliminary results on this analysis were reported at the Washington 1969 APS meeting.[2]

To facilitate our analysis we observed alpha particle elastic scattering on Ti^{48} at 21 MeV for laboratory angles from 20^o to 170^o. From RAROMP we obtained a number of optical model sets consisting of six parameter fits to the data and are currently investigating these in the (d,α) calculations.

Some tentative spin-parity assignments are for Sc^{48}: GS, 6+; 0.131, 5+; 0.253, 4+; 0.624, 3+; 1.097, 7+; 1.406, 2-; 2.518, 1+; and for Sc^{46}: GS, 4+; 0.052, 6+; 0.228, 3+; 0.281, 5+; 0.290, 2-; 0.628, 4+; 0.774, 5+; 0.973, 7+; 0.984, 2+; 1.125, 5+.

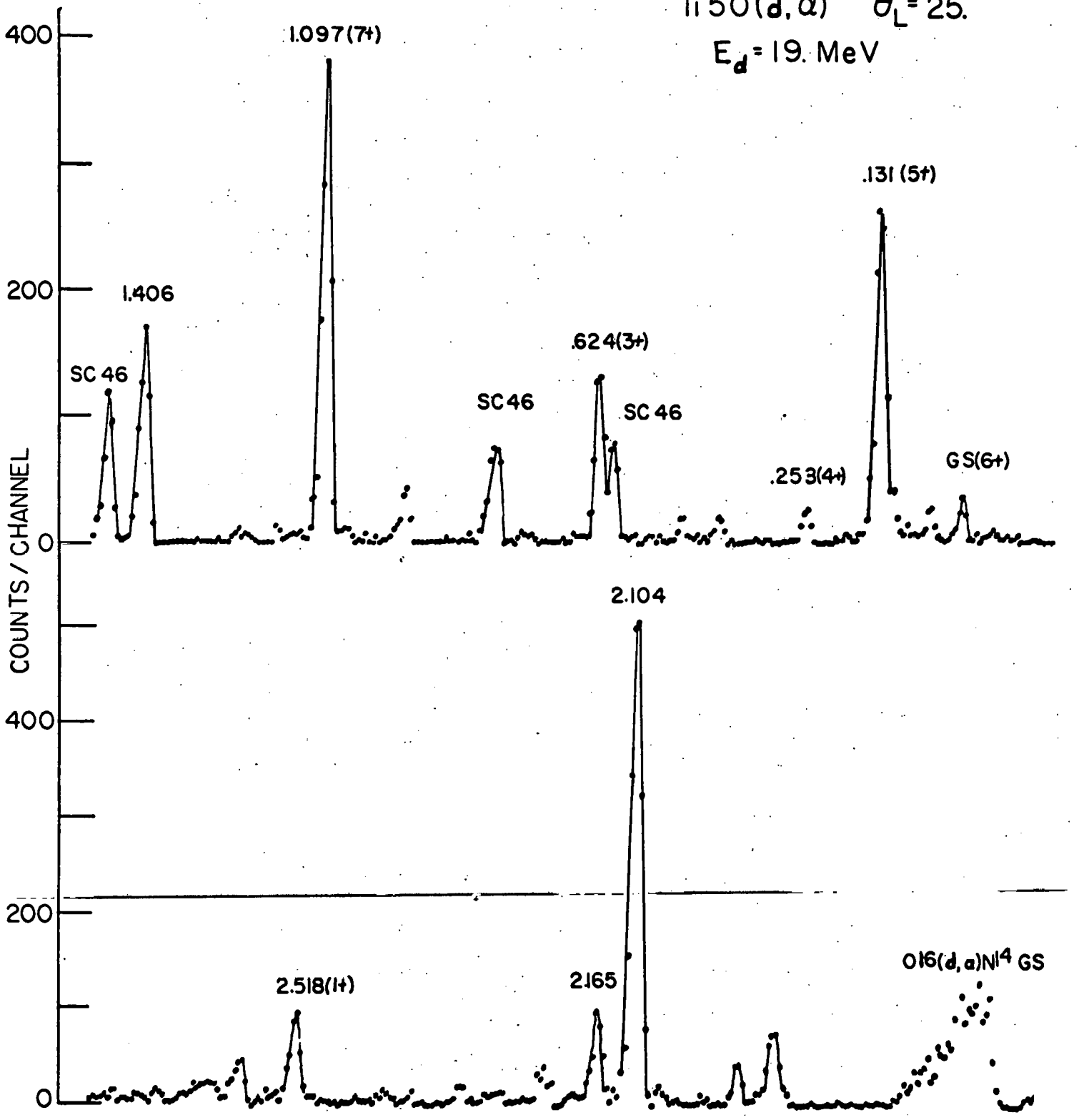
Ti 50 (d, α) θL = 25°
Ed = 19. MeV
COUNTS / CHANNEL
400
200
0
400
200
0
1.097(7+)
1.406
SC 46
SC46
.624(3+)
SC 46
.131 (5+)
.253(4+)
GS(6+)
2.104
2.518(1+)
2.165
O16(d, α)N14 GS

Fig. 14-1

References

1. W.W. Daehnick and Y.S. Park, Phys. Rev. 180, 1062 (1969).
2. R.A. Wallen, H. Ohnuma, N.M. Hintz, Bull, Am. Phys. Soc. 14, 601 (1960).
3. G.W. Greenlees, G.J. Pyle, and Y.C. Tang, Phys. Rev. 171, 1115 (1968).

15. $Ti^{49}(d,He^3)Sc^{48}$ Reaction

H. Ohnuma

The $Ti^{49}(d,He^3)Sc^{48}$ reaction has been studied with a 19.45 MeV deuteron beam from the Williams Laboratory tandem Van de Graaff. A split-pole magnetic spectrograph and position-sensitive detectors have been used to analyze reaction products. The target is a self-supporting metallic foil enriched to 77.3% in Ti^{49}. A typical spectrum at 15^{o}(lab) and the angular distribution for the ground state He^3 group is shown in Fig. 15-1 and Fig. 15-2 , respectively. States at 132, 254, and 624 keV in Sc^{48} are also excited by ℓ=3. Relative strength of these states are listed in Table 15-1 . As shown in the table, the present results are in good agreement with the previous (d,He^3) experiment[1] and the shell-model calculations[2,3], but in slight disagreement with the (t,α) results.[4]

References

1. H. Ohnuma and J.L. Yntema, to be published.
2. J.B. Ball, Bull Am. Phys. Soc. 11, 349 (1966).
3. S.S. Wong, Nucl Phys. A113, 481 (1968).
4. J.J. Schwartz, Phys. Rev. Letters 18, 174 (1967).

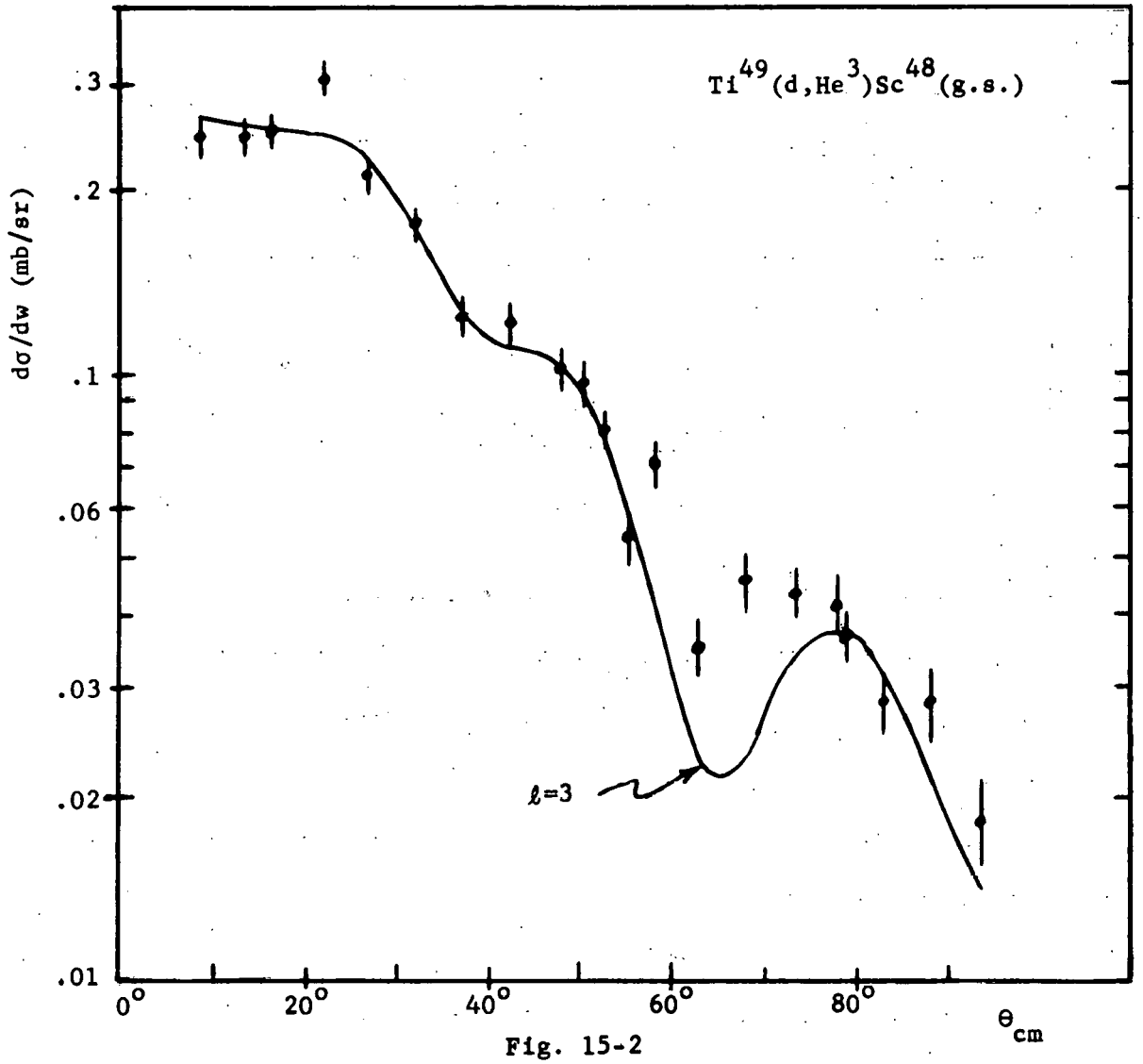

Fig. 15-2

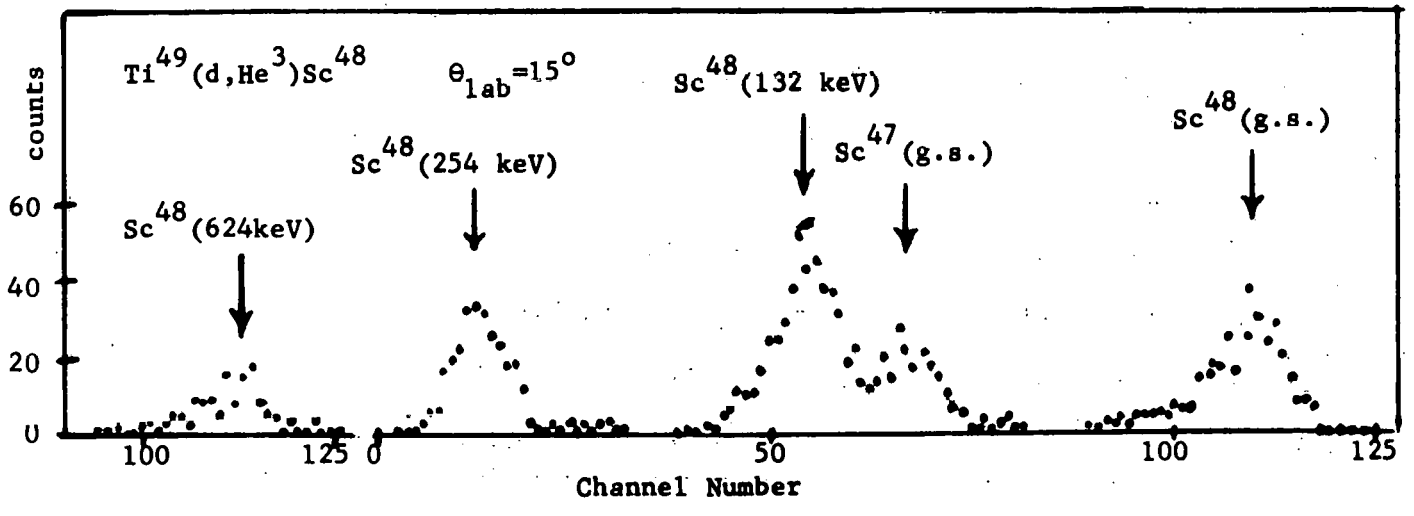

Fig. 15-1

TABLE 15-1 . Relative Strength of ℓ=3 Component in the Proton Pick-up Reactions from Ti^{49}.

State in Sc^{48}	(d,He^3) present	(d,He^3) previous	(t,α)	Calculations Ball	Wong
G.S. (6^+)	1.0	1.0	1.0	1.0	1.0
133 keV (5^+)	1.4	1.5	1.1	1.2	1.05
252 keV (4^+)	0.8	0.8	1.2	0.7	0.7
625 keV (3^+)	0.4	0.6	0.28	0.3	0.3
1145 keV (2^+)				0.5	0.08
1096 keV (7^+)			0.10(1.17MeV)	0.16	0.21
2525 keV (1^+)			0.33(2.70MeV)	0.002	0.01

16. States in Ti^{44} and Cr^{48} from (p,t) Reactions

D. G. Madland and N. M. Hintz

The $Ti^{46}(p,t)Ti^{44}$ and $Cr^{50}(p,t)Cr^{48}$ reactions have been studied with 40 MeV incident protons from the Minnesota Linear Accelerator. The reaction products were momentum analyzed with the 180° magnetic spectrograph and detected with an array of 32 solid state detectors. The over-all resolution for the experiment was ± 60 keV.

The three targets used in the experiment had the following properties:

	target	isotopic purity	areal density	contaminants	
(1)	Ti^{46}	77.1%	1.07 mg/cm^2	Ti^{48}	(17.3%)
(2)	Ti^{46}	86.4%	2.51 mg/cm^2	Ti^{48}	(9.6%)
(3)	Cr^{50}	95.9%	~4.5 mg/cm^2	C^{12},C^{13},H^1	(55%)

The experimental procedure was to take momentum spectra at two angles (10^{o} and 20^{o}) for each target. The excitation energies and their uncertainties, for all resolved states, were obtained from these spectra. Angular distributions were then taken on all such resolved states.

Analysis of the data using the two neutron transfer DWBA program, TWOPAR, by B. F. Bayman,[1] is partially complete. Parameters describing the incoming and outgoing distorted waves were taken from the generalized nucleon-nucleus optical potential of F. Becchetti[2] and an extrapolation of parameters obtained from 20 MeV triton elastic scattering experiments,[3] respectively.

$Ti^{46}(p,t)Ti^{44}$: Fig. 16-1 shows the momentum spectra taken at 10^{o} and 20^{o}. Resolved states in Ti^{44} are found at 0.00, 1.04, 2.10 and 2.65 MeV, and a doublet at approximately 3.56 MeV. A state is also assigned at 2.40 MeV on the basis of another experiment (see Fig. 16-5). All unlabeled states have been determined to be from the $Ti^{48}(p,t)Ti^{46}$ reaction by comparing the spectra taken with targets (1) and (2) which contain different amounts of Ti^{48}.

The angular distribution of the ground state transition is shown in Fig. 16-2 together with the DWBA prediction for picking up a pair of 1f 7/2 neutrons coupled to angular momentum, L=0. The theoretical curve is approximately 3^{o} out of phase with the data. This should not necessarily be taken as an indication of s-d or p components in the Ti^{46} ground state because changes in the triton optical parameters will also affect the phase. Fig. 16-3 shows the angular distribution of the state at 1.04 MeV which is assigned $J^{\pi}=2^{+}$, although we have not yet been able to fit the state despite using several admixtures of s-d and/or p together with f 7/2 neutrons coupled to angular momentum, L=2. On the other hand, the

state at 2.65 MeV (Fig. 16-4) is fit nicely with the transfer of two 1f 7/2 neutrons coupled to angular momentum, L=2 and is therefore assigned $J^{\pi}=2^{+}$. Thus the second 2^{+}(2.65 MeV) in Ti^{44} seems to be "pure" in the sense of being fit by transferring pairs from a pure (1f 7/2) configuration whereas the first 2^{+}(1.04 MeV) has to be made up of a mixture of configurations. Another possibility is that the first 2^{+} state is being excited by a combination of a one-step transfer process and a two-step inelastic and transfer excitation. The second 2^{+} state is also approximately 30% stronger than the first 2^{+} state and is at considerably lower energy than predicted by either pure f 7/2 calculations[4] (solid lines in middle of Fig. 16-5) or by f 7/2 - p 3/2 calculations[5] (dashed lines in middle of Fig. 16-5). In addition to the $Ti^{46}(p,t)Ti^{44}$ level diagram, Fig. 16-5 also shows results from several other research groups who have done $Ca^{40}(\alpha,\gamma)Ti^{44}$.

Work is continuing on fitting the 1.04 state and resolving the phase problem of the ground state.

$Cr^{50}(p,t)Cr^{48}$: Figs. 16-6 and 16-7 show the momentum spectra of this reaction at 10^{o}, 20^{o}, and 25^{o} (where the contaminant state is away from the first excited state). Resolved states in Cr^{48} are found at 0.00, 0.67, 1.63 (doublet), 3.15 (doublet) and 3.54 MeV (doublet).

The angular distribution of the ground state transition is shown in Fig. 16-8 together with the DWBA prediction for transferring two (1f 7/2) neutrons coupled to angular momentum, L=0. As in the case of the $Ti^{46}(p,t)Ti^{44}$ ground state, work must be done to remove the approximately 3^{o} phase difference between experiment and prediction. Fig. 16-9 shows the angular distribution of the first excited state at 0.67 MeV. The line drawn through the points has no theoretical significance. We have not yet been

able to fit this state with any degree of success, but feel that more configuration mixing is worth trying. It is worth noting that this state (assigned $J^{\pi}=2^{+}$) is the lowest first excited state of the even-even nuclei in the 1f 7/2 shell. The doublet at 1.63 MeV has been assigned as a mixture of 0^{+} and 4^{+} on the basis of its angular distribution in Fig. 16-10. Note that this group is very weak; about 2% of the ground state.

Fig. 16-11 summarizes what we know about the Cr^{48} system. The other experiment referred to is $Ti^{46}(He^{3},n)Cr^{48}$[6] which shows a state at the right energy (2.37 MeV) for the existence of a ground state rotational band. We did not see any state at that excitation energy and would put the upper limit of its strength at 1/10 of the 1.63 MeV group or, equivalently, 1/500 of the ground state.

References

1. B.F. Bayman, University of Minnesota, private communication.
2. Fred Becchetti, Jr., Phys. Rev. (in press).
3. E.R. Flynn, et al, LASL preprint = LA-DC-10367.
4. J.D. McCullen, B.F. Bayman, and L. Zamick, Phys. Rev. 134, B515 (1964).
5. J.B. McGrory and K.H. Bhatt, BAPS 14, 605 (1969).
6. R.G. Miller and R.W. Kavanagh, Nuc. Phys. A94, 261 (1967).

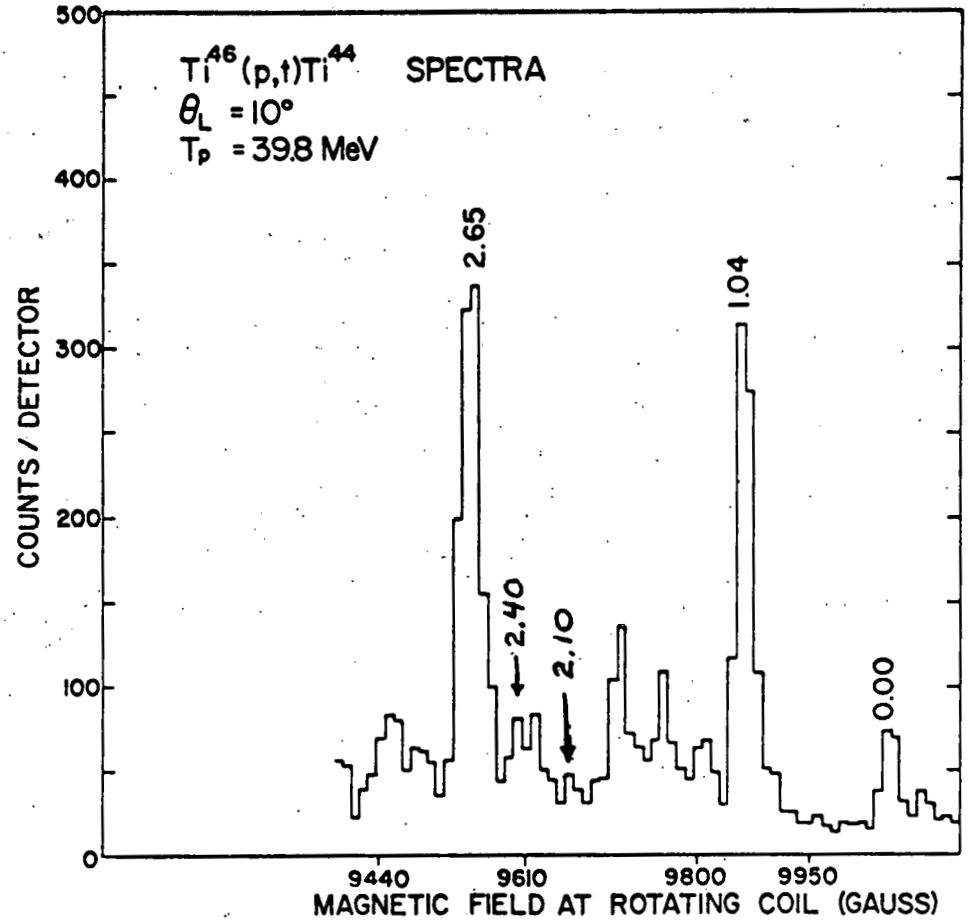
$Ti^{46}(p,t)Ti^{44}$ SPECTRA
θ_L = 10°
T_p = 39.8 MeV
COUNTS / DETECTOR
2.65
1.04
2.40
2.10
0.00
9440
9610
9800
9950
MAGNETIC FIELD AT ROTATING COIL (GAUSS)

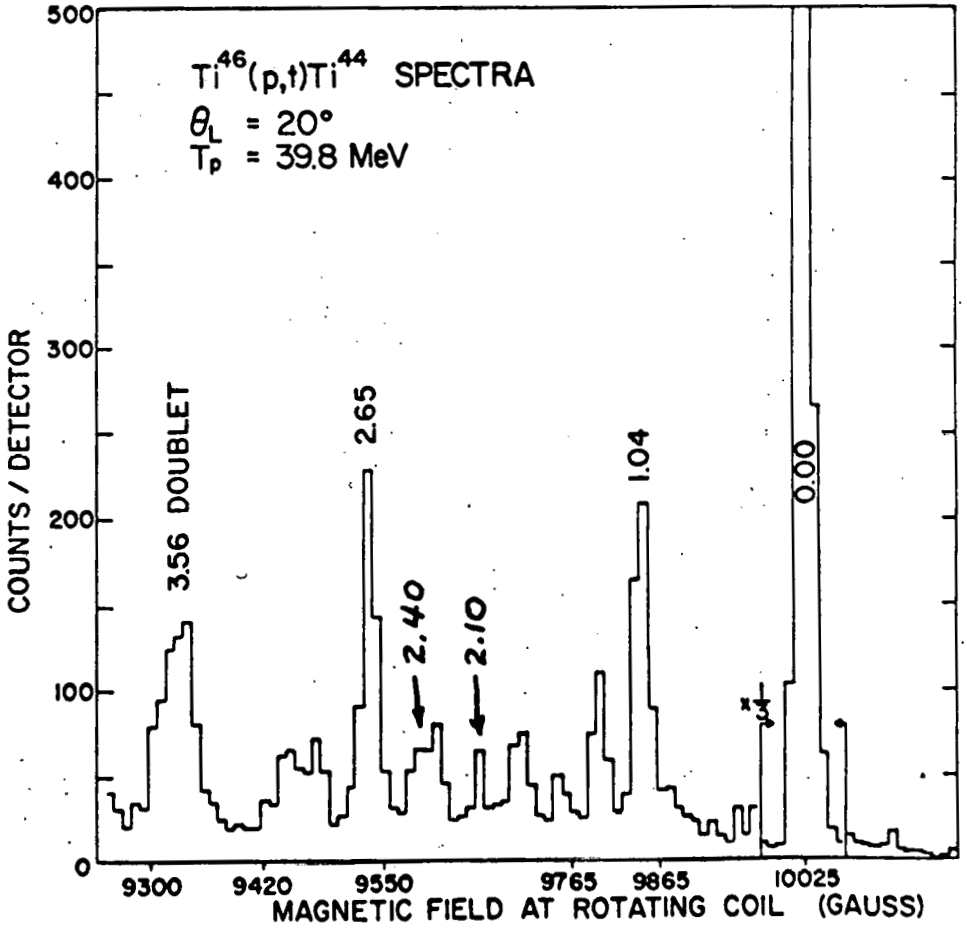
$Ti^{46}(p,t)Ti^{44}$ SPECTRA
θ_L = 20°
T_p = 39.8 MeV
COUNTS / DETECTOR
3.56 DOUBLET
2.65
2.40
2.10
1.04
0.00
9300
9420
9550
9765
9865
10025
MAGNETIC FIELD AT ROTATING COIL (GAUSS)

Fig.16-1

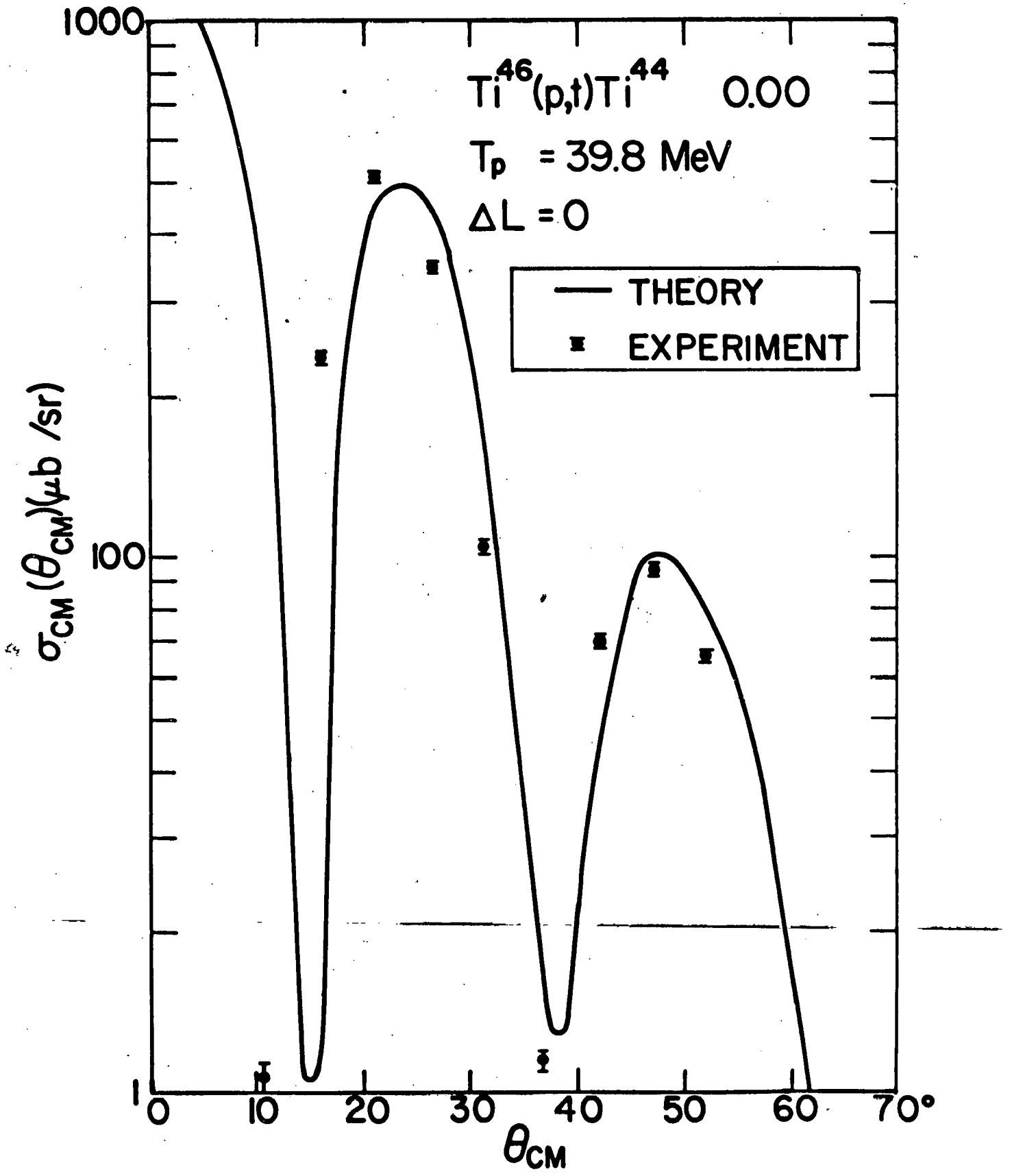
1000
100
1
$Ti^{46}(p,t)Ti^{44}$ 0.00
T_p = 39.8 MeV
ΔL = 0
THEORY
EXPERIMENT
$\sigma_{CM}(\theta_{CM})(\mu b/sr)$
0
10
20
30
40
50
60
70°
θ_{CM}

Fig. 16-2

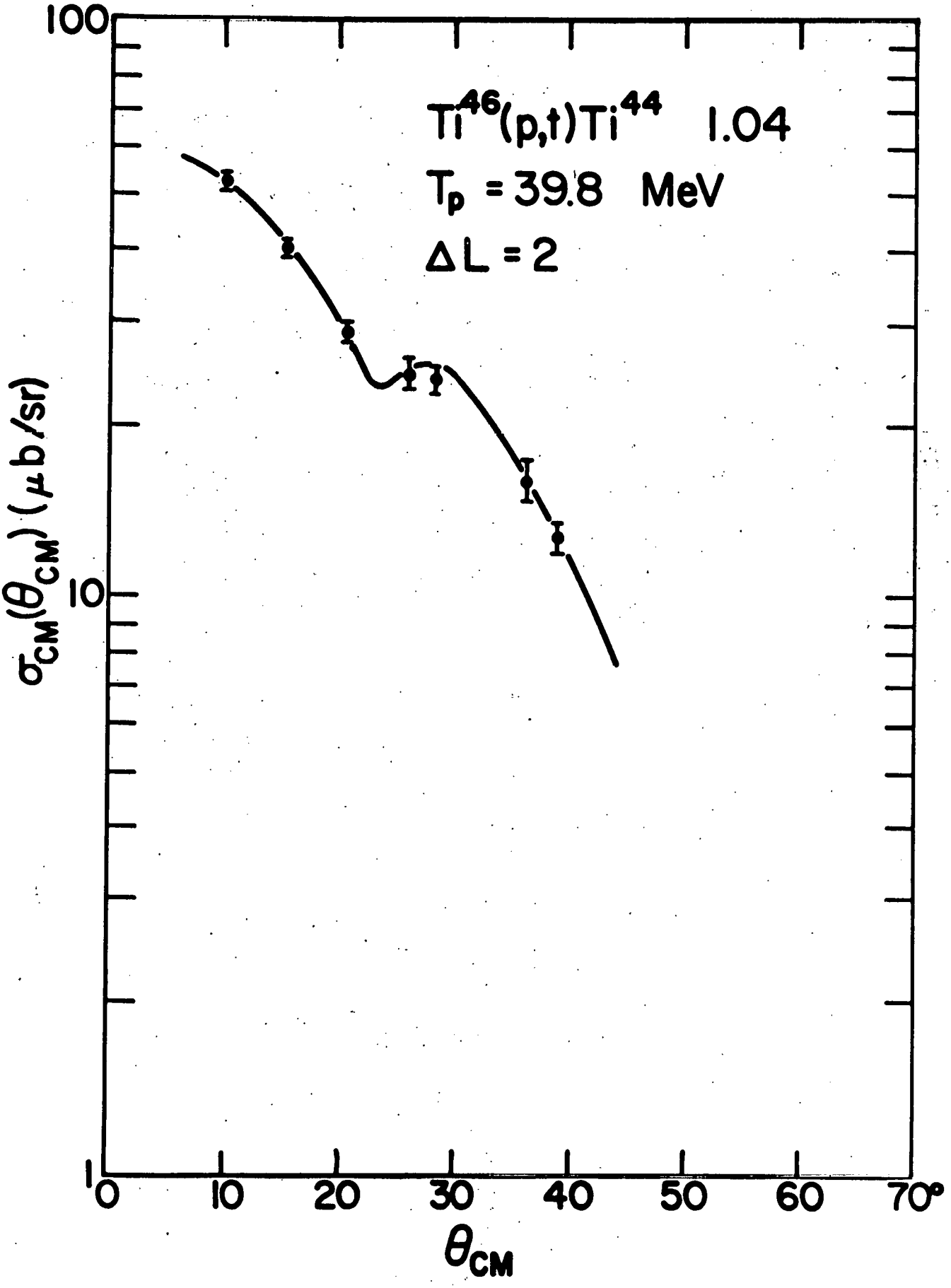
100
10
1
$Ti^{46}(p,t)Ti^{44}$ 1.04
T_p = 39.8 MeV
ΔL = 2
$\sigma_{CM}(\theta_{CM})$ (μb/sr)
0
10
20
30
40
50
60
70°
θ_{CM}

Fig. 16-3

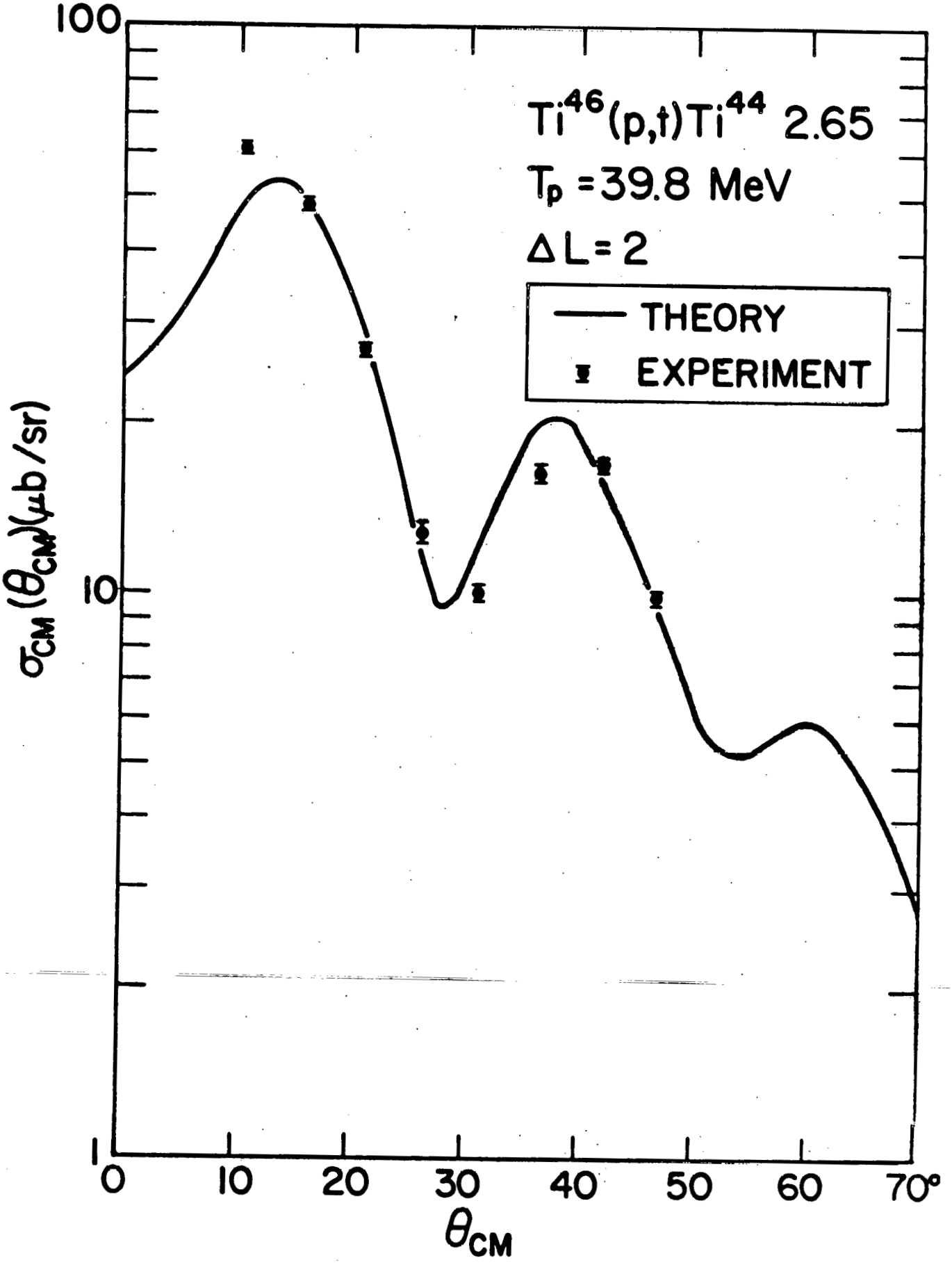
100
10
1
$\sigma_{CM}(\theta_{CM})(\mu b/sr)$
$Ti^{46}(p,t)Ti^{44}$ 2.65
T_p = 39.8 MeV
$\Delta L = 2$
THEORY
EXPERIMENT
0
10
20
30
40
50
60
70°
θ_{CM}

Fig. 16-4

LEVELS IN $^{44}_{22}Ti_{22}$

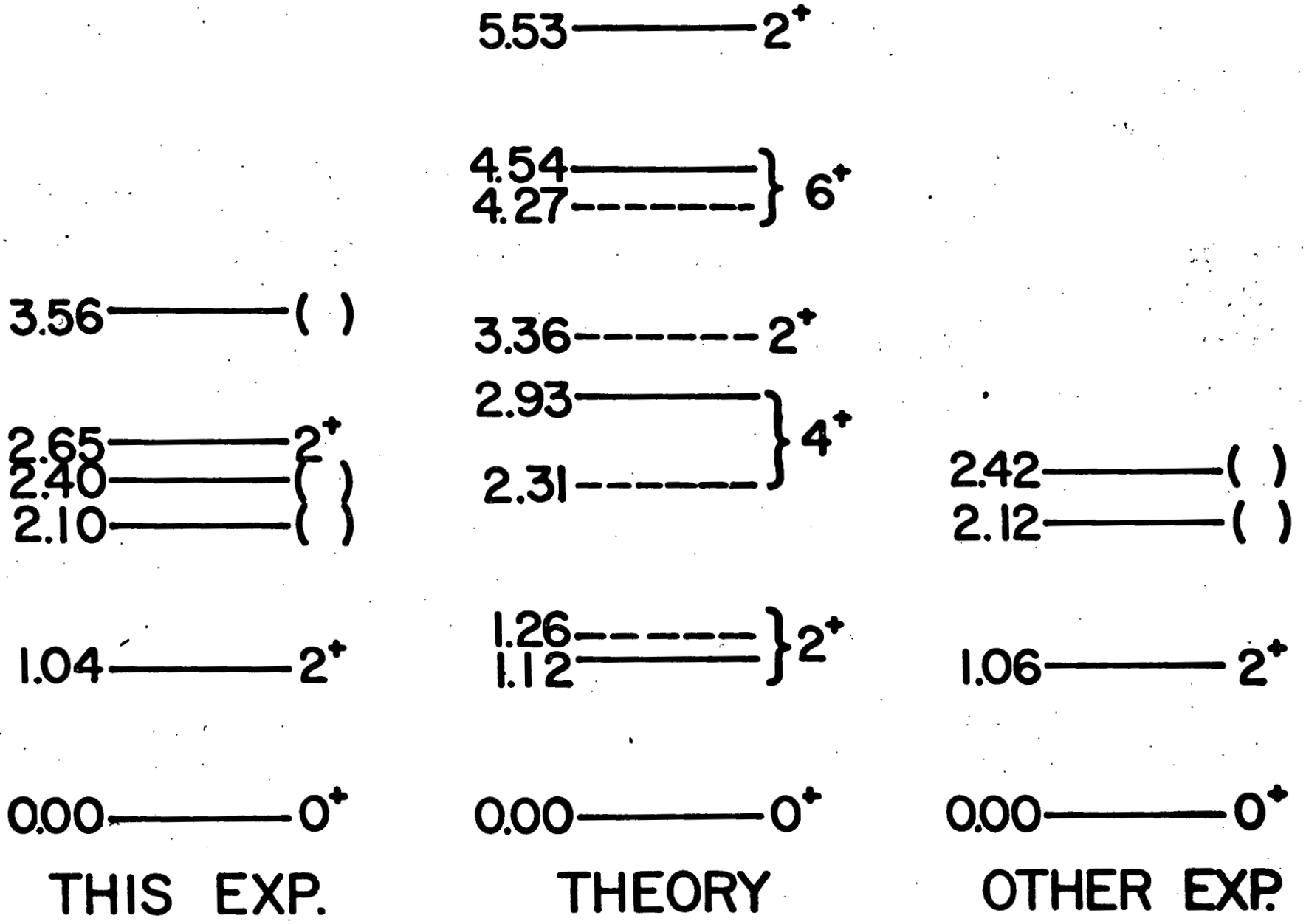

Fig. 16-5

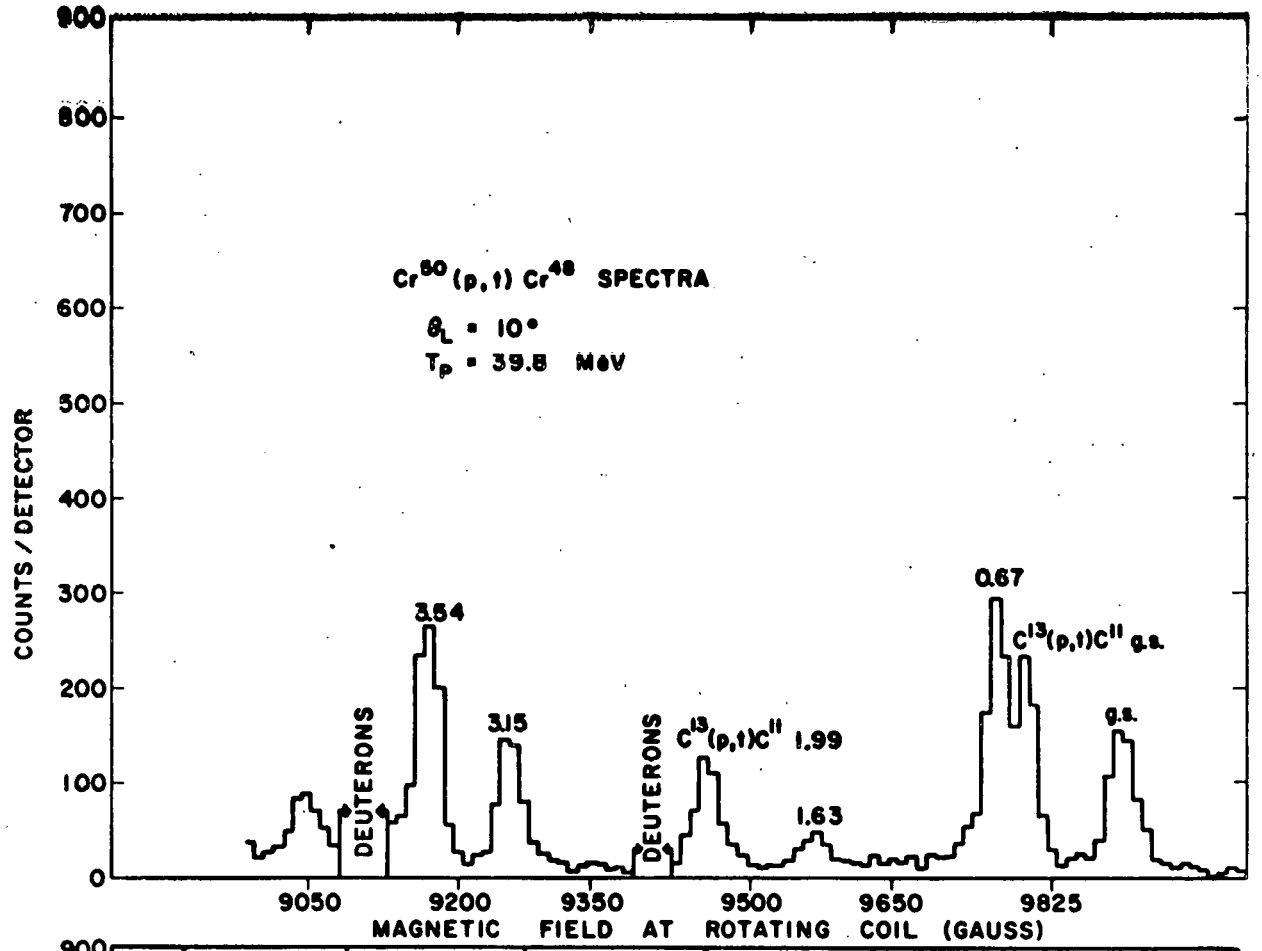
$Cr^{50}(p,t)\,Cr^{48}$ SPECTRA
θ_L = 10°
T_p = 39.8 MeV
COUNTS / DETECTOR
DEUTERONS
3.54
3.15
$C^{13}(p,t)C^{11}$ 1.99
1.63
0.67
$C^{13}(p,t)C^{11}$ g.s.
g.s.
9050
9200
9350
9500
9650
9825
MAGNETIC FIELD AT ROTATING COIL (GAUSS)

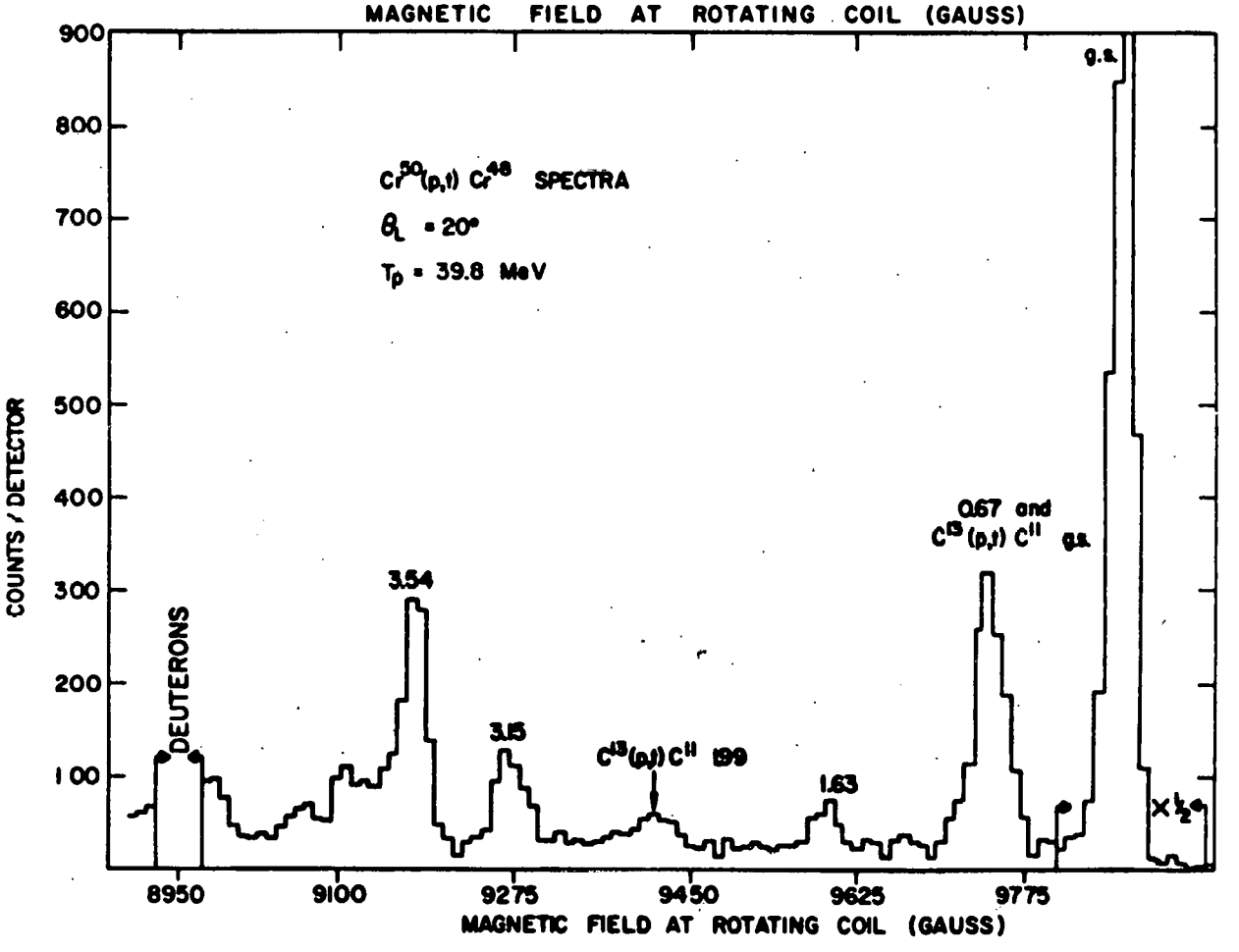
$Cr^{50}(p,t)\,Cr^{48}$ SPECTRA
θ_L = 20°
T_p = 39.8 MeV
COUNTS / DETECTOR
DEUTERONS
3.54
3.15
$C^{13}(p,t)C^{11}$ 1.99
1.63
0.67 and
$C^{13}(p,t)\,C^{11}$ g.s.
g.s.
$\times\frac{1}{2}$
8950
9100
9275
9450
9625
9775
MAGNETIC FIELD AT ROTATING COIL (GAUSS)

Fig. 16-6

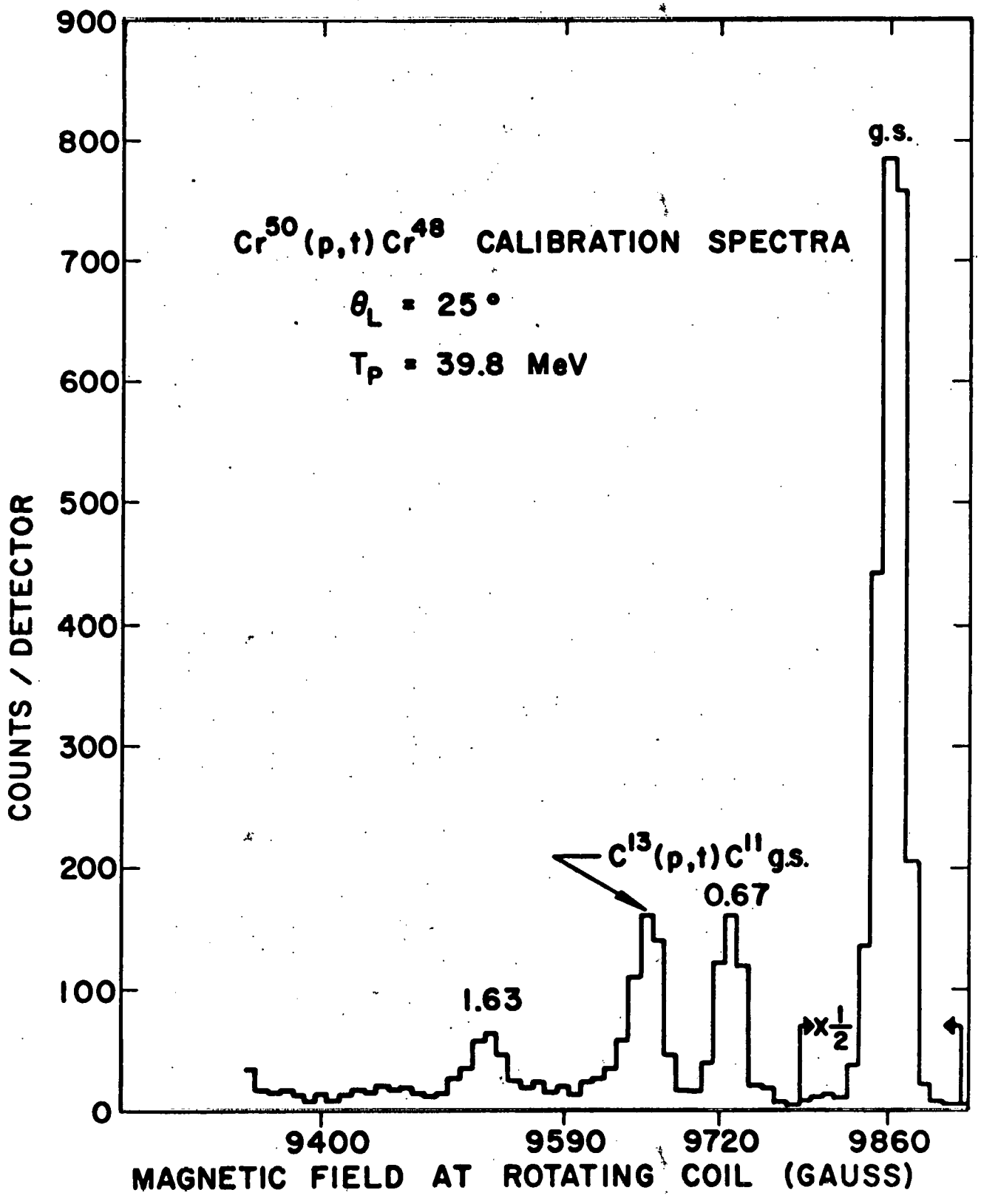
900
800
700
600
500
400
300
200
100
0
COUNTS / DETECTOR
Cr50(p,t)Cr48 CALIBRATION SPECTRA
θL = 25°
TP = 39.8 MeV
g.s.
C13(p,t)C11 g.s.
0.67
1.63
x1/2
9400
9590
9720
9860
MAGNETIC FIELD AT ROTATING COIL (GAUSS)

Fig. 16-7

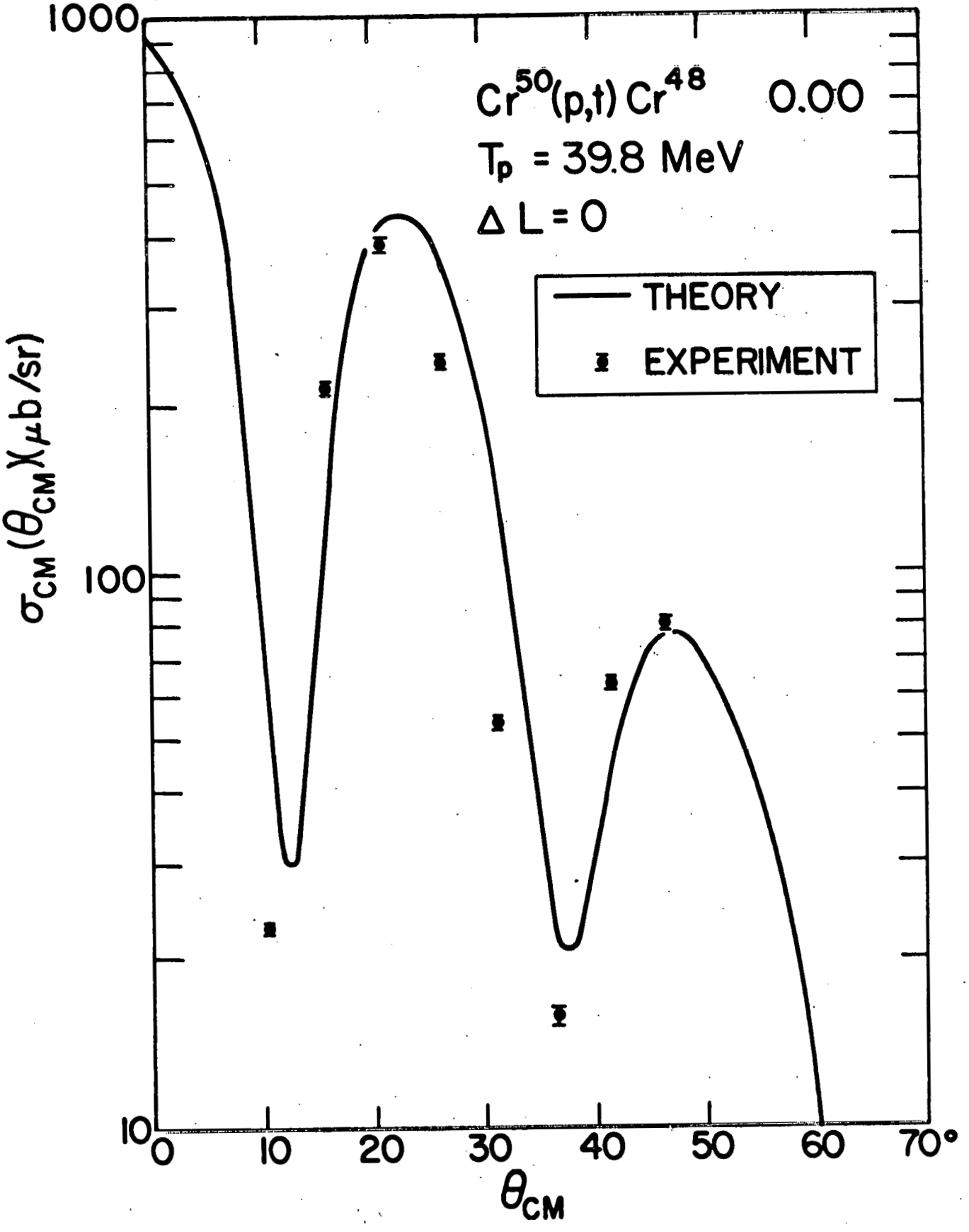
1000
100
10
$Cr^{50}(p,t)\,Cr^{48}$ 0.00
T_p = 39.8 MeV
Δ L = 0
THEORY
EXPERIMENT
$\sigma_{CM}(\theta_{CM})(\mu b/sr)$
0
10
20
30
40
50
60
70°
θ_{CM}

Fig. 16-8

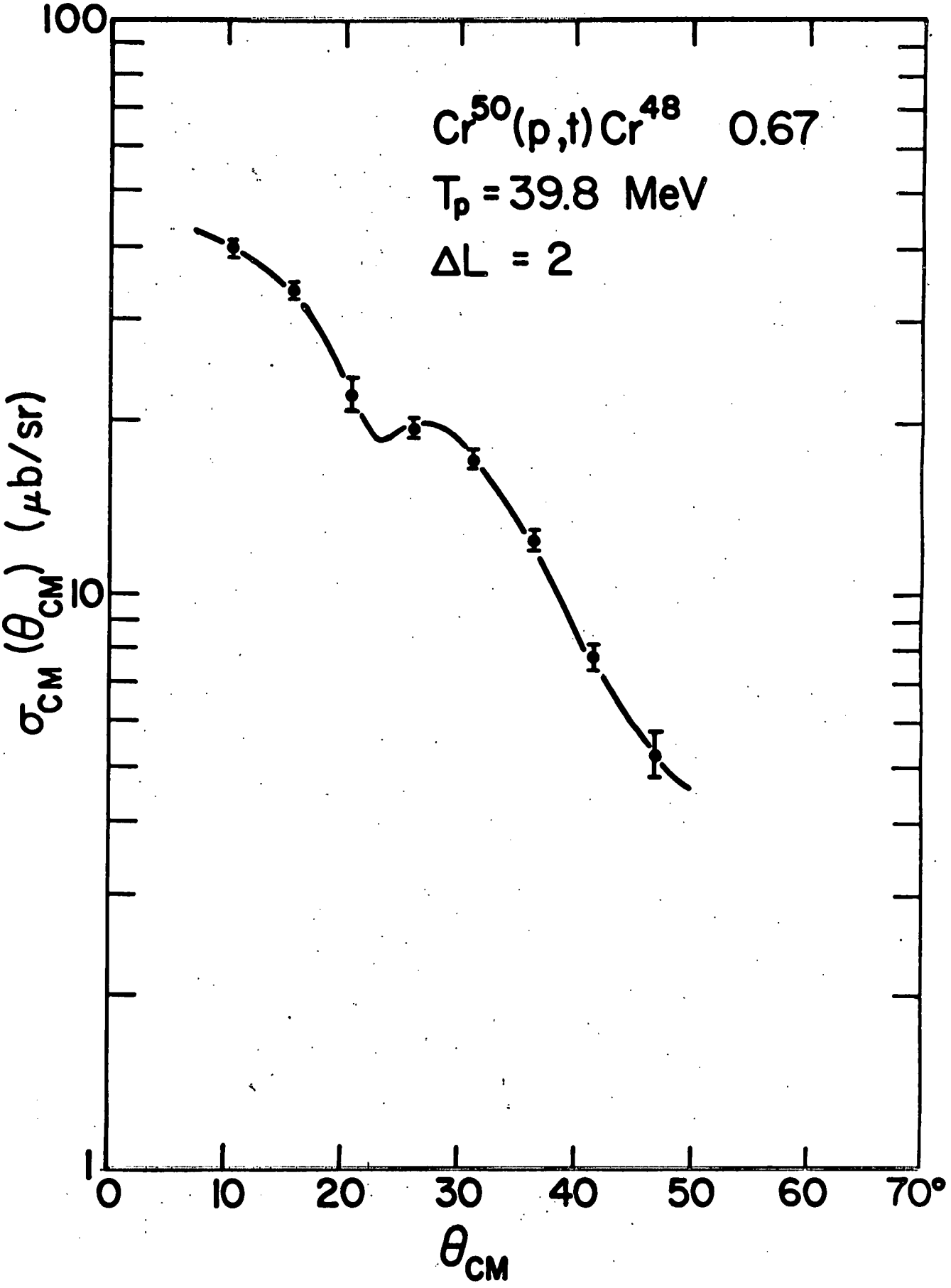
100
10
1
$Cr^{50}(p,t)Cr^{48}$ 0.67
T_p = 39.8 MeV
ΔL = 2
$\sigma_{CM}(\theta_{CM})$ (μb/sr)
0
10
20
30
40
50
60
70°
θ_{CM}

Fig. 16-9

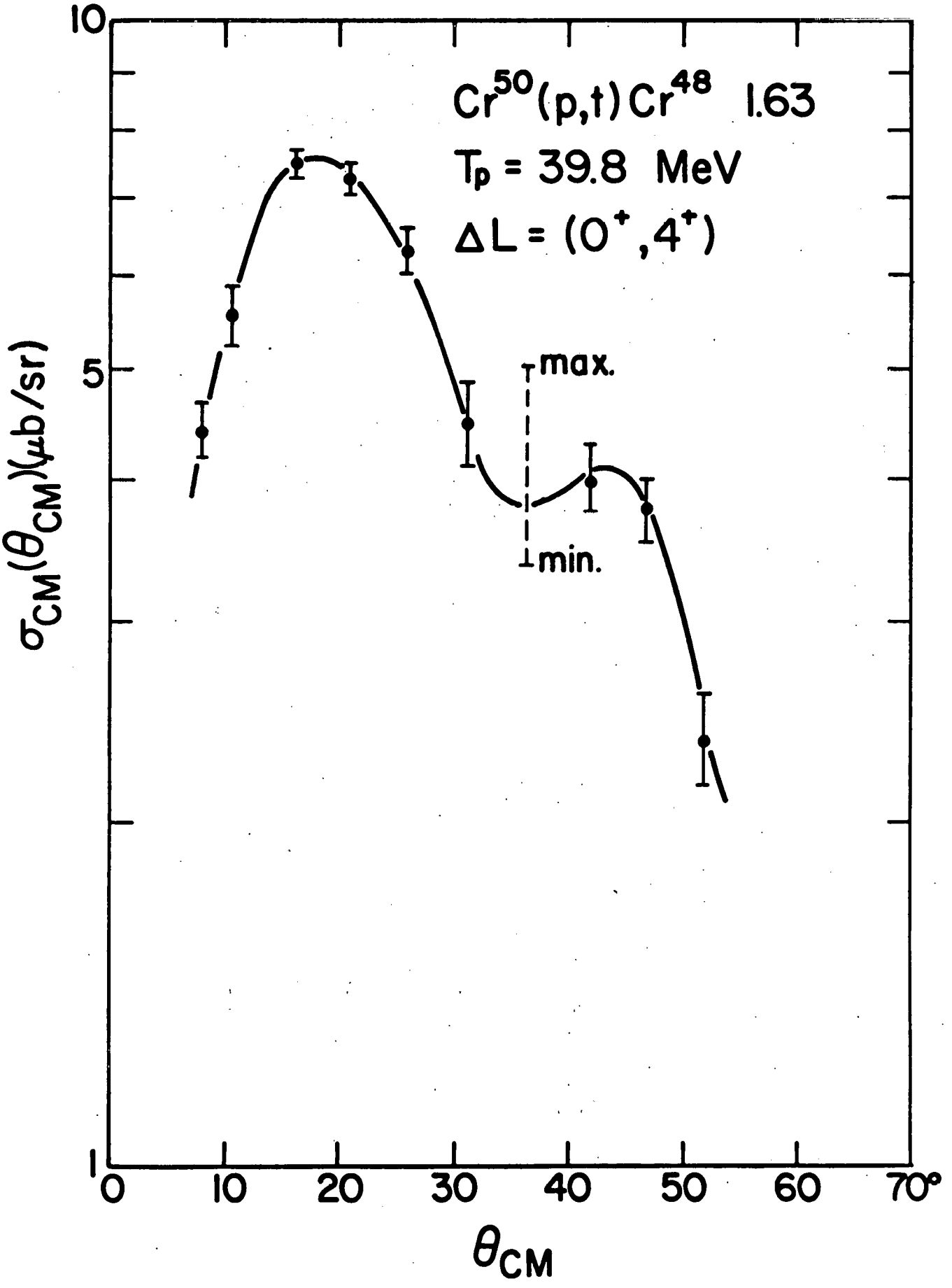
$Cr^{50}(p,t)Cr^{48}$ 1.63
T_p = 39.8 MeV
$\Delta L = (0^+, 4^+)$
max.
min.
$\sigma_{CM}(\theta_{CM})(\mu b/sr)$
10
5
1
0
10
20
30
40
50
60
70°
θ_{CM}

Fig. 16-10

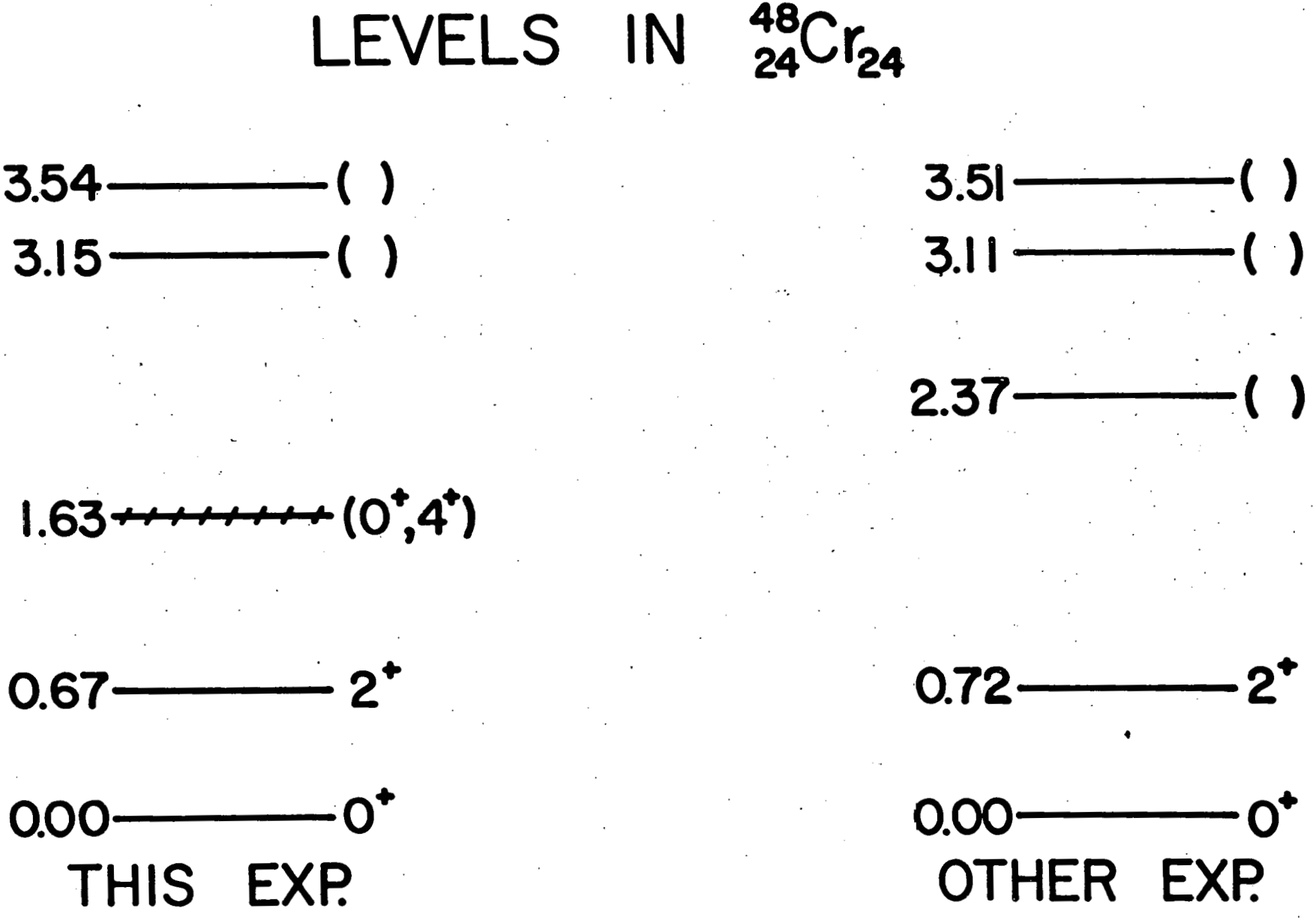
LEVELS IN $^{48}_{24}Cr_{24}$
3.54 ( )
3.15 ( )
1.63 (0⁺,4⁺)
0.67 2⁺
0.00 0⁺
THIS EXP.
3.51 ( )
3.11 ( )
2.37 ( )
0.72 2⁺
0.00 0⁺
OTHER EXP.

Fig. 16-11

17. Lifetime of the 40-keV Doublet in Ti^{45}

H. Ohnuma and A. A. Padmanabham

Recently two low-lying states, one at 37 keV and another at 40 keV, were found[1] in Ti^{45}. A comparison with a calculation[2] suggests that these are $3/2^-$ and $5/2^-$ states. The half-life of the 37-keV state was estimated to be between 1 μsec and 0.5 msec by Jett et al.[1] With our pulsed beam technique, it might be feasible to measure the lifetime or obtain a better limit for it, if one member of the doublet is $3/2^-$ and decays to the ground state by an E2 transition and if this transition is not enhanced.

The $Sc^{45}(p,n)Ti^{45}$ reaction was used to excite the doublet. The incident beam was a 10-MeV proton beam, pulsed to 140 μsec bursts with 600 μsec intervals. A 5 cc Ge(Li) detector was placed at 90^o to the beam. 37- and 40-keV gamma-rays were observed in the "beam-on" spectrum. They were not seen in the delayed spectrum taken during the 50 to 110 μsec interval after the beam bursts. We estimate the upper limit of the half-life of the doublet at about 25 μsec.

References

1. J.H. Jett, G.D. Jones, and R.A. Ristinen, Phys. Lett. 28B, 111 (1968).

2. F.B. Malik and W. Scholz, Phys. Rev. 150, 919 (1966).

18. States in V^{50} Studied with the (d,t) Reaction

A. Sourkes, H. Ohnuma and N. M. Hintz

States in V^{50} were studied by the V^{51}(d,t) reaction using 19.5 MeV deuterons incident from the Williams Laboratory Tandem Van de Graaff, a split pole magnetic spectrometer, and position sensitive detectors. The target was natural vanadium metal evaporated onto a thin carbon foil.

Fig. 18-1shows a typical triton spectrum with the states numerically labelled, where C is a contaminant peak. A previously reported triplet[1] at about 350 keV is clearly resolved. Fig. 18-2 exhibits a DWBA fit to the ground state angular distribution. The solid line is the sum of the dotted curves, consisting predominantly of ℓ=3 with a 2% ℓ=1 contribution.

Table 18-1shows the preliminary level energies and their spectroscopic factors. The energies are all referred to the ground state and have a 5 keV uncertainty. It seems that most ℓ=3 strength is exhausted by 1.3 MeV. A weak ℓ=1 component was observed indicating that there is a mixture of p-neutrons in the ground state of V^{51} as seen in other N=28 nuclei.[2,3]

References

1. J. B. Ball and R. F. Sweet, Phys. Rev. 140, B904 (1965).

2. E. Kashy and T. W. Conlon, Phys. Rev. 135, B389 (1964).

3. R. J. Peterson, Phys. Rev. 170, 1003 (1968).

TRITON SPECTRUM AT 15 DEGREES

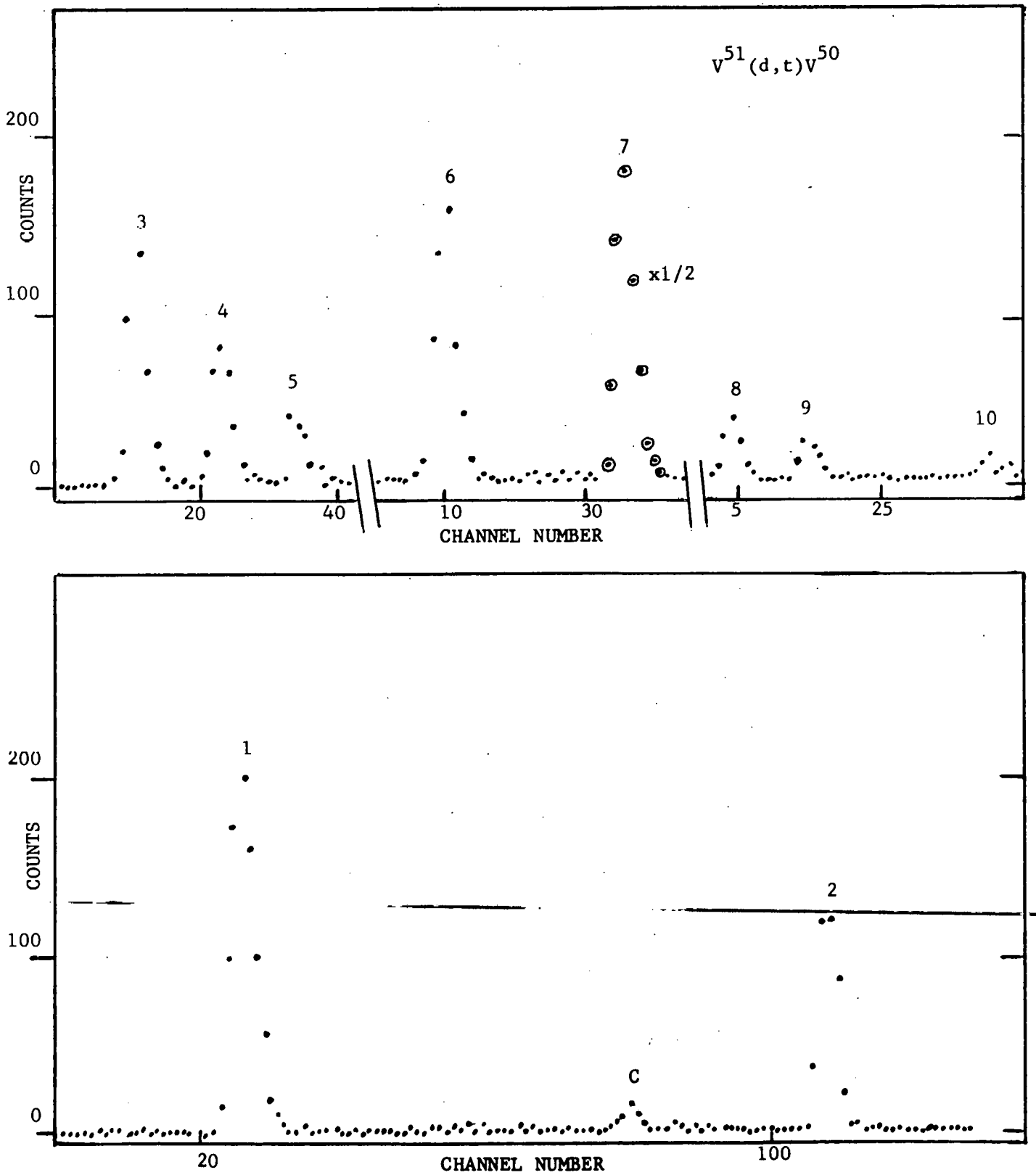

Fig. 18-1

DWBA FIT TO G.S. ANGULAR DISTRIBUTION

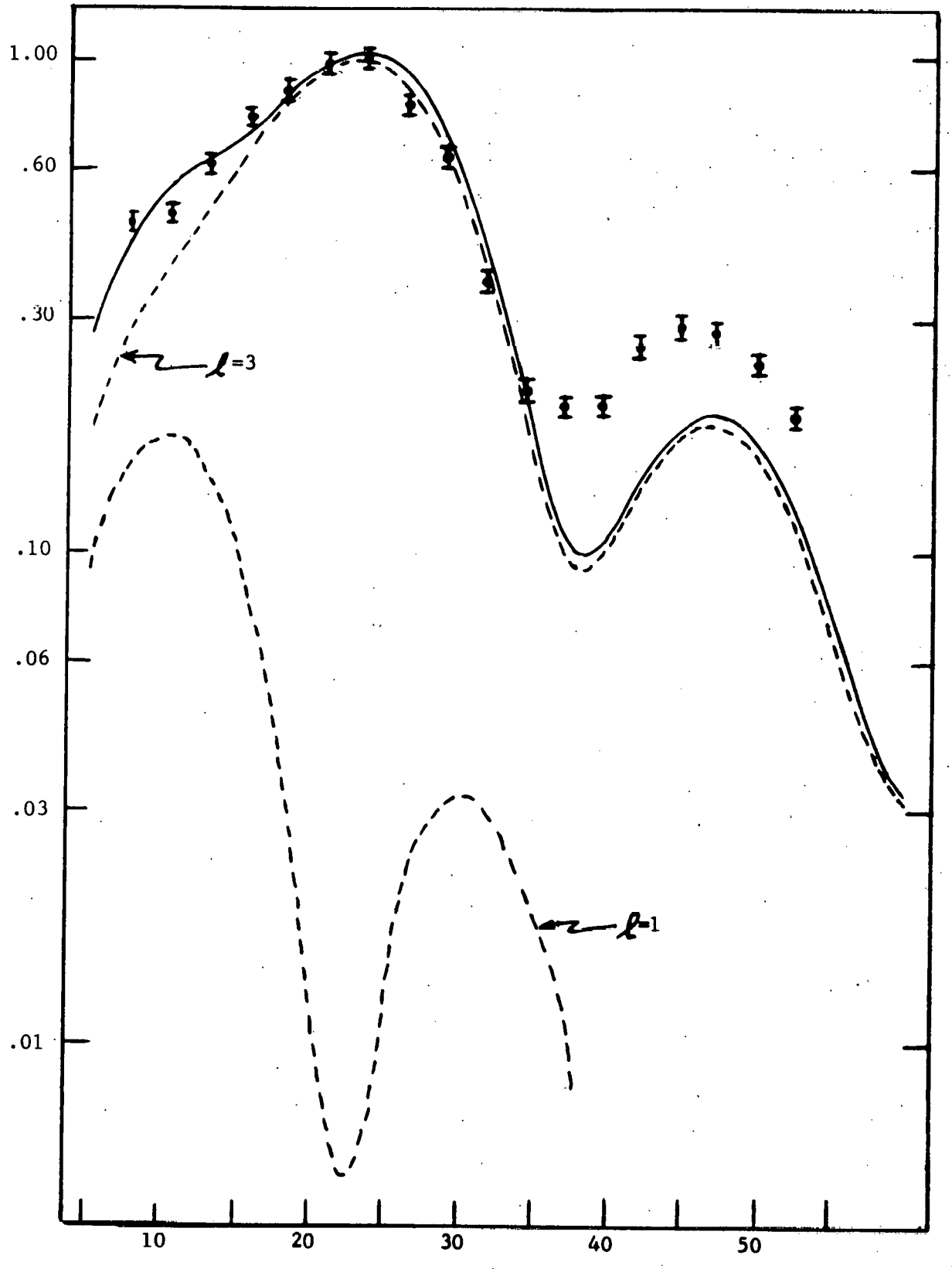

Fig. 18-2

TABLE 18-1

Energy levels and Spectroscopic Factors Seen in the V^{51}(d,t) Reaction

STATE NUMBER	E_x keV	c^2S $\ell=3$	c^2S $\ell=1$
1	0	1.57	.02
2	228±5	.66	.02
3	321	.99	.03
4	357	.56	.01
5	387	.32	.01
6	838	1.01	.04
7	911	2.67	.07
8	1301	.33	.003
9	1330	.23	.002
10	1402	-	.01

19. States in V^{50} Studied with the (He^3,d) Reaction

A. M. Sourkes, H. Ohnuma and N. M. Hintz

Using a 22 MeV He^{3++} beam from the Williams Laboratory Tandem Van de Graaff incident on a self-supporting 150 μgm Ti^{49} target of 77.2% enrichment and allowing the magnetically analyzed reaction products to fall on photographic plates covered with 45 mil polyethylene foil, states in V^{50} were observed up to about 6 MeV excitation, angular distributions being measured from 7-1/2° to 50° lab in 2-1/2° steps. Data are being analyzed.

20. A Study of the (He^3,t) Reaction on Ni^{58} and Ni^{60}

F. D. Becchetti, Jr and G. W. Greenlees

Angular distributions for the $0^+ \rightarrow 0^+$ IAS (isobaric analog state) and $0^+ \rightarrow 2^+$ IAS* (excited isobaric analog state) transitions for Ni^{58} (He^3,t)Cu^{58} and Ni^{60}(He^3,t)Cu^{60} as well as the $0^+ \rightarrow 1^+$ ground state transition in Cu^{58} have been measured at 24.6 MeV incident He^3 energy. The split-pole magnetic spectrometer was used in conjunction with an array of position-sensitive detectors and suitable monitor counters. Natural nickel foils were used to allow an accurate determination of the isotopic shift in the cross sections. The experimental results are shown in Fig. 20-1 .

The DWBA curve shown is a prediction for the $\Delta L=0$, $\Delta T=0$ IAS transition to Cu^{58} using a microscopic form factor calculated for a He^3 and triton with $\langle r^2 \rangle = 3F^2$, an isospin dependent nucleon-nucleon force with $\langle r^2 \rangle = 3F^2$, and a neutron excess configuration composed of a suitable mixture of $2p_{3/2}$ and $1f_{5/2}$ particles. The normalization corresponds to a volume integral of 180 MeV-F^3 for the isospin force. This is a value similar to those used in the (p,n) analysis of Greenlees et al[1] and the values obtained from the optical model analysis of nucleon-nucleus elastic scattering.[2] A preliminary set of general He^3 and triton optical model parameters were used (see Section 41).

The curve labeled "a" is a sum of the measured $\Delta L=0$ and $\Delta L=2$ angular distributions taken so as to give a reasonable fit to the $0^+ \rightarrow 1^+$

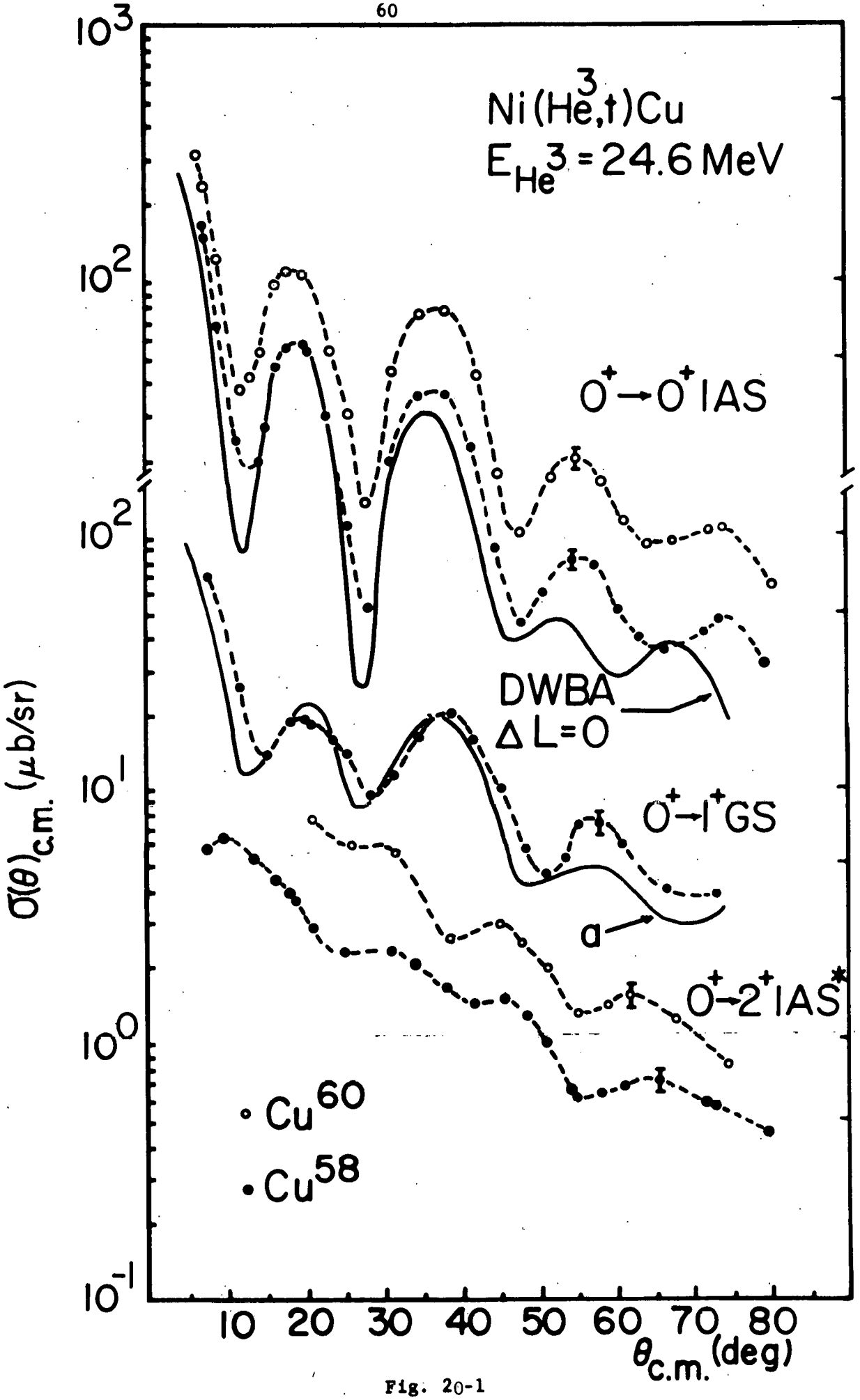
Ni(He3,t)Cu
E He3 = 24.6 MeV
0+ → 0+ IAS
DWBA
ΔL=0
0+ → 1+ GS
a
0+ → 2+ IAS*
Cu60
Cu58
σ(θ)c.m. (μb/sr)
θc.m. (deg)
10 20 30 40 50 60 70 80
10^3
10^2
10^2
10^1
10^0
10^-1

Fig. 20-1

cross section. This suggests that the $0^+ \rightarrow 1^+$ transition is primarily an incoherent sum of $\Delta L=0$ and 2.

More detailed DWBA calculations are in progress.

References

1. G. W. Greenlees, et al, Nucl. Phys. A127, 368 (1969)

2. F. D. Becchetti, Jr. and G.W. Greenlees, Phys. Rev, in press.

---

21. Analysis of Inelastic Proton Scattering from Ni^{58} and Ni^{60}

N. Lingappa and G. W. Greenlees

The coupled channels analysis of inelastic proton scattering at 40 MeV from Ni^{58} and Ni^{60} is described in the Ph.D. thesis of N. Lingappa. A paper on this topic is in preparation.

---

22. Review Article on $f_{7/2}$ Shell

N. M. Hintz

In collaboration with Ben Bayman (Minnesota), John McCullen (Arizona), and Larry Zamick (Rutgers), a review article is being prepared summarizing the current status of experiment and theory for nuclei in the $1f_{7/2}$ shell (Ca^{40} to Ni^{56}, inclusive). Attempts will be made to make critical comparisons between theory and experiment. It is already apparent that despite the large number of experiments on $f_{7/2}$ nuclei there exist many gaps in the data, especially electromagnetic transition probabilities, neutron pickup and proton transfer (resolution $\sim$ 25 KeV or better) and two particle transfer. Any recent or unpublished data would be welcome.

---

23. Gamma Rays from (α,xn) Reactions on f 7/2 Nuclei

A. R. Barnett, N. M. Hintz, H. Ohnuma and P. Ruenes

We have measured the 90° gamma ray yield with a 5cc Ge(Li) detector following (α,xn) reactions on several f 7/2-shell nuclei. Gamma rays of energies between 80 keV and 2 MeV were detected simultaneously using two ADC's and with an overall resolution of about 4 keV. Excitation functions were measured for alpha particle bombarding energies between 15 MeV and 30 MeV in order to help assign the origin of the numerous gamma rays seen.

Fig. 23-1 shows a partial spectrum obtained at 25 MeV from a pure ^{48}Ti 1 mg/cm^2 target. Gamma rays from the ^{48}Ti(α,2n)^{50}Cr and ^{48}Ti(α,np) ^{50}V reactions are prominent. We can also identify transitions following (α,p) and α,α') reactions. Table 23-1 lists some of the strong lines and their origins. By calibrating the system with various standard sources, including ^{56}Co(^{56}Fe(p,n) on the tandem), we obtain accuracies of ± 0.5 keV in gamma ray energies. To this order of accuracy no non-linearities can be detected in the gamma system, which comprises a TC135 preamplifier, a Canberra 1416 active filter amplifier and biased HP 5415A ADC's.

Bombardments at 25 MeV on the target nuclei ^{42}Ca and ^{46}Ti showed that the dominant reaction was (α,np) to the odd-odd nuclei ^{44}Sc and ^{48}V. We had been interested in observing states in the self-conjugate 4n nuclei ^{44}Ti and ^{48}Cr through γ decays following the (α,2n) reaction on ^{42}Ca and ^{46}Ti. Contrary to the mass-50 case the (α,2n) reaction was

weak and could not be identified. Both ^{44}Ti and ^{48}Cr have been studied[1] with the (p,t) reaction at 40 MeV.

We have used information from the ^{42}Ca(α,npγ) ^{44}Sc reaction to complement the study of ^{44}Sc by the Sc^{45}(d,t) and the Ca^{42}(α,d) reactions.[2,3] Energy differences between levels can be obtained to ± 1 keV and the existence of expected γ transitions adds weight to assignments based on transfer data or on theoretical grounds. For example, the 7^+ member of the pure f 7/2 configuration is expected[4] to lie at about 1 MeV. Strong transitions are seen in both (d,t) and (α,d) to a state at 971 ± 5 keV which is thought to be the 7^+ state.[2,3] We see a clear 697 ± 1 keV transition which we attribute to the decay of this state to the 271 ± 5 keV, 6^+ member of the f 7/2 configuration and no 971 keV γ, as expected. In a similar manner the decays in ^{50}V can be related to the spectroscopic information obtained from the ^{49}Ti(^{3}He,d)^{50}V and ^{51}V(d,t)^{50}V reactions.[5,6]

Further useful γ-ray data can be obtained using the resources of the tandem for the reactions (^{3}He,nγ), (p,nγ), and (p,2nγ) at suitable energies on appropriate targets.

References

1. D. Madland and N. Hintz, This report, Section 16.
2. A. Sourkes, H. Ohnuma, N. Hintz, This report, Section 13.
3. R. Cornett, H. Ohnuma, N. Hintz, This report, Section 12.
4. J.D. McCullen, B.F. Bayman, L. Zamick, Phys. Rev. 134, B515 (1964).
5. A. Sourkes, H. Ohnuma, N. Hintz, This report, Section 15.
6. A. Sourkes, H. Ohnuma, N. Hintz, This report, Section 18.

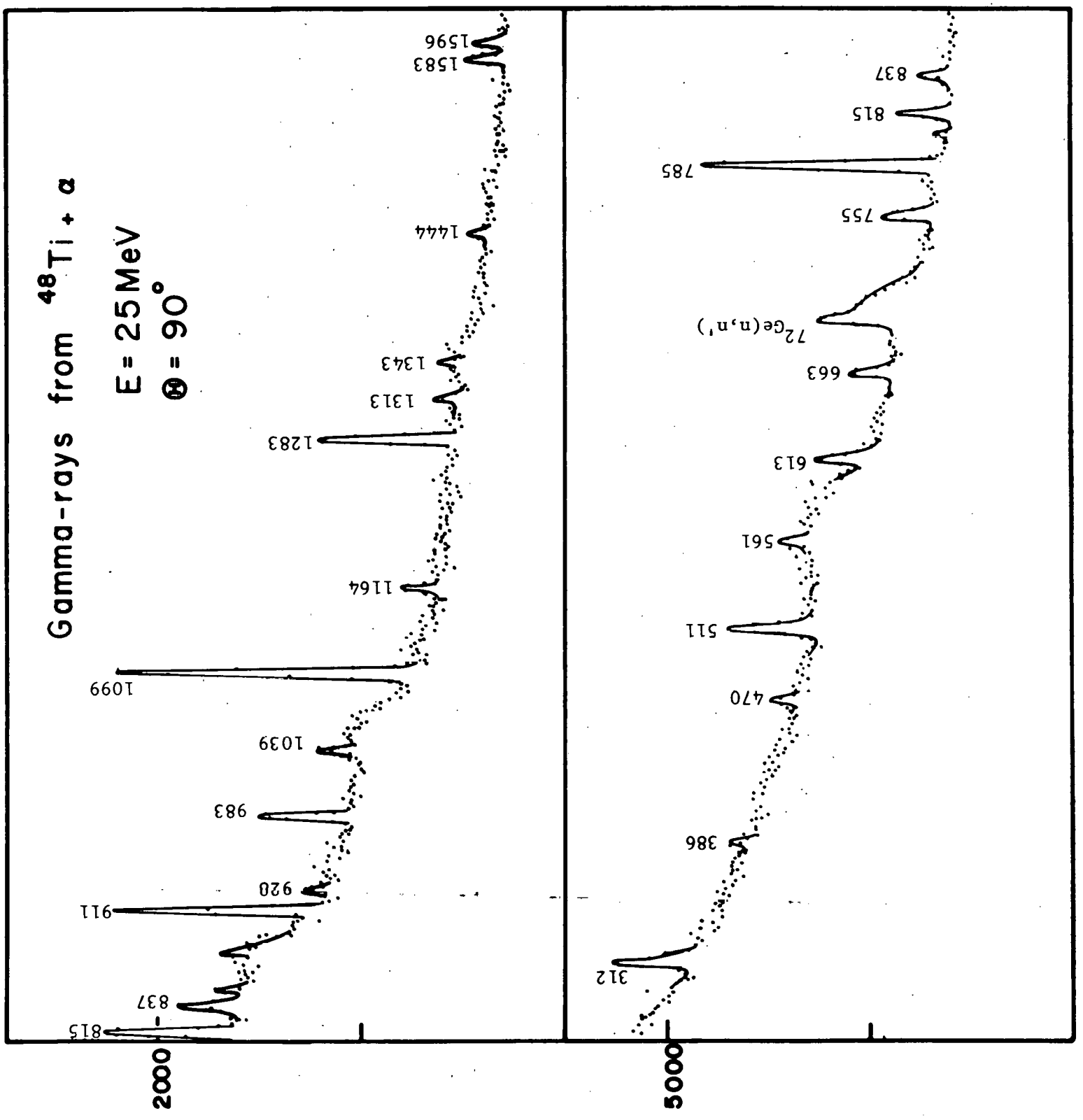
Gamma-rays from $^{48}Ti + \alpha$
E = 25MeV
⊗ = 90°
815
837
911
920
983
1039
1099
1164
1283
1313
1343
1444
1583
1596
312
386
470
511
561
613
663
$^{72}Ge(n,n')$
755
785
815
837
2000
5000

Fig. 23-1

TABLE 23-1. Some Gamma Rays Observed in $^{48}Ti+\alpha$ at 25 MeV.

γ Energy (keV)	Reaction	Levels (keV)		keV	J Values
96	$(\alpha,np)^{50}V$	319→225	=	94	(4+→5+)
162	$(\alpha,np)^{50}V$	385→225	=	160	(2+→5+)
228	$(\alpha,np)^{50}V$	225→0	=	225	(5+)→6+
317	$(\alpha,p)^{51}V$	320→0	=	320	5/2-→7/2-
511	annihilation				
783	$(\alpha,2n)^{50}Cr$	783→0	=	783	2+→0
834	$(\alpha,np)^{50}V$	833→0	=	833	?→6+
928	$(\alpha,p)^{51}V$	928→0	=	928	3/2-→7/2-
983	$(\alpha\alpha')^{48}Ti$	983→0	=	983	2+→0+
1039	$(\alpha\alpha')^{48}Ti$	3340→2295	=	1040	6+→4+
1099	$(\alpha,2n)^{50}Cr$	1880→783	=	1097	4+→2+
1283	$(\alpha,2n)^{50}Cr$	3161→1880	=	1281	6+→6+
1313	$(\alpha\alpha')^{48}Ti$	2295→983	=	1312	4+→2+

IV. SPECTROSCOPY OF DEFORMED NUCLEI

24. The (p,t) Reaction On Even Samarium Isotopes

P. Debenham and N. M. Hintz

$Sm^{152}(p,t)$

The $Sm^{152}(p,t)Sm^{150}$ reaction connects the two transitional samarium nuclei, whose ground states are mixtures of spherical and deformed components. Spherical components seem to predominate in the Sm^{150} ground state mixture, while the Sm^{152} ground state appears to be mostly deformed.

Angular distributions of tritons from the reaction at E_p = 19 MeV were analyzed with the split-pole spectrometer and recorded on nuclear track plates. The plates have been scanned over a region corresponding to excitations of up to 2.8 MeV in Sm^{150}. A typical triton spectrum was presented in the 1968 edition of the annual report.[1] As is typical of direct reactions, the L=0 angular distributions for different final 0^+ states are practically identical (see Fig. 24-1).

Fig. 24-2 shows L=2 angular distributions for several final states whose J-values are well established to be 2. The 1.194 MeV and 1.417 MeV state angular distributions are similar to each other but are markedly different from the distribution of the 0.334 MeV state. One explanation for this difference is that tritons leave the reaction with enough energy to overcome the Coulomb barrier only if the Sm^{150} nucleus is excited to less than some amount which lies between 0.334 and 1.194 MeV.

We eliminated this explanation by repeating the experiment with an additional 1 MeV of bombarding energy and observing no change in the angular distributions for these three states. This forces us to the

conclusion that the L=2 angular distributions are sensitive to the structure of the states involved. We hope to duplicate this sensitivity by performing DWBA calculations with intrinsic wave functions of the sort proposed by Kumar and Baranger[2] for transitional nuclei.

Maxwell, Reynolds and Hintz have proposed that the 1.256 MeV 0^+ state is largely deformed.[3] We have found a probable rotational band based on this state, with the 2^+ member being the 1.417 MeV 2^+ state and the 4^+ member being the 1.809 MeV state, whose J^π is unknown. The energy spacing of these states follows the J(J+1) rule closely and fits smoothly into the pattern of samarium ground state rotational bands, as Fig. 24-3 shows. We cannot determine whether the 1.809 MeV state has $J^\pi = 4^+$ until we can identify L=4 angular distributions unambiguously.

$Sm^{154}(p,t)$

Exposures have been made at E_p = 19 MeV at a number of angles for $Sm^{154}(p,t)$. The plates are currently being scanned.

References

1. P. Debenham and N.M. Hintz, Williams Laboratory of Nuclear Physics Annual Report (1968) 115.

2. Kumar and Baranger, Nucl. Phys. A122, (1968) 241-323.

3. Maxwell, Reynolds and Hintz, Phys. Rev. 151 (1966) 1000-1003.

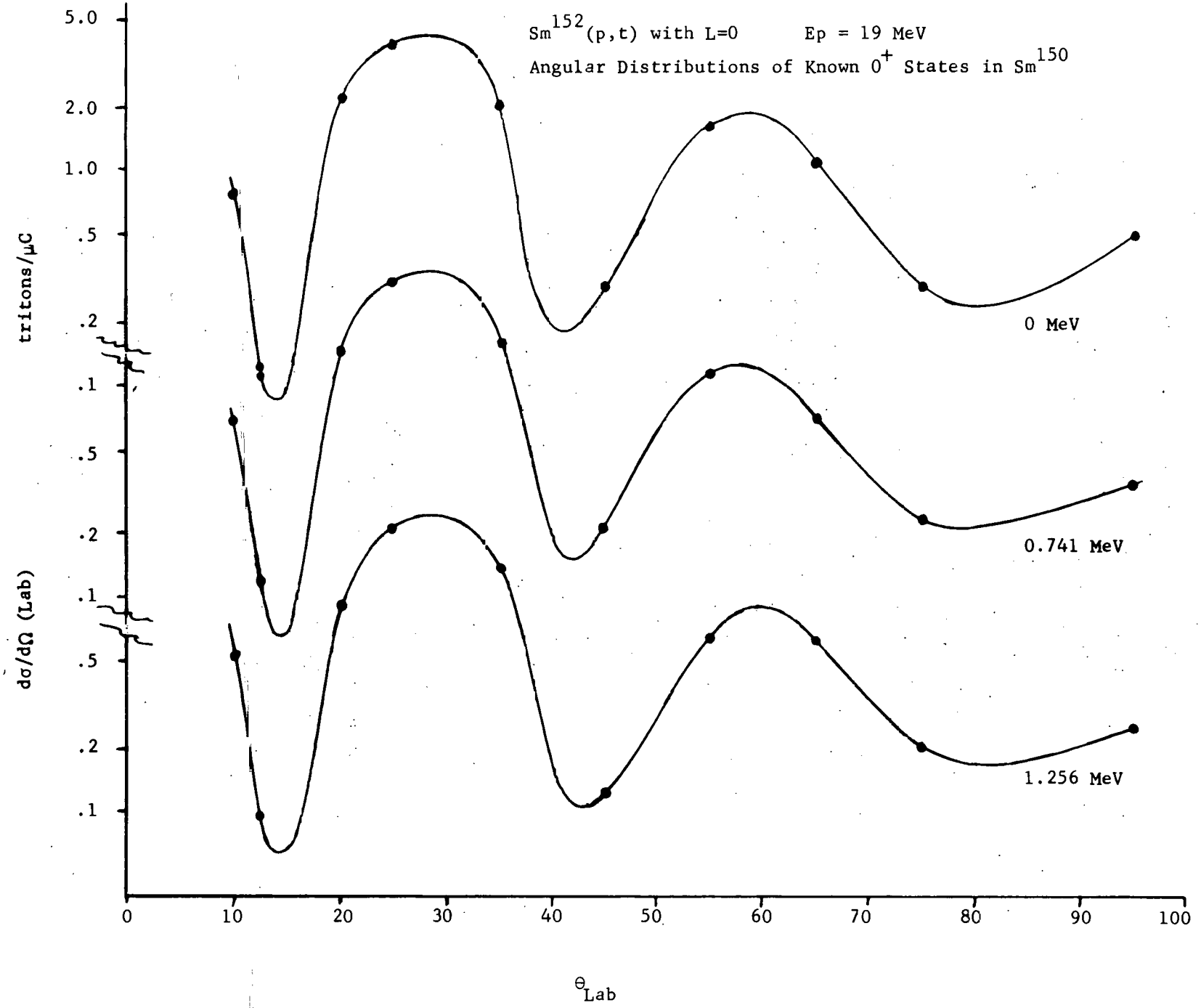
$Sm^{152}(p,t)$ with L=0 Ep = 19 MeV
Angular Distributions of Known 0^+ States in Sm^{150}
tritons/μC
dσ/dΩ (Lab)
5.0
2.0
1.0
.5
.2
.1
.5
.2
.1
.5
.2
.1
0 MeV
0.741 MeV
1.256 MeV
0
10
20
30
40
50
60
70
80
90
100
Θ_{Lab}

Fig. 24-1

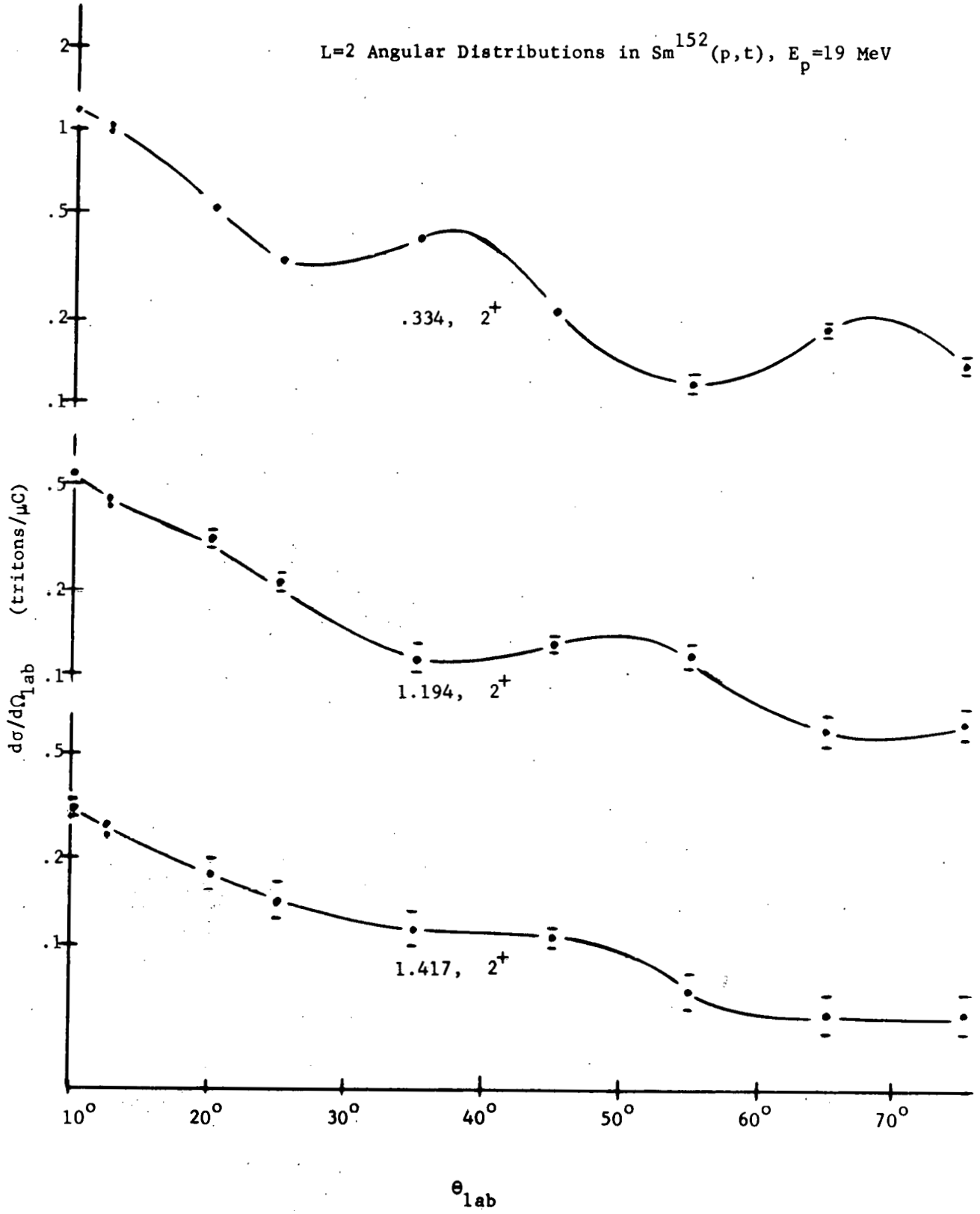
L=2 Angular Distributions in Sm152(p,t), Ep=19 MeV
.334, 2+
1.194, 2+
1.417, 2+
dσ/dΩlab (tritons/μC)
θlab
10°
20°
30°
40°
50°
60°
70°

Fig. 24-2

Energy Spacing in Samarium Rotational Bands. E_o=1.256 MeV for A=150, 0.0 MeV for all others.

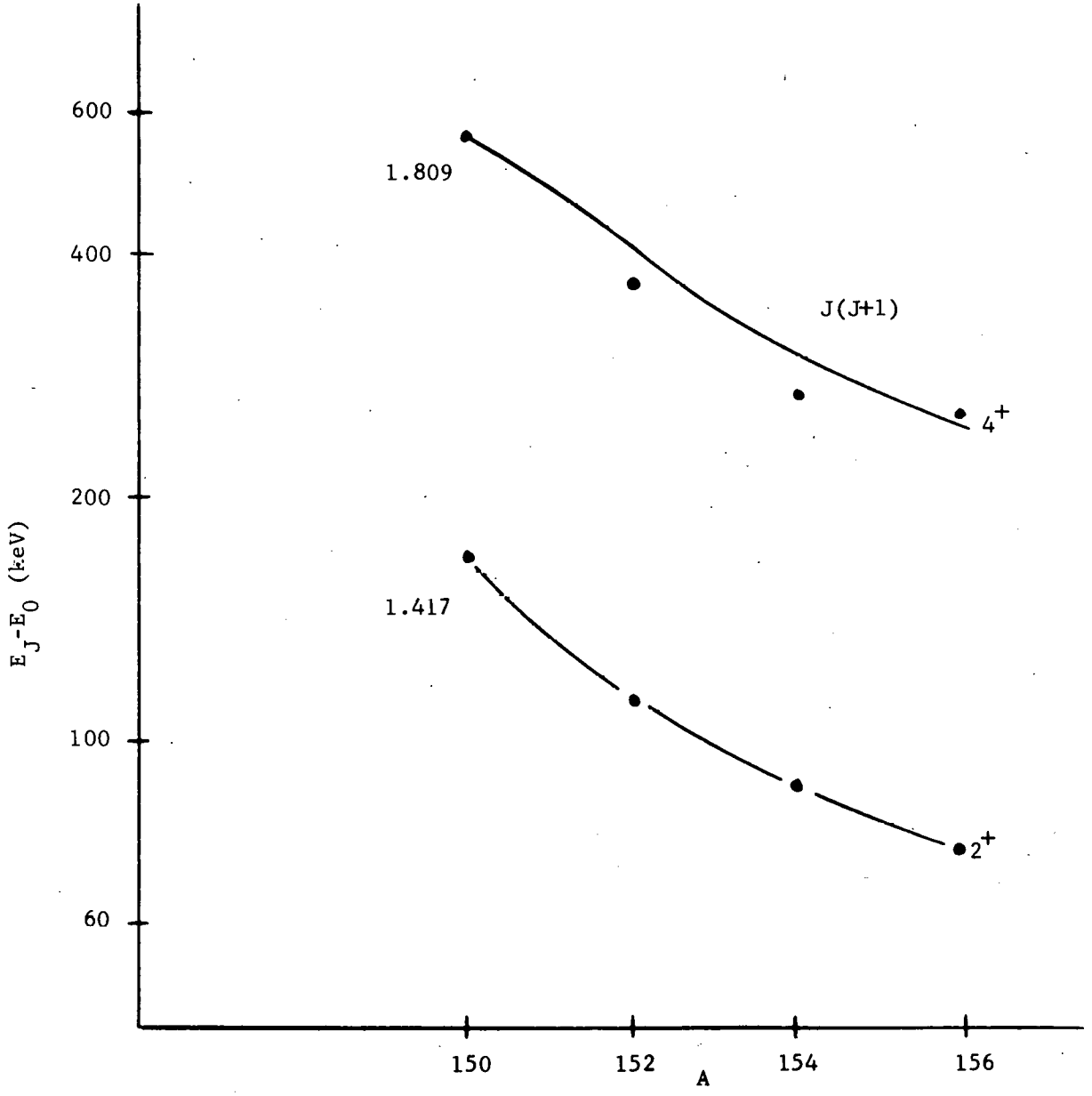

Fig.24-3

25. The (p,t) Reaction on Even Isotopes of Ytterbium

N. M. Hintz, M. Oothoudt and P. Vedelsby

During the past year a study of the even isotopes of ytterbium has been started using the (p,t) reaction. The Enge Split-Pole Spectrometer has been used to analyze the tritons which are collected on position-sensitive detectors or nuclear emulsion plates. Targets consist of 100-200 $\mu g/cm^2$ of enriched ytterbium isotopes from Oak Ridge National Laboratory on a backing of 30-60 $\mu g/cm^2$ of carbon.

Angular distributions (Fig. 25-1) from $\theta_{lab} = 10^\circ$ to 90° have been taken for the 0^+, 2^+, and 4^+ members of the ground state rotational band of ^{174}Yb populated by the reaction $^{176}Yb(p,t)$. The $\ell=0$ state takes its maximum at $27\ 1/2^\circ$; the ratio to Rutherford gives an absolute cross-section of 450 ± 100 μ barns/sterradian. The 0^+, distribution has been fitted very well by a DWBA code,[1] using the proton optical model parameters of Becchetti and Greenlees[2] and the 20 MeV triton parameters for ^{182}W of Flynn, et al.[3] However, the fits to the 2^+ and 4^+ states are poor. It may be necessary to include inelastic excitation in both the proton and triton channels.

Fig.25-2a shows the excitation spectrum up to about 2 MeV for the reaction $^{176}Yb(p,t)^{174}Yb$ at $\theta_{lab} = 25^\circ$. Table 25-1 lists the levels seen in this experiment and those seen previously. Note in particular the strong states at 1491 and 1888 keV which are shown to be 0^+ states by angular distributions at five angles. Possible rotational bands built on these states are indicated. Results for $^{174}Yb(p,t)$ and $^{172}Yb(p,t)$

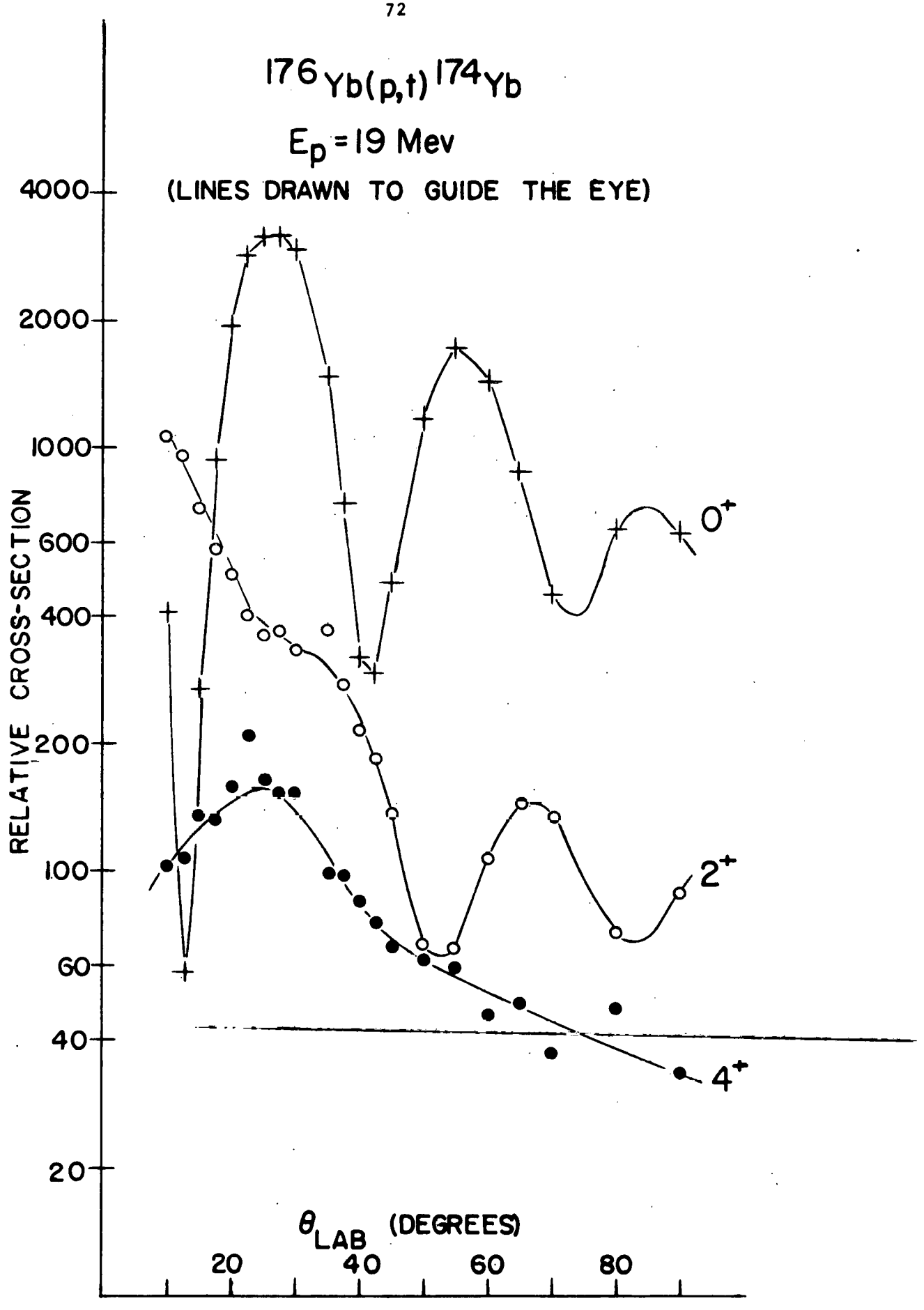
176Yb(p,t)174Yb
Ep = 19 Mev
(LINES DRAWN TO GUIDE THE EYE)
RELATIVE CROSS-SECTION
4000
2000
1000
600
400
200
100
60
40
20
0+
2+
4+
θLAB (DEGREES)
20
40
60
80

Fig. 25-1

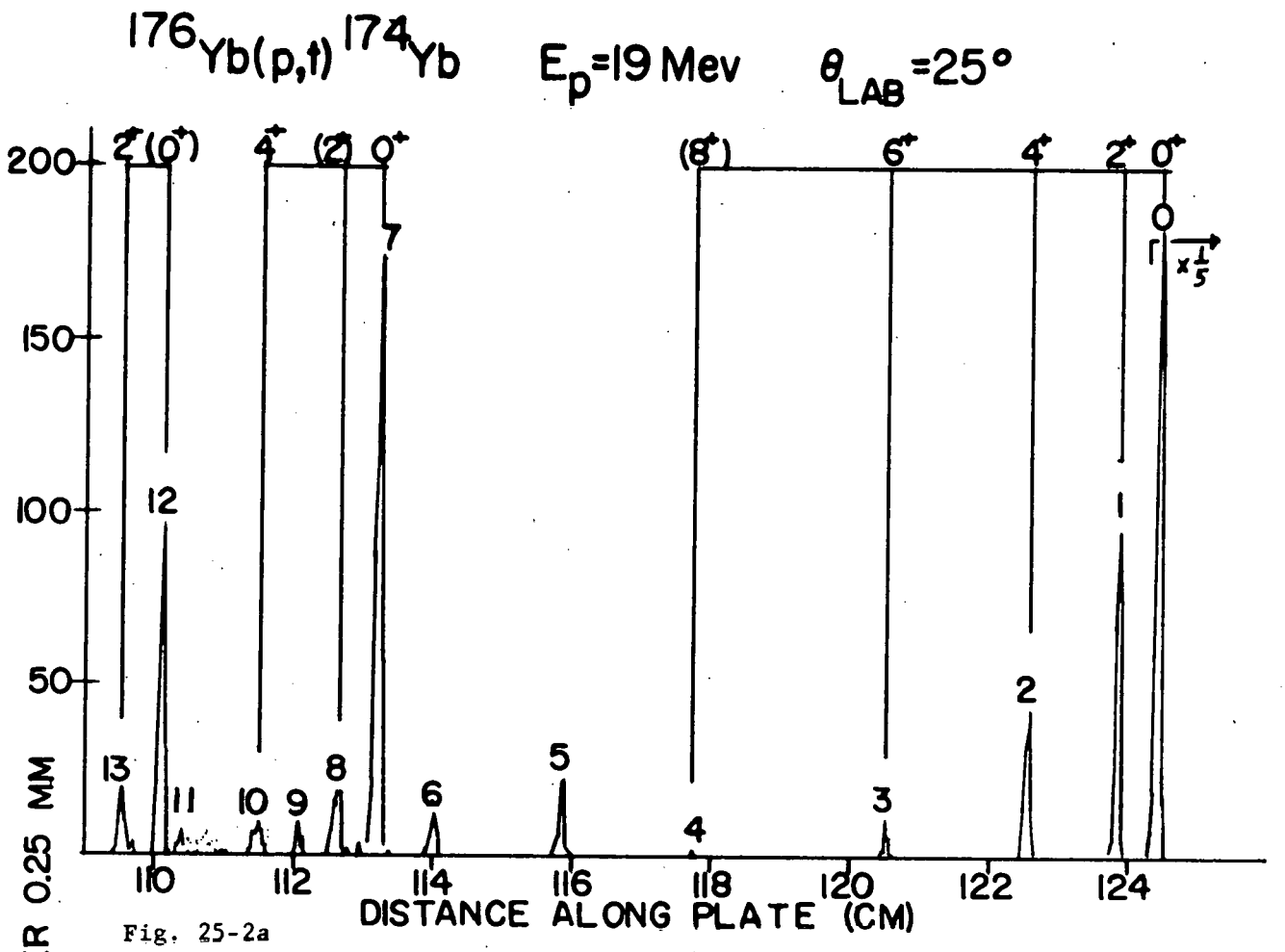

Fig. 25-2a

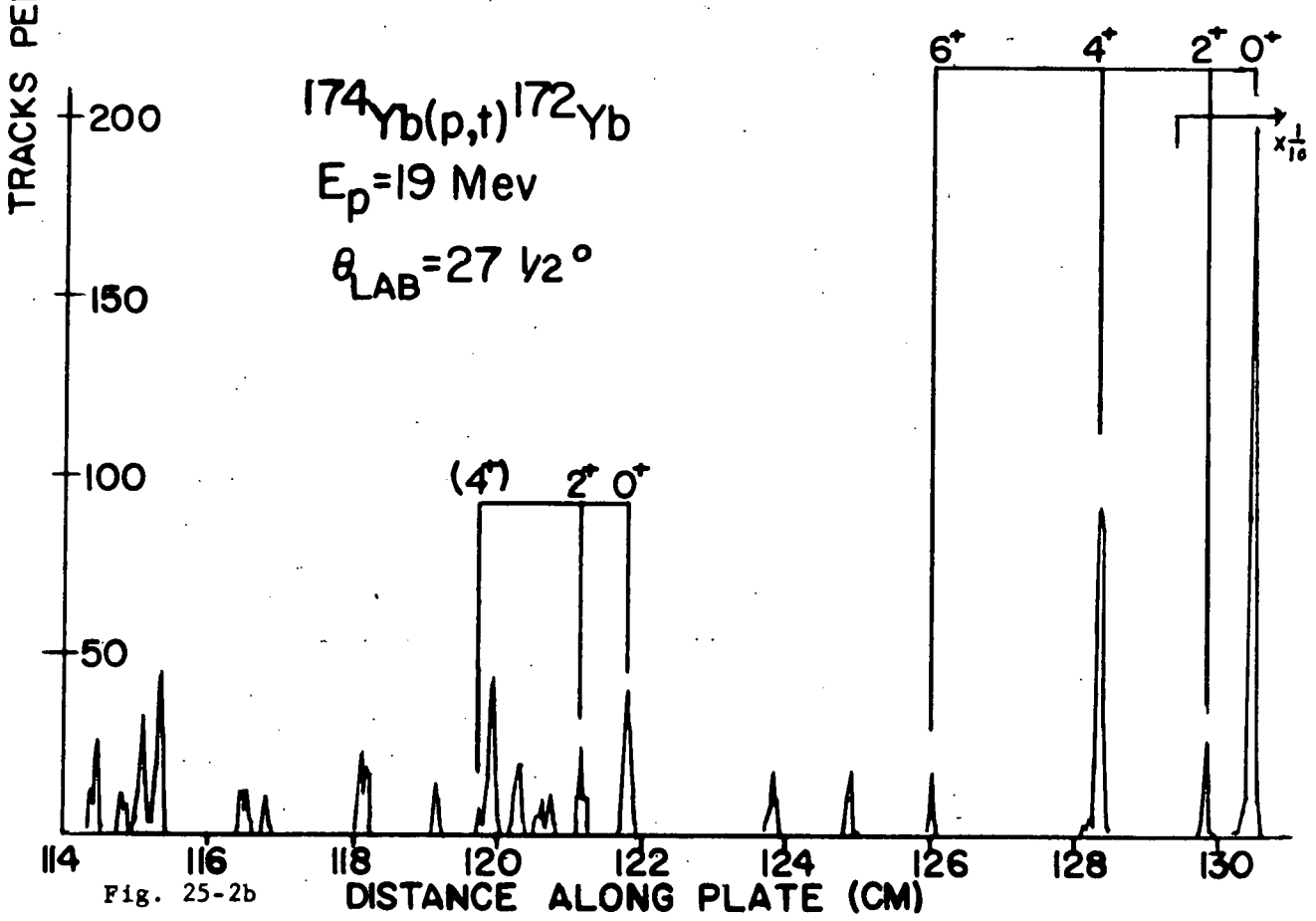

Fig. 25-2b

TABLE 25-1 : Levels in ^{174}Yb

	This Work			Previous Work		
level number	Ex. (keV)	J^π	Yield at 25°	Ex. (keV)	J^π	Reference
0	0	0^+	100.0	0.0	0^+	4
1	78±10	2^+	10.3	76.5	2^+	4
2	254±10	4^+	4.7	253.0	4^+	4
3	529±10		0.9	525.9	6^+	4
4	896±10		0.1	889.	8^+	4
5	174 Yb(p,t) ground state					
6	1385±10		1.7	1380.	3^-	5
7	1491±10	0^+	22.3			
8	1566±10	(2^+)	3.7			
9	1637±10		0.9	1630.	2^+	5
10	1711±10	4^+	1.7			
11	1854±10		1.0			
12	1888±10	(0^+)	11.0	1884.	(5^-)	4
13	1960±10	2^+	2.0			

show no such strongly excited states (Figs. 25-2band 25-2c). A 0^+ level is seen in ^{174}Yb(p,t) at 1043 keV but it is only 2 1/2% of the ground state.

A possible explanation for this difference comes from the positions of the Nilsson levels[6] (Fig. 25-3). A large gap exists between the energy levels of the last two neutrons in ^{176}Yb (7/2-, [514]) and the next highest energy level (5/2-, [512]). This gap provides the conditions for excitation of states described as pairing-vibrations. We could then say that the 1491 keV 0^+ level in ^{174}Yb results from picking up a pair in the region below the gap and the 1888 keV 0^+ level results from picking up a pair from below the next lowest gap.

For ^{174}Yb(p,t) and ^{172}Yb(p,t), however, a neutron pair is picked up from three closely spaced levels; since we have strong pairing forces here, we have a superfluid region and the entire 0^+ strength from (p,t) must go to the ground state.

According to this picture, the gap for ^{170}Yb(p,t) should produce spectra similar to those for ^{176}Yb(p,t). We are at present taking data to check this.

References

1. PROGRAM TWOPAR written by B. Bayman, University of Minnesota.
2. F.D. Becchetti, Jr. and G.W. Greenlees, John H. Williams Laboratory of Nuclear Physics Annual Progress Report, 1967, pp. 85-87.
3. E.R. Flynn, D.D. Armstrong, J.G. Beery, and A.G. Blair, preprint.

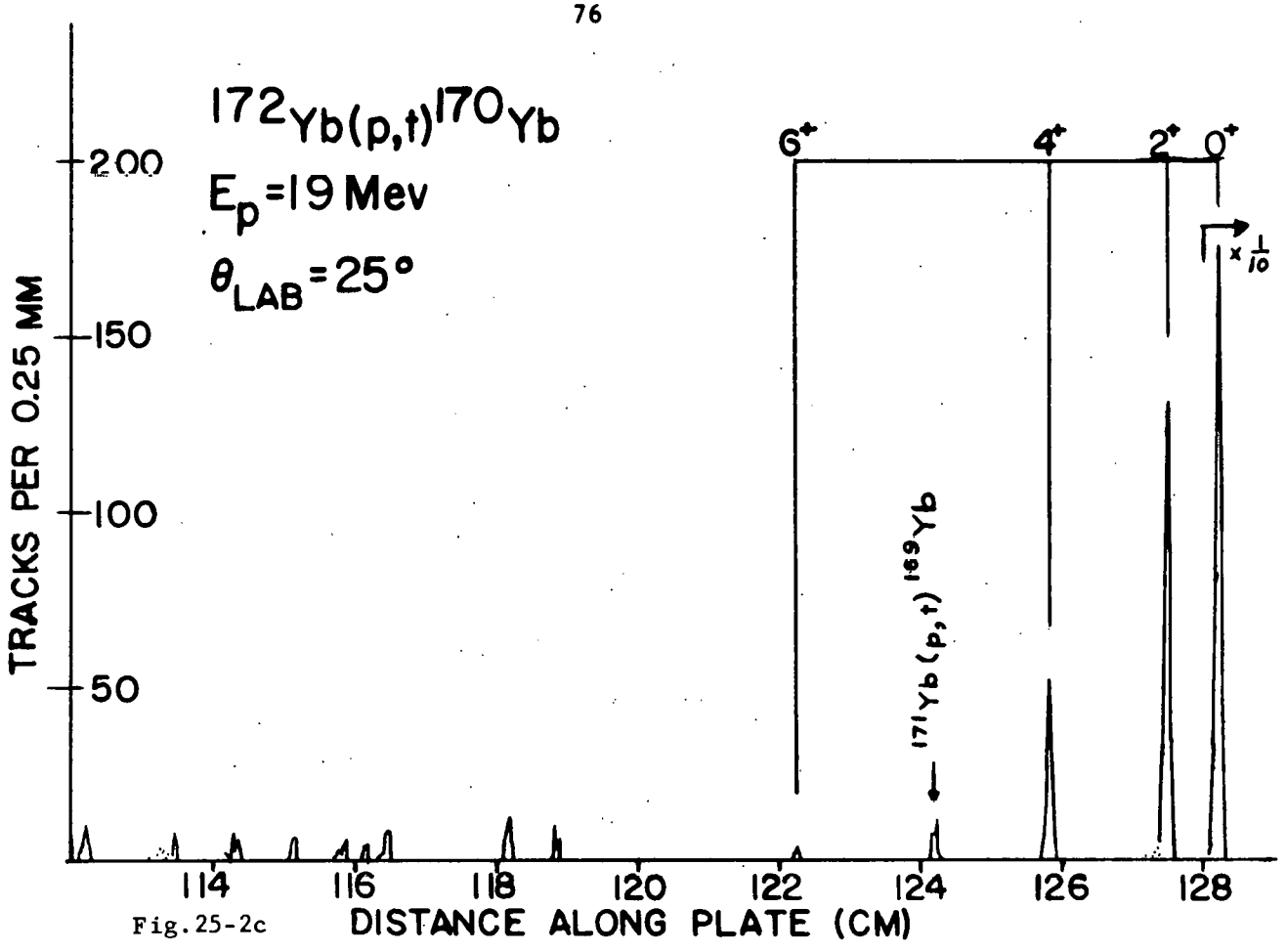

Fig.25-2c

APPROXIMATE ENERGY SPACINGS BETWEEN NILSSON STATES IN THE Yb REGION[6]

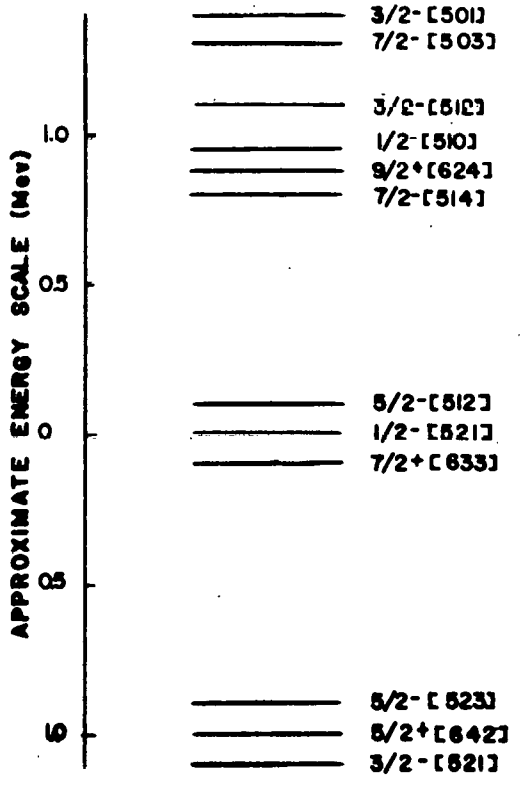

Fig. 25-3

4. J. Kantele, E. Liukkonen, and A. Sarmanto, Zeits fur Phys., 204, 456-461 (1967).

5. D.G. Burke and B. Elbek, Mat. Fys. Medd. Dan. Vid. Selsk., 36, no. 6 (1967), p. 13.

6. D.G. Burke, B. Zeidman, B. Elbek, B. Herskind, and M. Olesen, Mat. Fys. Medd. Dan. Vid. Selsk., 35, no. 2 (1966), p. 43.

---

26. Isomeric States in Tm^{165} and I^{122}

A. A. Padmanabham and G. W. Greenlees

The investigation of the 40 MeV proton induced reactions on $Te^{125,124}$ and Er^{168} responsible for the previously reported[1] gamma rays was continued. Bombardment of Er^{166} with 20 MeV pulsed protons and of Te^{166} with 20 MeV pulsed deuterons yielded the gamma rays of interest with measurable intensity. The energies and half-lives of these gamma rays were in good agreement with the previously reported work.[2,3] The reactions were identified by an accurate measurement of the energies of the k_α component of the X-ray involved following the internal conversion of these states and by measuring the excitation functions for these gamma rays.

The 70 keV, $T_{1/2}$ = 80 μ secs transition from Er^{166} Target

The energy of the k_α component of the X-ray involved, 50.5 keV, demands that the metastable level be assigned to a thulium nucleus. The possible reactions are thus $Er^{166}(p,n)Tm^{166}$; $Er^{166}(p,2n)Tm^{165}$ and $Er^{166}(p,3n)Tm^{164}$. The excitation function for this state indicates a threshold of about 13.0 MeV for this reaction. This result excludes the

possibility of a (p,3n) reaction whose threshold is about 17.0 MeV. The diminishing yield below E_p=16.0 MeV also excludes the possibility of a (p,n) reaction whose threshold is about 3.0 MeV. This conclusion is supported by the fact that if the reaction were Er^{166}(p,n), we should expect to observe the isomer even more strongly in Er^{167}, since at 19.0 MeV the cross section for (p,2n) is larger than that for (p,n); however, it was not seen at all when the Er^{167} target was used. Thus we conclude that the isomeric state is produced by the reaction Er^{166}(p,2n)Tm^{165}.

By measuring the intensities of the X-ray and the gamma ray we obtained a value of 1.7 ± 0.4 for the conversion coefficient α_k, indicating that the transition is E2 in character and not E1, as reported by Conlon.[2] The E2 character of this gamma ray is in agreement with the measurements on the magnetic spectrometer by Paris.[4] These observations, coupled with the fact that there was no evidence for any other isomeric transition in this reaction, indicate that the isomeric level of interest is the $7/2^+(404)$ level in Tm^{165} decaying by an E2 transition to the $3/2^+$ first excited state.

61.7, 94.0, 159.7 and 188.0 keV; $T_{1/2}$ = 80 μsecs Transitions from Te^{122} Target

An accurate measurement of the X-ray energy could not be made in this case because of the large background at this low energy and due to the energy spread in the peak following scattering in the aluminum cap around the detector and the dead layer in the detector itself. However, the decaying X-ray as observed during the "beam off" time is found to be at a higher energy than that of the characteristic tellurium X-ray observed during the "beam on" time. Thus the isomeric state is assigned to one of the iodine isotopes. The possible reactions

are thus (d,n) (d,2n) and (d,3n) with Q-values of +2.6 MeV, -7.3 MeV and -15.6 MeV respectively.

The excitation functions for all these gamma rays are found to peak up around E_d = 18.0 MeV with negligible intensity for deuteron energies less than 13.0 MeV indicating a (d,2n) reaction. This is supported by the data obtained with the linear accelerator where 40 MeV proton bombardment on Te^{125} and Te^{124} gave rise to these isomeric transitions, with a slightly larger yield from Te^{125}, suggesting the $Te^{124}(p,3n)I^{122}$ and $Te^{125}(p,4n)I^{122}$ reactions. Thus we assign the metastable state to I^{122}.

References

1. John H. Williams Laboratory of Nuclear Physics, Annual Progress Report, 1968, p. 126.

2. T.W. Conlon et al, Nuclear Phys. A104, No. 1 1967.

3. A.C. Ghosh and W.M. Martin, Canadian Journal of Physics, Vol. 41, 1963.

4. P. Paris, Le Journal de Physique, Tome 28, 1967.

V. INTERACTION OF SINGLE PARTICLE AND VIBERATION STATES

27. (p,p') and (p,t) on Silver and Palladium Isotopes

A. W. Kuhfeld and N. M. Hintz

Ag^{107} and Ag^{109} have been suggested as nuclides whose excitations are well-describable in terms of the phonon-core model, with a p1/2 proton (or proton hole) coupled to collective vibrations of the neighboring palladium or cadmium isotones. Experiments involving electromagnetic transition rates and Coulomb excitations,[1,2] inelastic proton scattering,[3,4] and inelastic alpha scattering[5] all tend to support this description; with a slight preference for descriptions in terms of palladium states rather than cadmium states. It was decided to study these various isotopes with particle-transfer reactions as well as inelastic scattering, to see how well the model holds under these more complex reactions. So far we have done (p,p') and (p,t) on Ag^{109} and Pd^{108}, using the Enge split-pole magnetic spectrometer and position-sensitive detectors for resolution and particle identification. $Pd^{106}(He^3,d)Ag^{107}$ and the inverse reaction are planned also, as are similar reactions on Cd^{108} and Cd^{110}.

The results of the (p,p') experiments on silver and palladium were quite incomplete because of the great number of contaminants in the targets; the only levels for which good angular distributions were obtained were the ground state and the octupole vibrational state(s) near 2 MeV excitation. Normalization was done using the Becchetti optical model program OMD[6] to predict ground state angular distributions; this procedure should give good relative normalizations, and fair absolute normalizations. The angular distributions for the Pd^{108} 2.030 MeV, 3- level and

the very similar Ag^{109} 2.17 MeV level were very similar in shape, but the magnitude of the silver octupole angular distribution was only about 35% that of the palladium angular distribution at the 18 MeV proton bombarding energy. No nearby states with similar angular distributions were noted. This phenomenon of "missing strength" has been observed in Ag^{109} (alpha,alpha') at 42 MeV lab incident by Stewart, Baron and Leonard,[5] and in Ag^{107}(p,p') at 13 MeV lab incident by Ford, Robinson and collaborators.[3,4]

In $Ag^{109}(p,t)Ag^{107}$ with 19 MeV incident protons, several states of approximately equal strength were seen clustered near the 2.19 MeV octupole level; their approximate excitations were 2.21, 2.24, 2.26, and 2.29 MeV. (These states were seen at 45^{o} lab on a spectrum extending out to 2.60 MeV excitation. Ford et al[3] saw no trace of these levels in Ag^{107}(p,p') at 13 MeV. Angular distributions for these higher levels are scheduled for the next (p,t) run.)

Angular distributions for the Ag^{109} and Pd^{108} (p,t) reactions were obtained in 5^{o} steps for lab angles from 10^{o} to 75^{o}; all known levels were included between 0 and 1.2289 MeV excitation for $Pd^{108}(p,t)Pd^{106}$, and 0 to 0.9490 for $Ag^{109}(p,t)Ag^{107}$. This region included the one- and two-quadrupole-phonon levels in Pd^{106} and the one-quadrupole-phonon 2+ multiplet by Ford et al.[3] Angular distributions for these levels are given in Fig. 27-1 . (The lines connecting data points are for visual purposes only.)

The ground state angular distributions for the two reactions are extremely similar in both shape and magnitude. (While the Ag distribution

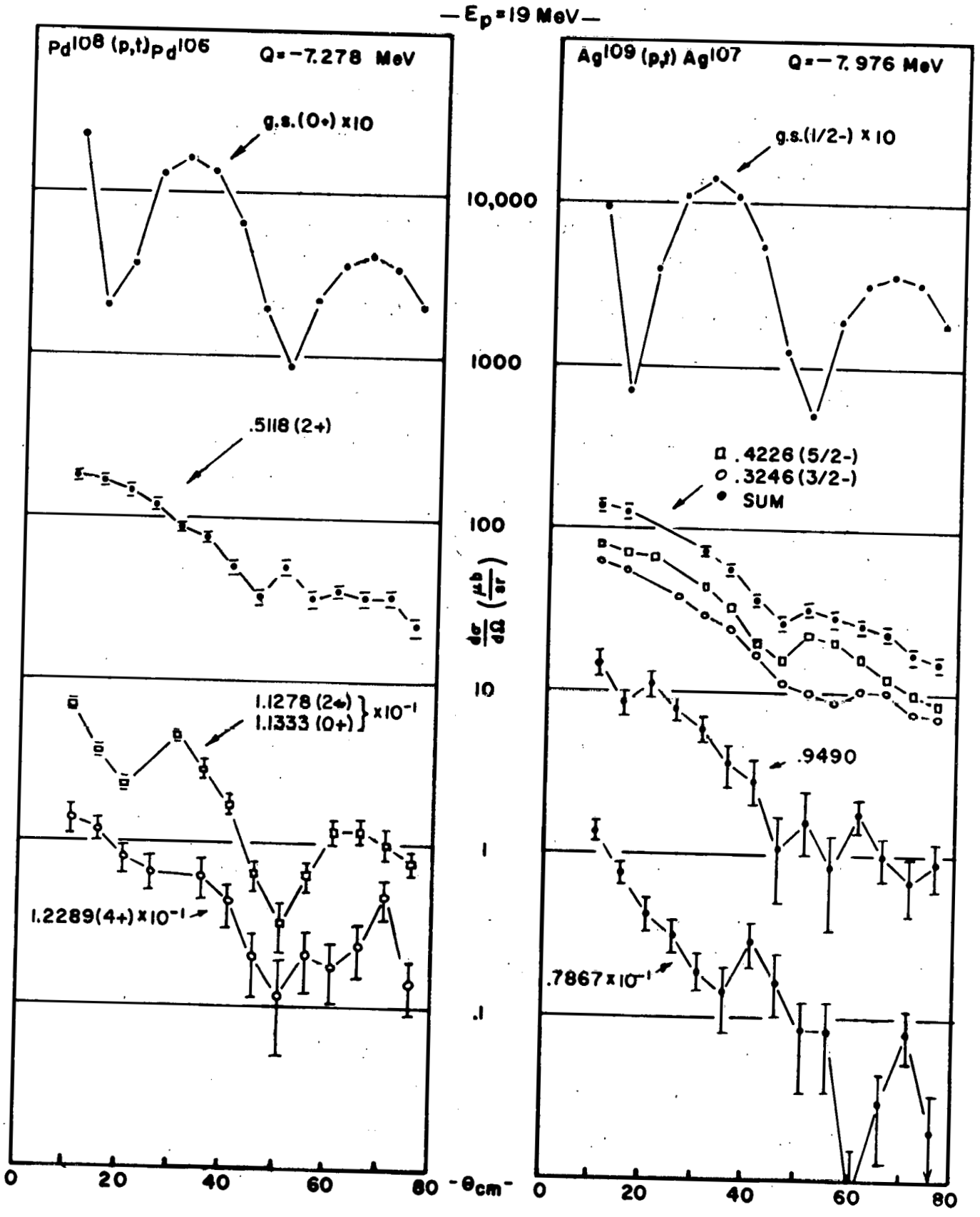
— E_p = 19 MeV —
$Pd^{108}(p,t)Pd^{106}$ Q = −7.278 MeV
g.s.(0+) x10
.5118 (2+)
1.1278 (2+)
1.1333 (0+)
} x10⁻¹
1.2289(4+) x10⁻¹
$Ag^{109}(p,t)Ag^{107}$ Q = −7.976 MeV
g.s.(1/2-) x 10
.4226 (5/2-)
.3246 (3/2-)
SUM
.9490
.7867 x10⁻¹
10,000
1000
100
10
1
.1
$\frac{d\sigma}{d\Omega}$ ($\frac{\mu b}{sr}$)
0
20
40
60
80
-θcm-

Fig. 27-1

has a lesser magnitude than the Pd distribution, this is largely a mere Q-dependent effect: the tritons are coming out near the Coulomb barrier, but have some 600 KeV more energy in $Pd^{108}(p,t)$ than in $Ag^{109}(p,t)$.) Likewise the angular distribution for the summed first 3/2- and 5/2- levels of Ag^{107} is very similar to the angular distribution for the first 2+ level in Pd^{106}. In addition, the two Ag levels obey the (2J+1) intensity rule expected of members of a core multiplet quite well, except for the region from 40^{o} to 60^{o}. This could be J-dependence, or a proton spin-flip L=0 contribution to the 3/2- state. A theoretical analysis is underway using two-nucleon-transfer program TWOPAR.

The two-quadrupole-phonon terms in the Pd reaction are surprisingly strong, since excitation of pure two-phonon states is forbidden in first order for simple pickup. This could be due to inelastic processes or following particle transfer, or perhaps an admixture of the 0+ ground state and the 2+ excited state into the 0+,2+ doublet. Unfortunately, the two states are only 5.5 keV apart and could not quite be resolved.

The 0.7867 and 0.9490 MeV levels in Ag^{107} have been assigned to the 2QP 2+ multiplet. Both have approximately the correct magnitude for this assignment; the 0.9490 angular distribution fits the L=2 shape without greatly exceeding its error bars. Better statistics will be acquired for definite comment.

References

1. A. DeShalit, Phys. Rev. 122, 1530 (1961).

2. J.L. Black, W. Gruhle, and D.W. Heikkinen, Phys. Lett. 22, 598 (1966).

3. J.L.C. Ford, Jr., Cheuk-Yin Wong, Taro Tamura, R.L. Robinson, and P.H. Stelson, Phys. Rev. 158, 1194 (1967).

4. R.L. Robinson, J.L.C. Ford, Jr., P.H. Stelson, and G.R. Satchler, Phys. Rev. 146 , 816 (1966).

5. W.M. Stewart, N. Baron, and R.F. Leonard, Phys. Rev. 171, 1316 (1968).

6. F.D. Becchetti, Jr., and C.W. Greenlees, Univ. of Minn. Report COO-1265-59.

---

28. The Coulomb Excitation of ^{209}Bi and the Weak Coupling Model

R. A. Broglia, J. S. Lilley, R. Perazzo and W. R. Phillips

The preliminary analysis of the Coulomb excitation of ^{209}Bi reported last year[1] has been completed and a comparison made with theoretical calculations.

In this experiment, a thick bismuth target was bombarded with 19 MeV α-particles and the γ-decays of levels populated via Coulomb excitation were observed with a 25 cc Li-Ge detector.

Fig. 28-1 summarizes the results of the γ-intensity measurements. The energies of the levels are those measured in this experiment and are accurate to $\pm$ 0.5 keV, except for the 2.598 MeV, 2.581 MeV and 2.563 MeV levels, which were Doppler shifted and broadened, and are believed accurate to $\pm$ 1 keV. The numbers quoted in the Figure are thick target γ-yields in units of 10^6 per 1.6 mC of 19 MeV He^{++}.

Table 28-1 lists the reduced transition probabilities measured in the experiment. The values for the upward E3 and E2 transitions were calculated from the thick target yields using Coulomb excitation theory.[2] The values for the individual levels of the multiplet can only be inferred,

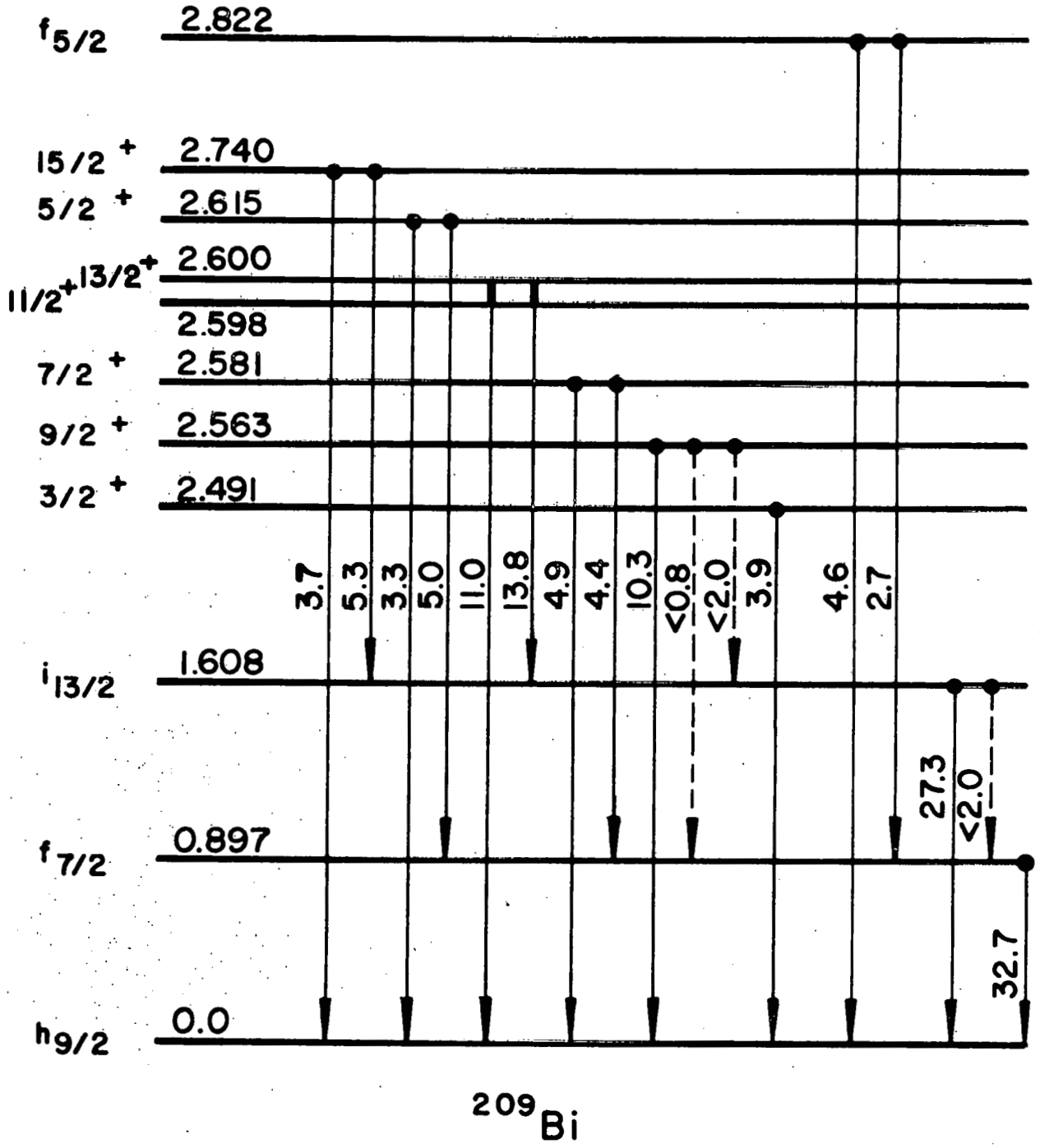
f5/2
2.822
15/2 +
2.740
5/2 +
2.615
11/2+13/2+
2.600
2.598
7/2 +
2.581
9/2 +
2.563
3/2 +
2.491
3.7
5.3
3.3
5.0
11.0
13.8
4.9
4.4
10.3
<0.8
<2.0
3.9
4.6
2.7
i13/2
1.608
27.3
<2.0
f7/2
0.897
32.7
h9/2
0.0
209Bi

Fig. 28-1

TABLE 28-1 Reduced Transition Probabilities

Transition	Type	Method of Measurement	$B(EL)_{exp}$ b)	B(EL) THEORY I	B(EL) THEORY II	$\frac{B(EL)_{exp}}{B(EL)_{s.p.}}$ c)
$0 \rightarrow 2.6$ a)	E3	γ-Intensities	$(.57 \pm .03) e^2 b^3$	---	---	31.5
$0 \rightarrow 1.608$	E3	γ-Intensities	$(1.24 \pm .32) \times 10^{-2} e^2 b^3$	$1.3 \times 10^{-2} e^2 b^3$	$1.3 \times 10^{-2} e^2 b^3$	0.68
$0 \rightarrow 0.897$	E2	γ-Intensities	$(1.39^{+.16}_{-.23}) \times 10^{-3} e^2 b^2$	$0.15 \times 10^{-3} e^2 b^2$	$1.23 \times 10^{-3} e^2 b^2$	3.8×10^{-2}
$0 \rightarrow 2.822$	E2	γ-Intensities	$(2.90 \pm 1.00) \times 10^{-2} e^2 b^2$	$0.3 \times 10^{-2} e^2 b^2$	$3.4 \times 10^{-2} e^2 b^2$	0.79
$2.581 \rightarrow 0$	E1	Lifetime and γ-Intensities d)	$(1.45 \pm 0.58) \times 10^{-6} e^2 b$	$1.25 \times 10^{-3} e^2 b$	$1.5 \times 10^{-6} e^2 b$ ($k(\tau=1)=4.1$)	2.1×10^{-5}
$2.581 \rightarrow 0.897$	E1	Lifetime and γ-Intensities d)	$(4.60 \pm 1.85) \times 10^{-6} e^2 b$	$2 \times 10^{-4} e^2 b$	$4 \times 10^{-6} e^2 b$ ($k(\tau=1)=5.5$)	6.8×10^{-5}
$2.563 \rightarrow 0$	E1	Lifetime and γ-Intensities	$\gtrsim 4.5 \times 10^{-6} e^2 b$	$9 \times 10^{-4} e^2 b$	$8.8 \times 10^{-5} e^2 b$ ($k(\tau=1)=5.5$)	$\gtrsim 7 \times 10^{-5}$
$2.598 \rightarrow 0$	E1	Lifetime and γ-Intensities	$\gtrsim 4.5 \times 10^{-6} e^2 b$	$2.4 \times 10^{-3} e^2 b$	$1.6 \times 10^{-5} e^2 b$ ($k(\tau=1)=5.5$)	$\gtrsim 7 \times 10^{-5}$

a) Summed E3 strength to septuplet.

b) Errors quoted do not include error in absolute efficiency of detector.

c) $B(EL)_{s.p.} = (2L+1) \frac{e^2}{4\pi} \left(\frac{3}{3+L}\right)^2 R_o^{2L}$: $R_o = 1.2 A^{1/3} \times 10^{-13}$ cms.

d) Assumes that the $7/2^+$ level has significant decays to ground and $f_{7/2}$ only.

since there exist transitions within the multiplet which were not observed in this experiment. The B(E1) values were calculated from lifetimes given by an analysis of the Doppler-broadened lives. The Doppler effects were small and so the resulting B(E1) values have a large uncertainty. However, even an approximate number gives quite a sensitive test to the theory.

In addition to the reduced matrix elements discussed above, there are several relative transition rates measured in the experiment that can be compared with the theoretically predicted values. These are shown in Table 28-2 . Most of them came in a straightforward manner from the relative γ-ray intensities shown on Fig. 28-1 . Two of them arise from an analysis of γ-ray angular distributions.

The results have been analyzed in terms of the particle-vibration weak-coupling model. Initially, only the 2.6 MeV, 3-vibrational state of the ^{208}Pb core was allowed to couple--Approximation I. The B(E3) for the octupole state was taken to be 0.58 e^2b^3.[3] Calculations using Approximation I are given in column 5 of Table 28-1 . Agreement with experiment is good for the B(E3) values only, and it is clear that other degrees of freedom must be included to account for the other observed transition strengths.

This has been done in Approximation II (column 6 of Table 28-1) in which the 2^+ state at 4.07 MeV and the 1^- state at 12 MeV in ^{208}Pb were also included in the coupling. The theoretical results given in Table 28-2 were calculated also using Approximation II. A B(E2) value of 0.3 e^2b^2 for the 2^+ state[4] gives excellent agreement with experiment. The coupling strength k(T=1) for the 1^- state was treated as a parameter. All the data can be fixed with k(T=1) = 5.2 ± 1.0, which is approximately a constant as it should be. No attempt has been made to determine the

Table 28-2 Relative Transition Rates.

Transitions	Type	Method of Measurement	Ratio Exp.	Ratio Theory
$\frac{0.897 \rightarrow GD}{0.897 \rightarrow GD}$	$\frac{E2}{M1}$	Ang. Dist.	0.7 - 1.3	1.1
$\frac{1.608 \rightarrow 0.897}{1.608 \rightarrow GD}$	$\frac{E3}{E3+M2}$	γ-Intensities	$\lesssim 0.07$	10^{-4}
$\frac{2.563 \rightarrow 0.897}{2.563 \rightarrow GD}$	$\frac{E1}{E1+M2+E3}$	γ-Intensities	$\lesssim 0.08$	0.08 ($k(\tau=1)=5.9$)
$\frac{2.563 \rightarrow 1.608}{2.563 \rightarrow GD}$	$\frac{E2}{E1+M2+E3}$	γ-Intensities	$\lesssim 0.20$	10^{-3} ($k\tau=5.5$)
$\frac{2.581 \rightarrow 0.897}{2.581 \rightarrow GD}$	$\frac{E1}{E1+M2+E3}$	γ-Intensities	0.88 ± .08	0.8 ($k\tau=4.1$)
$\frac{*2.598 \rightarrow 1.608}{2.598 \rightarrow GD}$	$\frac{M1+E2}{E1+M2+E3}$	γ-Intensities	1.25 ± .09	1.2 ($k\tau=6.2$)
$\frac{2.615 \rightarrow 0.897}{2.615 \rightarrow GD}$	$\frac{E1}{M2+E3}$	γ-Intensities	$1.51\ ^{+.4}_{-.8}$	1.0 ($k\tau=5.5$)
$\frac{2.615 \rightarrow GD}{2.615 \rightarrow GD}$	$\frac{E3}{M2}$	Ang. Dist.	0.8 -25.0	8
$\frac{2.740 \rightarrow 1.608}{2.740 \rightarrow GD}$	$\frac{M1+E2}{E3}$	γ-Intensities	1.44 ± .18	3
$\frac{2.822 \rightarrow 0.897}{2.822 \rightarrow GD}$	$\frac{M1+E2}{E2}$	γ-Intensities	0.6 ± 0.3	2

* Separate $11/2, 13/2^+$ contributions unresolved.

sensitivity to the values of the unbound single-particle energies used in the calculations.

A more complete treatment of the E1 transitions has been made recently[5] in which the influence of the giant dipole is taken into account through an effective charge $e_{eff}(E1) = 0.3$. The corresponding B(E1) values are in good agreement with this experiment.

A detailed report of this work has been completed and submitted for publication.

References

1. John H. Williams Laboratory, Annual Report 1968, p. 123.
2. K. Alder, A. Bohr, J. Huus, B. Mottelson and A. Winther, Revs. Mod. Phys. 28, 432 (1956).
3. A.R. Barnett and W.R. Phillips, to be published.
4. J.F. Ziegler and G.A. Peterson, Phys. Rev. 165, 1337 (1968).
5. I. Hamamoto, The Decay Scheme of the Septuplet in the Nucleus ^{209}Bi, preprint, May 1969.

---

29. Alpha Particle Reaction Cross Sections on ^{208}Pb and ^{209}Bi Below the Coulomb Barrier

A. R. Barnett, J. S. Lilley and F. Chwieroth

Total (α,n) cross sections for ^{208}Pb between 16 and 22 MeV and for ^{209}Bi between 18 and 22 MeV have been measured by observing the α-activity of the residual nuclei ^{211}Po and ^{212}At.

The (α,n) channel is the most important one at these energies. Inelastic α scattering is known to be small (approximately 0.3 mb at 19 MeV) and is dominated by Coulomb excitation which is calculable. Other possi-

ble channels, (α,p) and (α,γ), also lead to characteristic α-active nuclei. They are not expected to compete significantly with neutron emission and no evidence has yet been seen for them. Thus a measurement of $\sigma(\alpha,n)$ below the $(\alpha,2n)$ threshold should be a good measure of the total reaction cross section, σ_R.

Normally, it is difficult to measure σ_R accurately, particularly for energies below the Coulomb barrier. However, in this energy region it is one of the few measurable quantities that is sensitive to the nuclear interaction. As soon as the bombarding energy approaches and exceeds the Coulomb barrier, the elastic scattering deviates significantly from Rutherford scattering. The scattering and reaction cross section, determined for a range of energies near the Coulomb barrier, will be analyzed using an optical model description. In this way it is hoped to obtain information about α-penetrabilities and to learn some details about the distribution of matter in the outer regions of the nucleus.

Above 18 MeV the α-activity peaks were observed in the energy spectra of scattered α particles. These peaks were clearly identifiable among the prompt α-distribution. Their energies corresponded to the known α-decay energies, their angular distributions were isotropic, and they exhibited no kinematic shift with either bombarding energy or scattering angle. Measurements relative to the elastic peak gave accurate determinations of the (α,n) cross section since σ_{el} was measured independently to within a few percent. Fig. 29-1 shows the (α,n) results.[1]

The $^{208}Pb(\alpha,n)$ cross section has been measured below 19 MeV using a chopped beam and detecting the delayed activity. The beam was chopped with a pneumatically operated Faraday cup in a time short compared with the half-lives being measured. After each beam burst, the target was

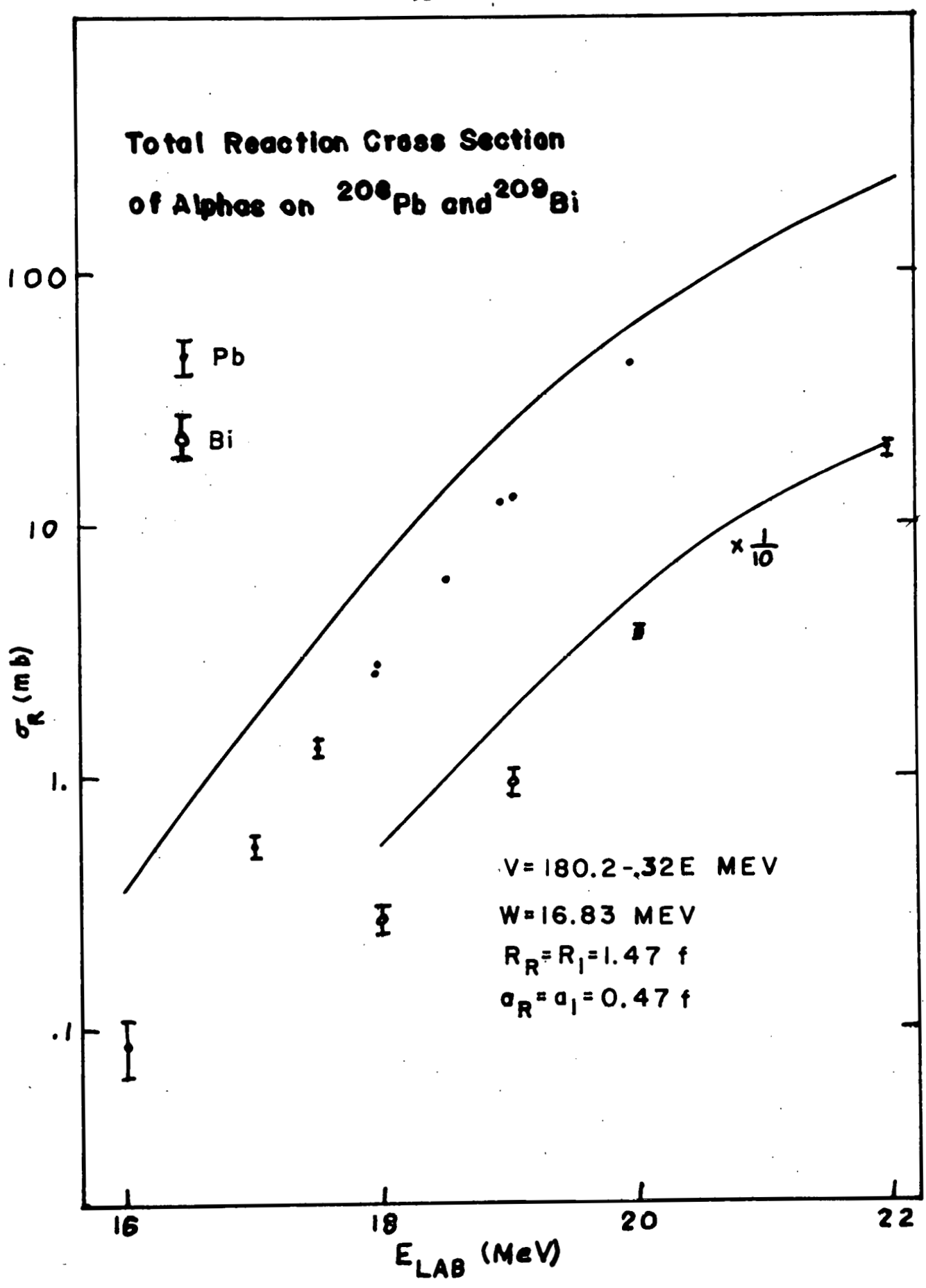
Total Reaction Cross Section
of Alphas on ^{208}Pb and ^{209}Bi
100
10
1.
.1
σ_R (mb)
Pb
Bi
$\times \frac{1}{10}$
V = 180.2 - .32E MEV
W = 16.83 MEV
$R_R = R_I = 1.47$ f
$a_R = a_I = 0.47$ f
16
18
20
22
E_{LAB} (MeV)

Fig. 29-1

moved between two detectors giving a large solid angle and complete freedom from beam background. Operation of the experimental equipment and on-line analysis of the data was carried out by the CDC-3100 computer using a general-purpose "activity" routine ACT. Both the α-particle energy spectrum and the measured half-life $T_{1/2} = 0.505 \pm 0.035$ sec confirm the identification of the activity as ^{211}Po.

Cross sections determined by both methods agree quite well. The advantages of the latter technique allow measurements to be made down to energies approaching the α,n threshold at 15.25 MeV. (See Fig. 29-1.)

We have also measured the elastic scattering angular distributions for both ^{208}Pb and ^{209}Bi at 19, 20, and 22 MeV and normalized the data to distributions at 16 MeV which were taken to be pure Rutherford. The overall accuracy of the data is about 2%. These data are given in Figs. 29-2 and 29-3 together with the results of a simultaneous optical model fit to all the scattering data using the global search routine BOMB.[2] The model parameters are given in Fig. 29-1 together with the predicted curves for the σ_R excitation functions.

The calculated values for σ_R are uniformly higher than the experimental ones by factors of 2 to 3, although the energy dependence of the reaction cross sections is reproduced best by small values of the diffuseness parameters a_R and a_I. A preliminary search for optical parameters which fit the reaction and the scattering data simultaneously gives significantly poorer fits to the elastic scattering data.

References

1. The value shown for bismuth at 22 MeV includes a contribution of 66 mb for the (α,2n) reaction (Ramler et al., Phys. Rev. 114, 154 (1959)).

2. F.D. Becchetti, Jr., M.S. Thesis, University of Minnesota, June 1968, unpublished.

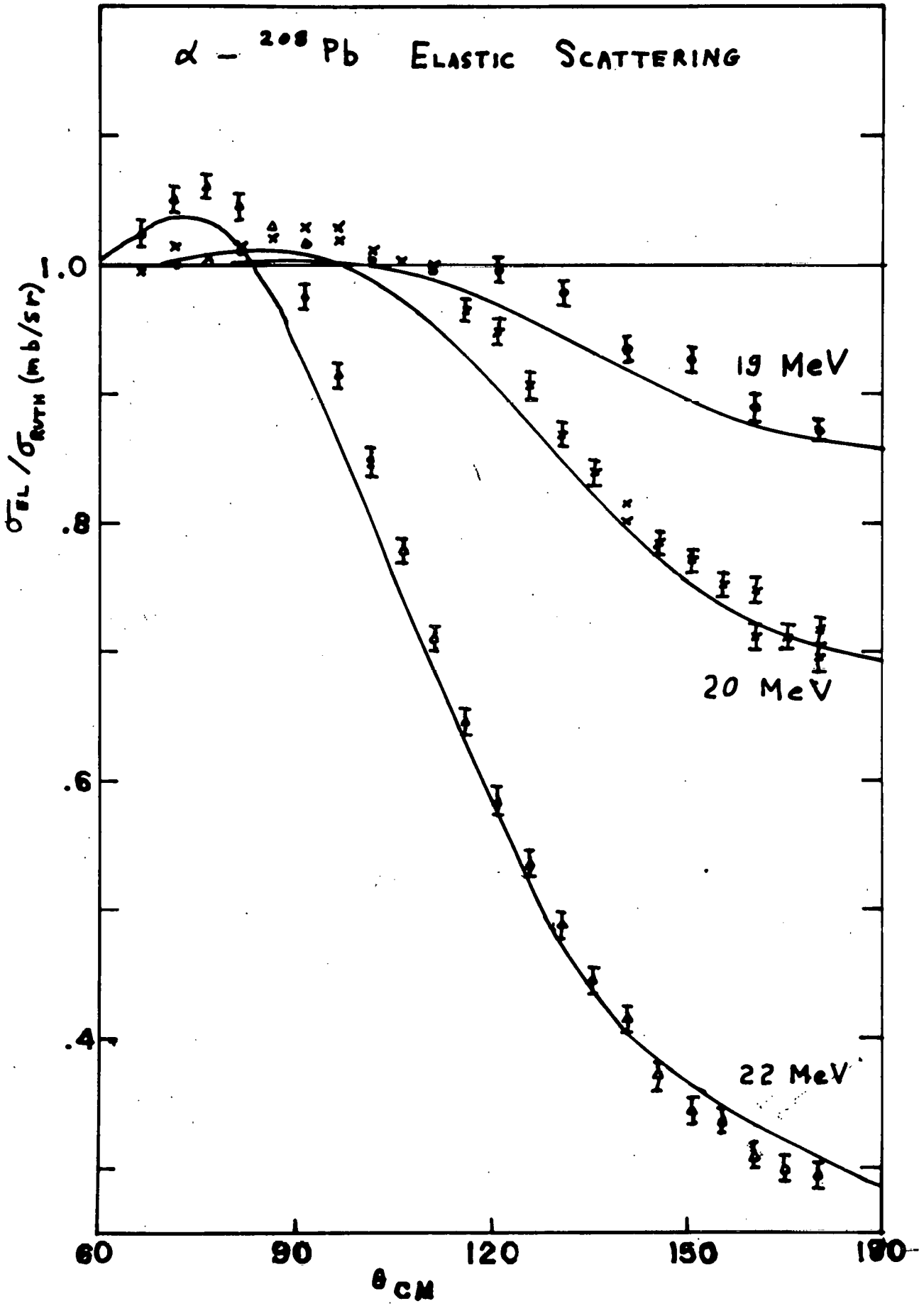
α – 208 Pb ELASTIC SCATTERING
σEL /σRUTH (mb/sr)
1.0
.8
.6
.4
19 MeV
20 MeV
22 MeV
60
90
120
150
180
θCM

Fig. 29-2

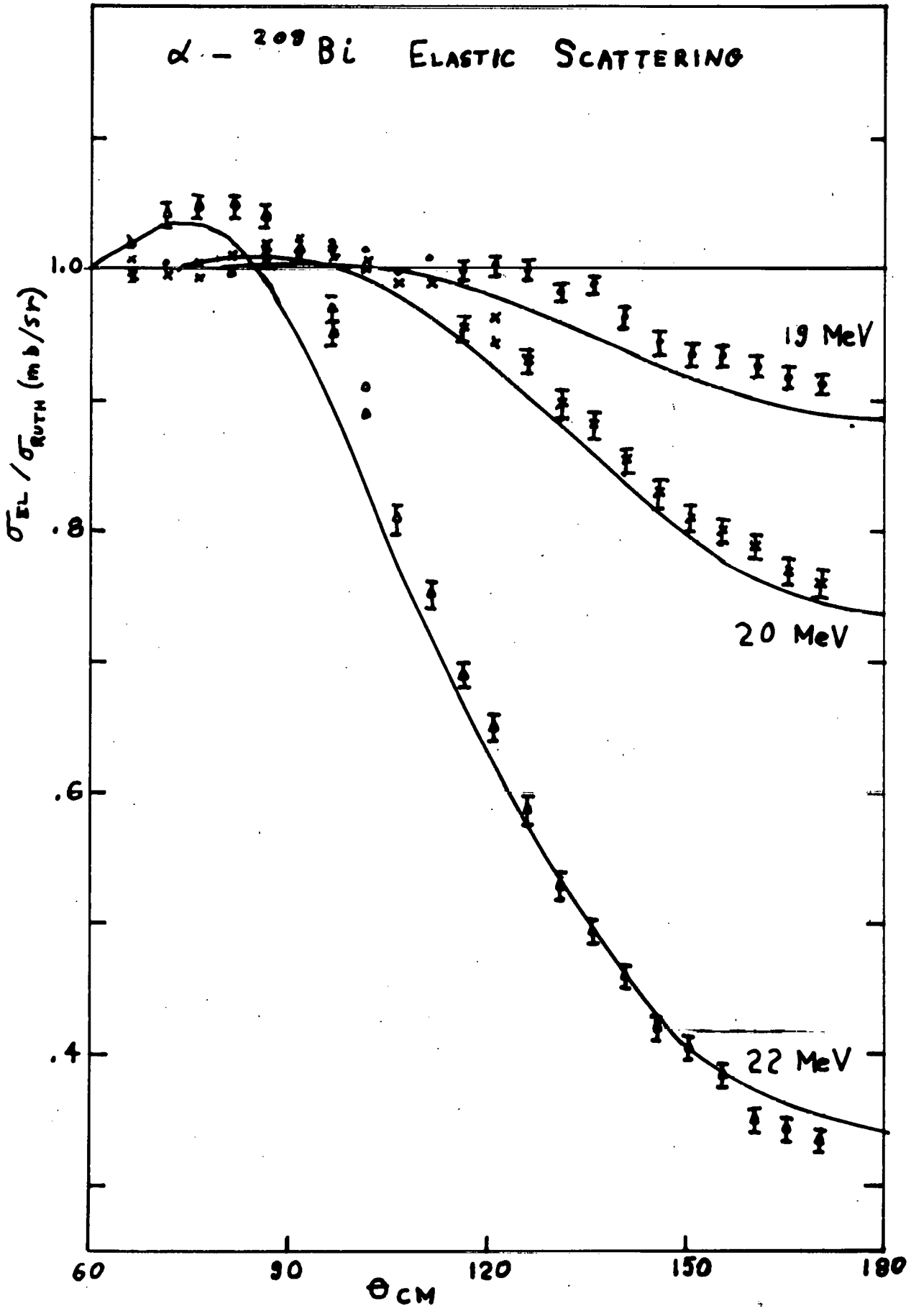
α - 209 Bi ELASTIC SCATTERING
1.0
.8
.6
.4
σEL / σRUTH (mb/sr)
19 MeV
20 MeV
22 MeV
60
90
120
150
180
θCM

Fig. 29-3

30. The Quadrupole Moment of the 2.6 MeV 3^- State in ^{208}Pb

A. R. Barnett and W. R. Phillips

The static quadrupole moment, Q, of the 2.614 MeV 3^- level in ^{208}Pb has been measured by observing the angular distribution of inelastically scattered ^4He and ^{16}O ions following E3 Coulomb excitation. The reduced matrix element for the E3 transition $0^+(g.s.) \rightarrow 3^-$, $BE3\uparrow$, was also obtained. The deviation of the angular distributions from first order theory (the reorientation effect) directly depends on Q and in special cases, as here, there are no other competing second order processes. Both the sign and magnitude of Q can be determined. The results are

$$Q = -1.3 \pm 0.6 \text{ b}$$

and $$BE3\uparrow = 0.58 \pm 0.04 \ e^2b^3.$$

Experimental angular distributions were taken over the angular range 80°-170° using a multiple solid state detector array at α energies of 19, 18, and 17.5 MeV and at an oxygen energy of 69.1 MeV. Differential inelastic cross sections are in the range 10-40 μb/sr for α's, and 200-300 μb/sr for oxygen*. As discussed earlier[1] the 19 MeV data showed strong interference between the CE amplitude and an amplitude from direct nuclear excitation even though the bombarding energy was "safely below the Coulomb barrier" according to usual prescriptions. The other three data sets showed no such interference and are considered to be examples of pure E3 Coulomb excitation. They were analyzed simultaneously

---

*An example of the oxygen data is given in Fig. 31-1 of this Report.

using the symmetrized semi-classical Coulomb excitation theory of Alder et al[2] in terms of the two parameters quoted above. Fig. 30-1 shows the correlation between BE3↑ and Q; the curve encloses parameter regions such that χ^2 for the 26 data points $\leq 2\chi^2_{min}$ and defines an acceptable region. Our quoted errors are shown and are considerably larger than those arising from the least squares analysis (also shown on the figure); however, we feel they are appropriate to the data and the uncertainties in the theoretical analysis.

Interim results of this study have been presented[3,4] and the final report[5] will appear in The Physical Review.

References

1. A.R. Barnett and W.R. Phillips, Annual Report 1968, J.H. Williams Laboratory, p. 119.

2. K. Alder, et al, Revs. Mod. Phys. 28, 432 (1956).

3. A.R. Barnett and W.R. Phillips. B.A.P.S. 13, 1470 (1968).

4. A.R. Barnett and W.R. Phillips, Proceedings of the Heidelberg Heavy Ion Conference, July 1969.

5. J.H. Williams Laboratory, preprint, COO-1265-73.

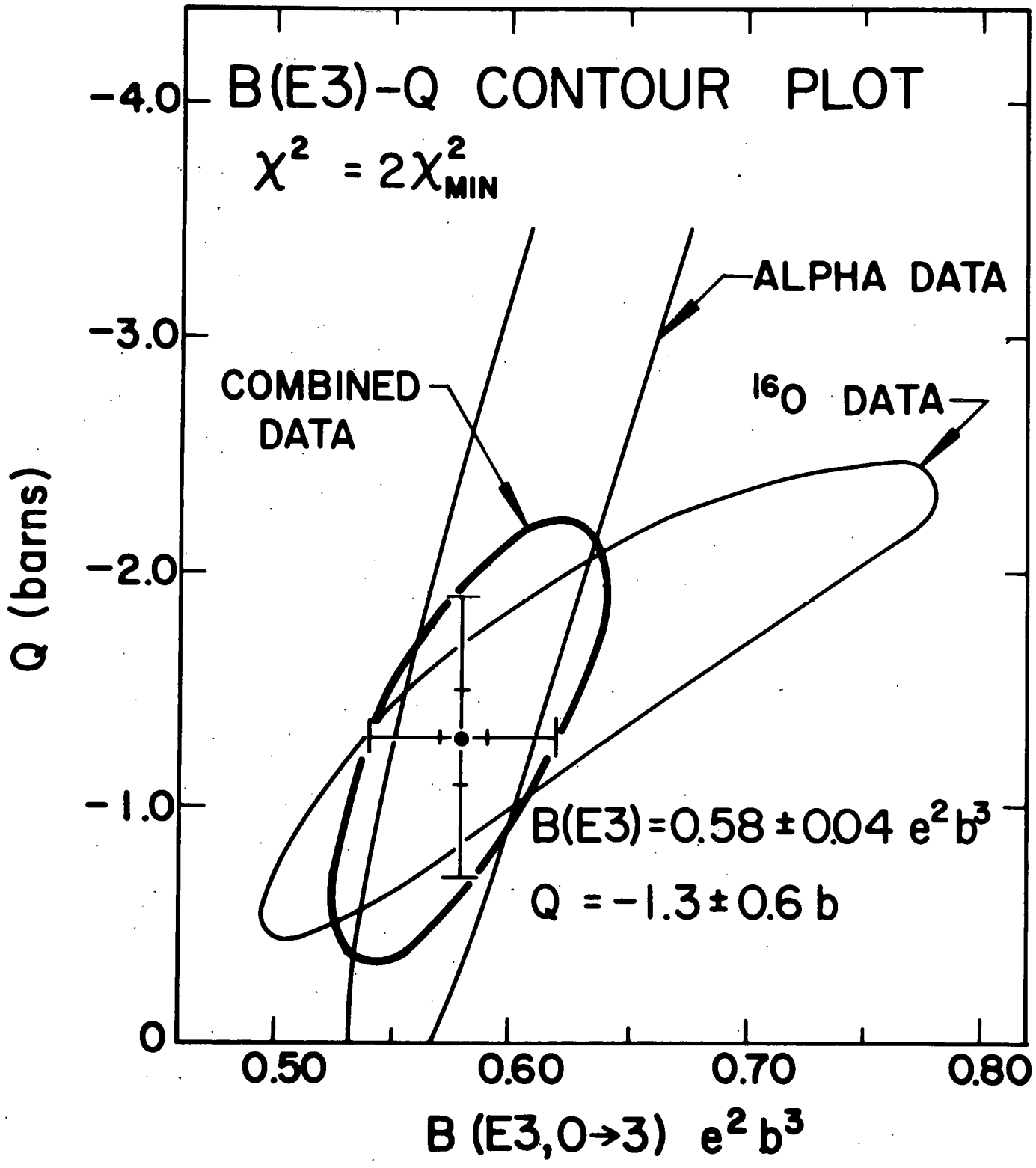
B(E3)-Q CONTOUR PLOT
$\chi^2 = 2\chi^2_{MIN}$
ALPHA DATA
COMBINED DATA
^{16}O DATA
B(E3)=0.58 ± 0.04 e^2b^3
Q = −1.3 ± 0.6 b
Q (barns)
B (E3,0→3) e^2b^3
−4.0
−3.0
−2.0
−1.0
0
0.50
0.60
0.70
0.80

Fig. 30-1

31. Neutron and Proton Tunnelling Reactions on ^{208}Pb

W. R. Phillips and A. R. Barnett

Neutron pickup and proton stripping reactions below the barrier have been measured for 69.1 MeV ^{16}O ions on ^{208}Pb. The bombarding energy is 11 MeV below a "barrier height" E_C given by $E_C = Z_1 Z_2 e^2/R$ with $R = 1.5(A_1^{1/3} + A_2^{1/3})F$.

Reaction products were observed over the angular range 100°-170° in six solid state detectors arranged in a precision scattering chamber. In order to observe the reaction groups below the intense elastically scattered group, it was necessary to obtain a peak to valley ratio of 10^5:1 in the detectors; this was achieved by careful attention to beam definition and collimator edges. Fig. 31-1 shows two typical spectra, at 160° and at 170°. Below the elastic peak (whose scale is x 1/1000) is a group arising from Coulomb excitation of the 3^- level in ^{208}Pb (see Section 30 in this report), next an overlapping series of groups arising from the stripping reaction $^{208}Pb(^{16}O,^{17}O)^{207}Pb$. The next series of groups comes from the pickup reaction $^{208}Pb(^{16}O,^{15}N)^{209}Bi$, the strong state being from the $^{15}N_{g.s.} + {}^{209}Bi_{0.895\ MeV}$ reaction. The peak at channel 295 is an elastically scattered ^{16}O group of a different energy and serves as a calibration line; the other groups were identified by their kinematic variations with angle.

The differential cross sections were obtained in a straightforward way by comparison with the elastic peak; the elastic scattering was shown

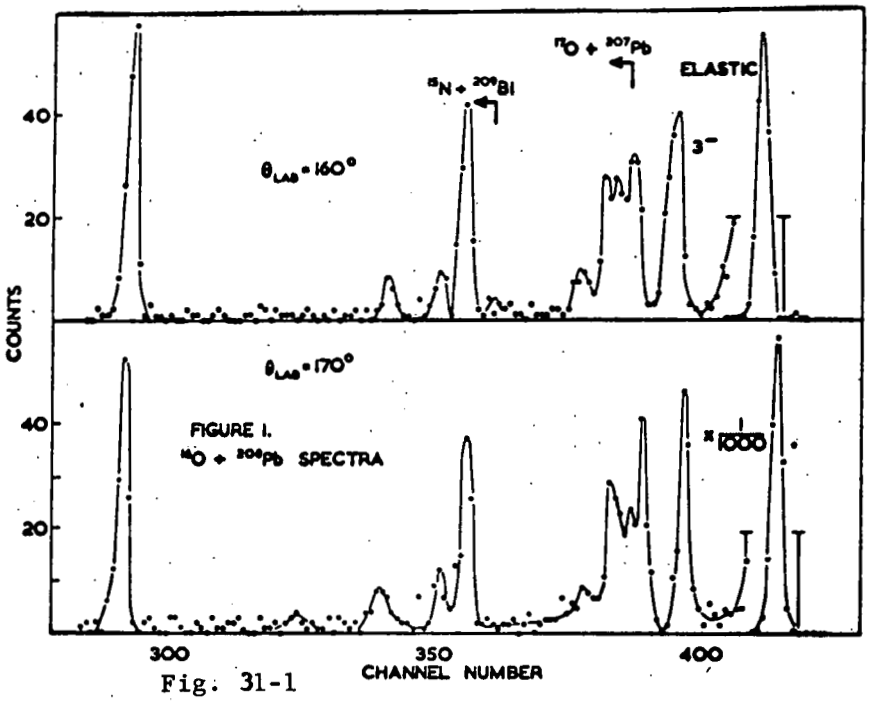

Fig. 31-1

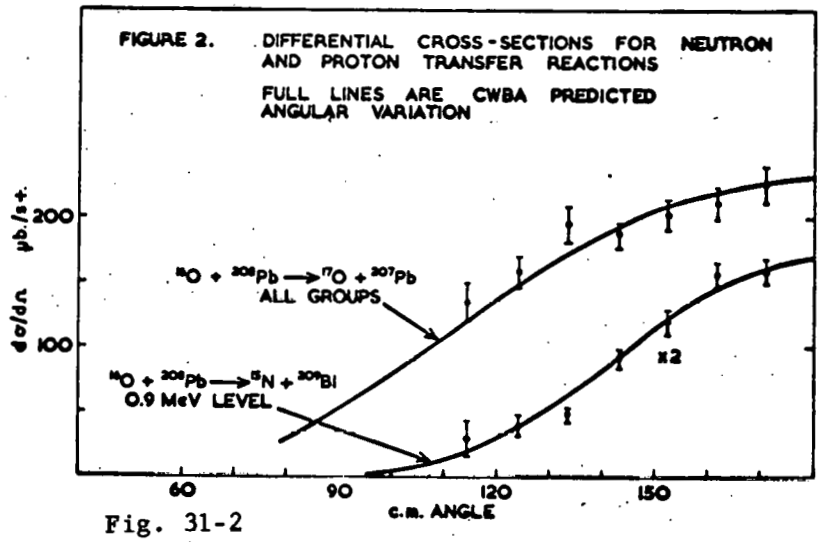

Fig. 31-2

to be pure Rutherford to ± 0.3%. Fig. 31-2 shows the values obtained for the sum of all the transitions leading to levels in $^{17}O + ^{207}Pb$, and for the proton tunnelling leading to the 0.895 MeV f 7/2 state of ^{209}Bi. Table 31-1 gives estimates of the relative total cross sections for the individual neutron tunnelling reactions.

The total cross section for neutron pickup involving all levels is 2.2 ± 0.1 mb. This figure includes a correction for the Coulomb excitation of the 2^+ 4.07 MeV state of ^{208}Pb, which contributes to the partially resolved neutron spectrum. Table 31-2 gives values for the total cross sections for the individual proton tunnelling reactions. These data have been reported at a recent Heavy Ion Conference.[1]

Tunnelling reactions below the barrier can be analyzed using DWBA;[2] the distorted waves become Coulomb wave functions and uncertainties associated with optical model parameters disappear. This and the increased versatility of heavy ion reactions would make tunnelling a useful source of spectroscopic information if the mathematical analyses could be improved, as has been realized since the early work in the field.[3] If one makes various approximations in the CWBA expression[4] for the transition amplitude, then the angular distribution of the nucleon tunnelling groups is given by

$$d\sigma(\theta)/d\Omega = C \operatorname{cosec}^3\theta/2 \exp\left[-2\eta\chi k^{-1} \operatorname{cosec} \theta/2\right]$$

where η and k are the mean Sommerfelt parameters and wavenumber in the two channels. The quantity χ for neutron transfer is related to the neutron binding energy in ^{17}O, B_n by $\chi = (2m_n B_n/\hbar^2)^{1/2}$, but for proton

TABLE 31-1 $^{208}Pb + {}^{16}O \rightarrow {}^{17}O + {}^{207}Pb$

Main Configuration of ^{17}O Level	Main Configuration of ^{207}Pb Level	Q MeV	Relative σ_{Total}
$d^5/_2$	$(p^1/_2)^{-1}$	-3.23	1.0
$d^5/_2$	$(f^5/_2)^{-1}$	-3.80	0.75 ± 0.15
$d^5/_2$	$(p^3/_2)^{-1}$	-4.12	0.70 ± 0.15
$s^1/_2$	$(p^1/_2)^{-1}$		
$d^5/_2$	$(i^{13}/_2)^{-1}$		
$s^1/_2$	$(p^3/_2)^{-1}$	-4.86	0.2 ± 0.08
$s^1/_2$	$(f^5/_2)^{-1}$		

TABLE 31-2 $^{208}Pb + {}^{16}O \rightarrow {}^{15}N + {}^{209}Bi$

Main Configuration of ^{15}N Level	Main Configuration of ^{209}Bi Level	Q MeV	σ_{Total} μb
$(p^1/_2)^{-1}$	$h9/_2$	-8.32	30 ± 25
$(p^1/_2)^{-1}$	$f7/_2$	-9.22	302 ± 16
$(p^1/_2)^{-1}$	$i13/_2$	-9.93	80 ± 20
$(p^1/_2)^{-1}$	$p1/_2$	-11.43	100 ± 18
$(p^1/_2)^{-1}$	$p3/_2$	-11.94	

transfer a value larger than that corresponding to the proton separation energy in ^{209}Bi, B_p, should be used.[2] This procedure leads to a more rapid fall off with angle than for the neutron transfer. The prediction for the angular distribution shape is nearly independent of angular momentum and should apply to all the neutron transfers and, separately, to the proton transfers. The full line of Fig. 31-2 is the curve for B_n=4 MeV and B_p =14 MeV. The good fits to the angular distributions using the CWBA suggest that such treatments of proton and neutron tunnelling reactions may be valid.

Recently[5] Buttle and Goldfarb have examined the ξ and Q value dependence of the cross sections ($\xi = \eta_f - \eta_i$) and can account quite well for the relative strengths of the different groups in both the proton and neutron cases. In particular, the very weak g.s. transition in the proton pickup reaction, $^{15}N_{g.s.} + {}^{209}Bi_{g.s.}$, compared with $^{15}N_{g.s.} + {}^{209}$Bi(0.90 MeV) can be understood. Further refinement in the calculations is needed before the absolute magnitude of the proton transfers can be predicted; for the neutron transfer the absolute magnitudes agree quite well with experiment.

References

1. W.R. Phillips and A.R. Barnett, Proceedings of the Heidelberg Heavy Ion Conference, July 1969.
2. P.J.A. Buttle and L.J.B. Goldfarb, Nucl. Phys. A115, 461 (1968).
3. See, for example, G. Breit and M.E. Ebel, Phys. Rev. 103, 679 (1956).
4. R.H. Lemmer, Nucl. Phys. 39, 680 (1962).
5. P.J.A. Buttle and L.J.B. Goldfarb, Proceedings of the Heidelberg Heavy Ion Conference, July 1969.

VI. ANALOG STATES AND COULOMB DISPLACEMENT ENERGIES

32. Isospin Mixing for Bound Analog States in ^{56}Co and ^{58}Co

T. G. Dzubay and R. Sherr (Princeton University)
and
F. D. Becchetti, Jr. and D. Dehnhard

Transitions to levels in the vicinity of the ground state analogs in ^{56}Co and ^{58}Co have been investigated using the Fe(^{3}He,t)Co reactions at 24.6 MeV. Two predominantly L=0 transitions, 70 keV apart, were observed where the analog state in ^{56}Co was expected to occur. For the analog state in ^{58}Co two pure L=0 transitions spaced at 20 keV were observed. Tentative assignments of 0^{+} are made for all four levels. These phenomena are described in terms of large isospin mixing of the analog state (T=To) with a T=To-1 state. The observed cross-section ratios and splittings are used to estimate off-diagonal matrix elements for the charge dependent part of the nuclear Hamiltonian of 33 keV for ^{56}Co and 10 keV for ^{58}Co. The results are being prepared for publication.

---

33. Measurement of Coulomb Displacement Energies Using the (He^{3},t) Reaction

F. D. Becchetti, Jr. and D. Dehnhard
and
T. G. Dzubay (Princeton University)

Coulomb displacement energies for thirty-three isotopes between Ca^{42} and Zn^{68} inclusive have been measured using the (He^{3},t) reaction at an incident energy of 24.6 MeV. Triton spectra were taken at $\theta_L=18^{o}$

using a calibrated position-sensitive detector in the focal plane of the split-pole magnetic spectrometer. Most of the measurements were made with isotopically enriched targets. The elastic He^3 yields at 18^o were used to extract the target thicknesses and compositions from which absolute and relative (He^3,t) cross sections were calculated.

In most of the spectra a single strong transition to the IAS (isobaric analog state) of the target nucleus could be identified and an unambiguous Coulomb displacement energy calculated from the Q value. For several of the odd-even targets analogs to the first excited state could also be identified. The triton spectra for several targets such as Ti^{50}, Fe^{56}, Fe^{58}, and Ni^{64} showed several strong transitions in the region expected for the analog state. In these cases the cross sections to any single state were lower than expected from the (He^3,t) cross section systematics. Two cases in particular, $Fe^{56}-Co^{56}$ and $Fe^{58}-Co^{58}$, were investigated further. For Co^{58} and probably Co^{56} the results indicate isospin mixing of the analog state with other 0^+ states in the residual nucleus (see Section 32).

The triton spectra obtained from Ni(He^3,t)Cu with A=58,60,61,62 and 64 are shown in Fig. 33-1 . One channel in the XE/E position spectrum corresponds to about 1.7 keV in energy. The bottom spectrum was obtained using a 68 $\mu g/cm^2$ natural nickel foil. The others are for 63, 31 and 34 $\mu g/cm^2$ enriched targets of $Ni^{61,62,64}$ respectively on 15 $\mu g/cm^2$ carbon backings. The states identified as ground state analogs (IAS) and first excited state analogs (IAS*) are labelled with arrows. The unlabeled peak in the A=58,60 spectrum is the 1^+ ground state in Cu^{58}. In Ni^{64} two peaks, 17 keV apart, are seen at the energy expected for the IAS.

The (He^3,t) spectra are being analyzed using the peak fitting rou-

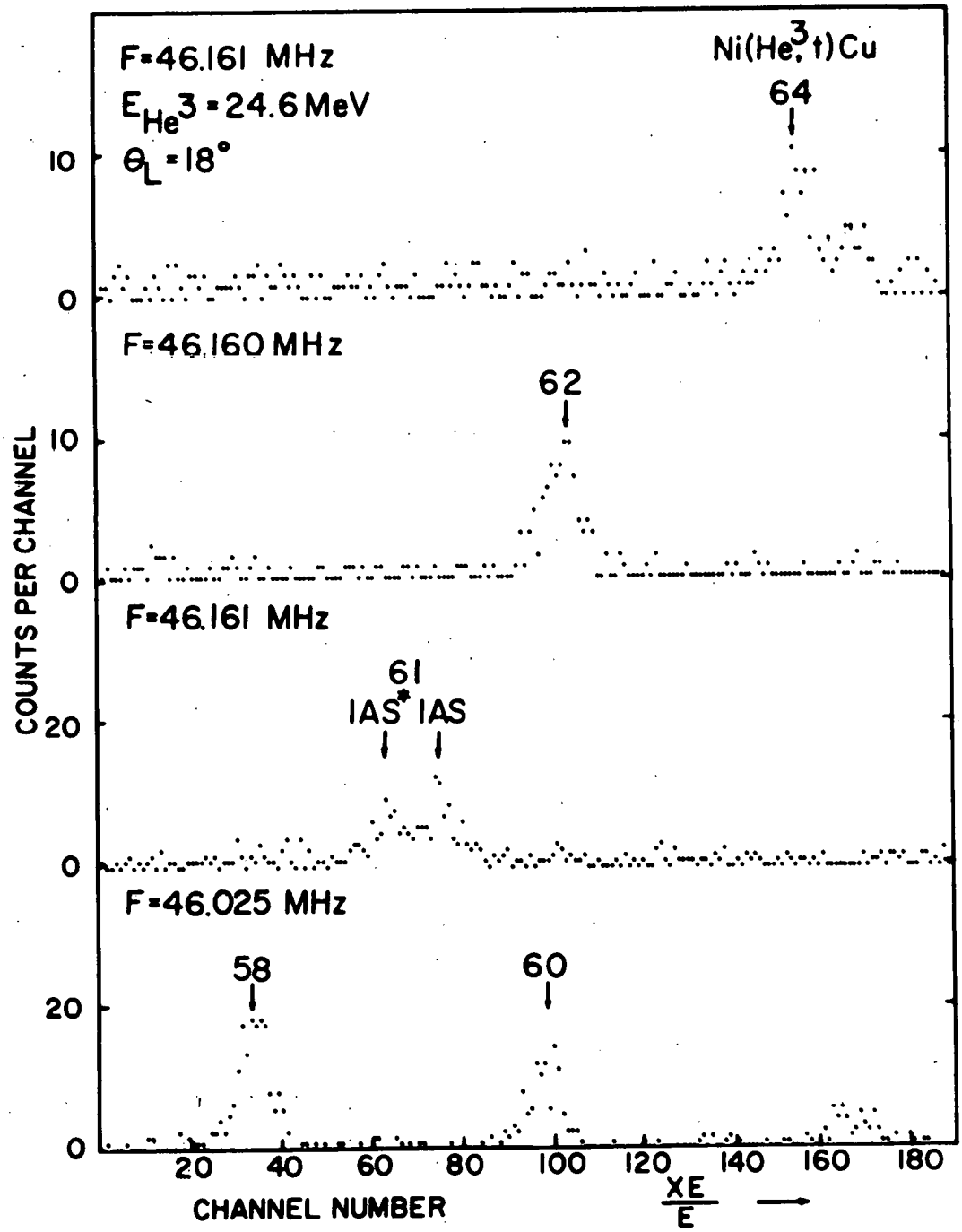
F=46.161 MHz
E_{He^3} = 24.6 MeV
θ_L = 18°
Ni(He^3, t)Cu
64
F=46.160 MHz
62
F=46.161 MHz
61
IAS*
IAS
F=46.025 MHz
58
60
COUNTS PER CHANNEL
CHANNEL NUMBER
XE/E

Fig. 33-1

tine GPF. Correction for energy losses in the target, etc., are included. The final Coulomb energies for most targets should be accurate to better than ± 5 keV relative to the calibration energies. The results are being prepared for publication.

---

34. Calculations of Coulomb Displacement Energies

F. D. Becchetti, Jr. and G. W. Greenlees

Calculations of Coulomb displacement energies based on the model of Nolen et al[1] have been performed for several 1f-2p shell nuclei as well as Zr^{90}, Sn^{120}, and Pb^{208}. This model yields a value for the ms radius of the neutron excess from which an estimate of the differences in the neutron and proton rms radii can be made. The results indicate such differences, Δ_{np}, for Ni^{58} of 0.00 ± .08 F, for Zr^{90} Δ_{np} = 0.02 ± .08 F, for Sn^{120} Δ_{np} = 0.05 ± 0.10 F, and for Pb^{208} Δ_{np} = 0.09 ± 0.10 F. The errors reflect uncertainties in the exchange and core overlap corrections, and the core neutron radii. These results are similar to those obtained by Friedman, et al,[2] and by Schiffer,[3] and in Section 38 of this Report, but indicate differences smaller than those calculated from reasonable single particle potentials.[4]

References

1. J.A. Nolen, J.P. Schiffer, and N. Williams, Phys. Lett. 27B, 1 (27 May 1968).

2. E. Friedman and B. Mandelbaum (preprint).

3. J.P. Schiffer, in Proc. of the Second Conf. on Nuclear Isospin, Asilomar (to be published).

4. C.J. Batty and G.W. Greenlees, Nucl. Phys., in press.

VII. THE OPTICAL MODEL OF THE NUCLEUS

35. The Elastic Scattering of 9.8 MeV Protons

Watson, Sievers, Greenlees, Poppe

During the past 12 months the measurements of the elastic scattering of 9.8 MeV protons have been completed. Cross section and polarization angular distributions have been measured for the isotopes ^{54}Fe, ^{59}Co, ^{58}Ni, ^{64}Ni, ^{68}Zn, ^{90}Zr, ^{120}Sn, and ^{181}Ta over the angular range 17.5° to 160.0°. The polarization data were taken using the polarized beam from the Linear accelerator and the cross sections using a 9.8 MeV proton beam from the MP Tandem. The cross section data have an absolute normalization uncertainty of at most 2% over the whole angular range. The uncertainties in the polarization data range from 0.005 at the forward angles to 0.05 at the backward angles.

The data are at present being analyzed in terms of the standard optical model and also using the approach of Greenlees, Pyle, and Tang.[1] Figs. 35-1 and 35-2 show fits obtained to some of the data.

References

1. Greenlees, Pyle and Tang, Phys. Rev. 171, 1115 (1968).

---

36. The Elastic Scattering of 16 MeV Protons

W. Makofske, H. Liers and G. W. Greenlees

A number of experimental modifications in measuring absolute differential cross sections for proton elastic scattering have been made in the past year. The angular acceptance of the Ortec chamber Faraday Cup has been enlarged to approximately 9° in order to avoid beam losses due to

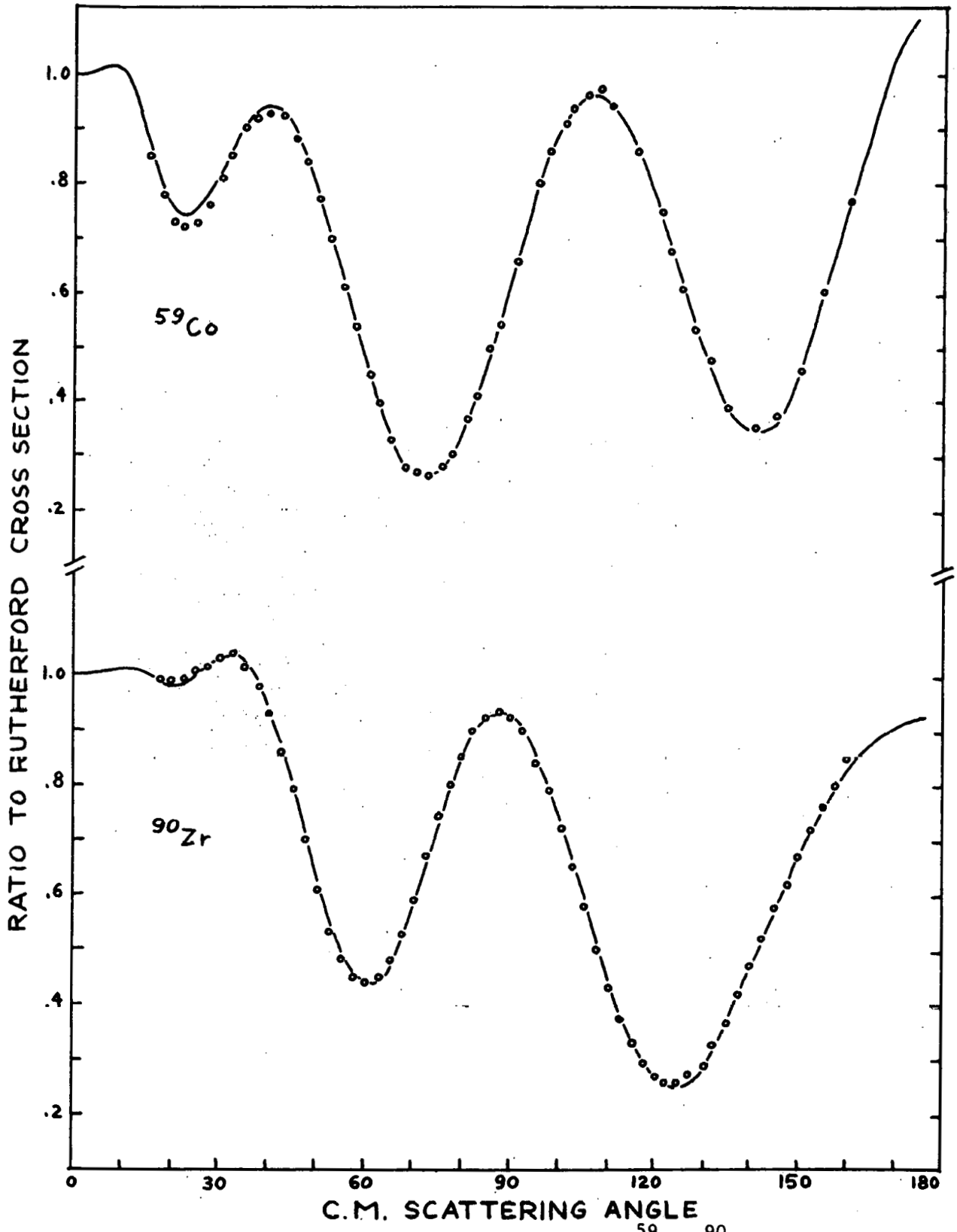

Proton elastic scattering cross-section data for ^{59}Co, ^{90}Zr at 9.8 MeV. The curve is a standard optical model fit to the data.

Fig. 35-1

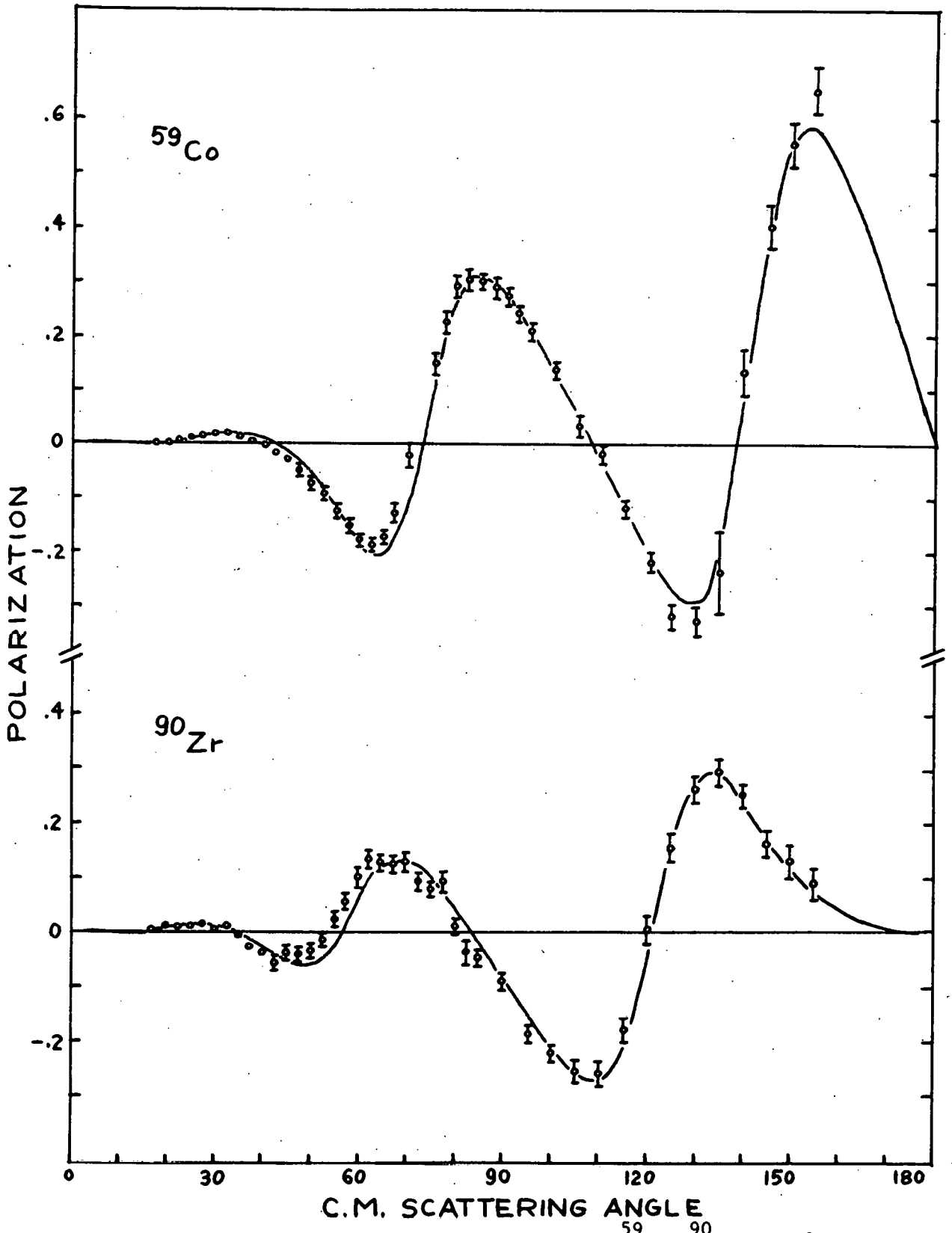

Proton elastic scattering polarization data for ^{59}Co, ^{90}Zr at 9.8 MeV. The curve is a standard optical model fit to the data.

Fig. 35-2

multiple scattering at low energies. This allows absolute normalizations to be determined with negligible error from multiple scattering for target thicknesses of up to 5 mg/cm^2 at an incident bombarding energy of 5 MeV. Tests have also been made verifying that errors in charge collection arising from knockout electrons from the target are negligible for an incident proton beam.

A system of two fixed-angle monitor detectors has also been designed and built for the Ortec chamber. These detectors can be mounted out of the scattering plane at a number of positions along the chamber wall. They allow monitoring of target thickness variations due to beam movements and target deterioration at all angles without interfering with the present method of measuring the cross section on either side of the beam at the same angle to average out angular shifts due to beam movements. This method also eliminates the need for overlap runs when changing target angle since the target thickness is measured for every run.

These changes, coupled with small beam defining collimators, allow us to take data of about 1% relative accuracy and 2% absolute accuracy with the present system. Thus far, absolute cross sections have been measured over the angular range between 15° and 160° in 2.5° steps for ^{58}Ni, ^{60}Ni and ^{120}Sn. Partial data has been taken on ^{62}Ni, ^{64}Ni, ^{90}Zr and ^{208}Pb.

37. The Elastic Scattering of 40-MeV Protons by Even Isotopes of Ni and Zn

H. S. Liers, R. N. Boyd, C. H. Poppe, J. A. Sievers and D. L. Watson

Measurements of the differential cross section and polarization for the elastic scattering of 40-MeV protons by the isotopes of ^{58,60,62,64}Ni and ^{64,66,68}Zn[1] have been completed. The data have been analyzed using both the standard optical model and the Greenlees, Pyle and Tang approach[2] in which the real part of the central potential and the spin orbit potential are obtained from the two-nucleon potential and the neutron, proton, and matter point-density distributions. Root-mean-square radii have been extracted from the data, but no systematic trend is evident for an isotopic sequence. Within the errors, no symmetry dependence is found for the ratio of the volume integral of the real central potential to the mass number.

A manuscript describing the experiment and the results of the analysis has been prepared for submission to the Physical Review.

References

1. Williams Laboratory of Nuclear Physics, Annual Report (1968), pp. 51-53.

2. G. W. Greenlees, G. J. Pyle, and Y. C. Tang, Phys. Rev. 171, 1115 (1968).

38.

An Analysis of Proton Elastic Scattering Using Potentials Derived from Nucleon Density Distributions and Two-Body Potentials

G. W. Greenlees, W. Makofske and G. J. Pyle

Recently Greenlees, Pyle, and Tang[1] developed an optical model in which the real parts of the potential were derived from nuclear matter distributions and the nucleon-nucleon force. When applied to proton elastic scattering at 14.5, 30.3, and 40 MeV the model was able to fit the data as well as standard optical model treatments despite having fewer adjustable parameters. For a given range of two-body force, values for the nuclear rms matter radii could be obtained. These values were greater than corresponding rms proton radii, derived from electron scattering and muonic x-ray work, and implied that the nuclear neutron rms radii were greater than the nuclear proton rms radii by about 0.6 F for all nuclei considered when a Yukawa two-body force of ms radius 2.25 F^2 was used.

Although the model, as developed in Ref. 1, gives a first order treatment of the problem, the actual analysis of data involved two additional assumptions in the calculation of the isospin and spin-orbit terms. In the present analysis, these approximations have been removed and proton data at 30.3 MeV analyzed using the complete model. It is found that the neutron-proton rms radii differences are reduced by 0.1-0.2 F for a Yukawa two-body force of ms radius 2.25 F^2. However, the fits to the data are found to be relatively insensitive to both the

magnitude of the isospin term and the range of the direct part of the nucleon-nucleon force. When these quantities are chosen to agree with a recent analysis of low energy nucleon-nucleon data, which used a Gaussian shape, a further reduction is effected in the nuclear neutron-proton rms radius differences to values around zero for medium-weight elements and 0.1-0.2 F for heavy elements.

Confirmation is provided that the volume integral and the rms radius of the real central potential are well-defined quantities which can be extracted from elastic scattering data as was suggested in Ref. 1 and by Becchetti et al.[2] This result is insensitive to detailed form of the potential used.

References

1. G. W. Greenlees, G. J. Pyle and Y. C. Tang, Phys. Rev. 171, 1115 (1968).

2. F. D. Becchetti, Jr. and G. W. Greenlees, Phys. Rev. (to be published).

39.

Further Optical Model Analysis of 30.3 MeV Proton Elastic Scattering Data

G. W. Greenlees and W. Makofske

Recently elastic scattering polarization data on ^{58}Ni, ^{120}Sn and ^{208}Pb at 30.3 MeV have become available over the angular range from 10°-165° in five degree intervals with an absolute accuracy of 0.005-0.02.[1] These data, together with the corresponding differential cross section data,[2] are being analyzed with the standard optical model and a

version in which the real parts of the effective interaction potential are derived from the nuclear density distribution and components of the nucleon-nucleon force.[3] Preliminary results seem to indicate that the model cannot fit medium weight nuclei nearly as well as heavy nuclei. This suggests that some feature, perhaps A dependent, is lacking in present formulations of the optical model.

References

1. G. W. Greenlees, J. Lowe, O. Karban and V. Hnizdo, Rutherford Laboratory Report RHEL/R170 (1968).

2. B. W. Ridley and J. F. Turner, Nucl. Phys. 58, 497 (1964).

3. G. W. Greenlees, G. J. Pyle and Y. C. Tang, Phys. Rev. 171, 1115 (1968); G. W. Greenlees, W. Makofske and G. J. Pyle (to be published).

40.

Optical Model Analysis of He^3 and Alpha-Particle Elastic Scattering

J. S. Lilley and D. D. Leavitt

Optical model analysis of 29 MeV He^3 elastic scattering data[1] revealed several parameter sets which gave approximately equivalent fits. The combination of large radius and small diffuseness fits to the data were as good as fits from a small radius and large diffuseness. Good fits to the data were achieved with radii from 0.99 $A^{1/3}$ to 1.3 $A^{1/3}$, diffuseness from 0.6 to 0.89, and potentials from 90 to 360 MeV. The potential form factors for all these fits shared a common point of intersection at a radius in the interaction region. Volume integrals for these fits ranged from 240 MeV-F^2 to 825 MeV-F^2. Data analyzed extended out to less than 100 degrees. For larger angles, the predicted cross

sections of the different fits varied significantly. To see if some of these ambiguities can be resolved, we are measuring scattering cross sections over the entire angular range. Measurements are presently being made on Ni^{58} and Ti^{48}, and will be extended to other isotopes. Since the counting rate at large angles is very small, the particle identification computer routine has been modified to handle incoming data from three detectors, allowing simultaneous measurements of three angles.

Compared to He^3 elastic scattering data, alpha scattering data displays much more diffraction structure and thus allows less ambiguity in the optical model parameters. Fits to alpha scattering data tend to favor a large radius and small diffuseness. Again, large angle data is scant. However, recent Polish data, $K^{39}(\alpha,\alpha)K^{39}$,[2] suggests a possible angular dependence of the parameters, that is, better fits at large angles with large diffuseness and small radius, while the forward angles are better fit with smaller diffuseness and large radius. We plan to investigate the complete angular scattering range for other nuclei to see if this same dependence is exhibited, and to determine what form factor is required to give a good fit over the entire angular range.

References

1. Baugh, Pyle, Rolph, and Scarrott, Elastic Scattering of 29 MeV He^3 by Complex Nuclei, preprint, University of Birmingham, England (1966).

2. Brobrowska, Budzanowski, Grotowski, Jarczyk, Micek, Hiewodniczanski, Strzalkowski, and Wrobel, Elastic Scattering of Alpha Particles on ^{39}K Nuclei in the Energy Range from 22.1 MeV to 28.2 MeV, I.N.T. Cracow Report, 613/PL.

41. Standard Optical Model Parameters

F. D. Becchetti, Jr. and G. W. Greenlees

The analysis of nucleon-nucleus elastic scattering using the standard optical model has been completed and the results are in press (Physical Review).

The technique used in the nucleon-nucleus analysis, i.e., the simultaneous fitting of a large amount of data in terms of explicit parameterization of the optical parameters with energy, (N-Z)/A, etc. is being extended to the analysis of He^3 and triton elastic data.

A preliminary set of parameters has been found that gives a reasonable fit to the He^3 and triton data analyzed ($\chi^2/N \simeq 13$). These parameters are:

He^3: $V_R = 136.4 - 0.17E + 55(N-Z)/A$

$W_V = 41.3 - 0.33E + 63(N-Z)/A$

triton: $V_R = 165.0 - 0.17E - 7(N-Z)/A$

$W_V = 46 - 0.33E - 110(N-Z)/A$

$r_R = 1.20$, $a_R = 0.72$, $r_I = 1.40$, $a_I = 0.86$, $W_{SF} = 0$, $V_{SO} = 0$

These parameters are in no way unique and represent only one of several sets that give comparable fits to the data. The inclusion of spin orbit coupling improves the fits only slightly ($\chi^2/N \simeq 9$) but for convenient use in DWBA calculation the parameters given here are for $V_{so}=0$.

VIII. EXPERIMENTAL AND DATA ANALYSIS PROCEDURES

42. Enge Split-Pole Spectrometer Programs

M. Oothoudt and P. Vedelsby

During the past year, five programs have been written to aid in analyzing photo-plate spectra. All of the programs use calibrations giving either the distance along the focal plane (d) as a function of the radius of curvature (ρ) in the main field of the magnet or ρ as a function of d. The calibration was obtained by making exposures at several magnetic field settings for a peak of known energy; a separate calibration must be made for each pair of settings for the screws which position the plate holder.

PROGRAM MMM reads scanning results from the card reader and displays the spectrum on the oscilliscope. Tagging channels of a peak result in integration of the peak and calculation of its center of gravity. From this distance the $B\rho$ value of the peak, its absolute energy, and its Q value are calculated.

PROGRAM ESPKIN is a kinematics program to aid in identifying peaks by their $B\rho$ and d values found with MMM. Given reaction data on a set of up to 150 reactions, the program calculates relativistically correct kinematics and prints out results in order of decreasing $B\rho$ and d.

PROGRAM F calculates the frequency necessary to place a peak at a given location along the focal plane.

PROGRAM D calculates the location of a peak for given reaction parameters. Using PROGRAMS F and D, one may calculate the frequency necessary to place the peak of highest $B\rho$ of interest at the highest convenient

d of the plates while making sure that other peaks of interest do not fall on file marks or in joints between plates.

PROGRAM Q calculates the absolute energy and reaction Q value of peaks found at given d values.

---

43. Q-Value Computation Programs

H. Ohnuma

A program which calculates nuclear reaction Q-values is developed. This program is small enough to fit to the CDC 3100 computer, so that an experimenter can calculate necessary Q-values in the course of his experiment. Q-values are based on the 1964 Mass Table[1] and additions and corrections are made according to recent literature.[2,3,4,5]

This program can

I) make a table of mass excesses and masses;

II) calculate Q-values for

1) one reaction on all known nuclei;

2) one reaction on all stable (normally available) nuclei;

3) reactions with one incident particle on one target nucleus and various outgoing particles;

4) one reaction on one target;

III) make a Q-value for up to 11 incoming particles and 22 outgoing particles on all stable (normally available) nuclei.

The program can take more than one outgoing particle for a reaction, thus enabling one to calculate Q-values for reactions such as (α,3n).

References

1. J.H.E. Mattauch, W. Thiele, and A.H. Wapstra, Nucl. Phys. 67, 1 (1965).
2. T. Lauritsen and F. Ajzenberg-Selove, Nucl. Phys. 78, 1 (1966).
3. C. Maples, G.W. Goth, and J. Cerny, Nuclear Data 2, 429 (1966).
4. P.M. Endt and C. Van der Leun, Nucl. Phys. A105, 1 (1967).
5. F. Ajzenberg-Selove and T. Lauritsen, Nucl. Phys. A114, 1 (1968).

---

44. Digital "Leaky Integrator" Routine to Compensate for Beam Intensity Variations

A. R. Barnett, J. H. Broadhurst and R. W. Goodwin

The standard methods of determining the effective charge in an activity measurement are:

1) Saturate the activity by bombarding for a time $T \gg T_{1/2}$, $T_{1/2}$ = the known half-life, so that the activity at the start of the counting cycle is proportional to the current (corrected for the time taken to turn off the beam and begin counting).

2) Bombard for a time $T \ll T_{1/2}$, thus approximating to an instantaneous charge Q at T=0, where $Q = \int I dt(1-1/2\lambda dt+\ldots)$ and λ is the decay constant, $\ln 2/T_{1/2}$.

3) Use a leaky current integrator and allow the accumulated charge to decay with a time constant set equal to the decay rate of the activity to be measured so that the effective charge at the start of the counting period is proportional to the activity.

Each of these methods has well known disadvantages. In method 1) undesired background activities can be built up and ideally the current

should be constant; in method 2) one approximates to the exponential activity increase by its linear first part but may not produce enough activity per cycle, again the current is assumed constant; and in method 3) one has the hardware problem of varying (often high) resistance values in order to achieve the correct decay constant in a separate preliminary experiment.

We have overcome many of these disadvantages in a simple manner by multiscaling the beam current integrator output; that is, by dividing the total bombarding plus wait period into (in our case) 128 equal time intervals and recording the number of beam current integration (BCI) pulses in each. For our BCI, full scale current gives an output of 100 pulses/sec. The data can be recorded in an array and processed on-line, or subsequently. The effective charge at any later time T (when the detectors began recording activity data) can be easily calculated as $\sum q_i e^{-\lambda(T-t_i)}$ where q_i is the charge recorded at the time element labeled t_i. The activity data are recorded in a normal multiscaling system such as by the program ACT.[1] Since the beam intensity fluctuations have been recorded, accumulated over as many bombarding recording cycles as desired, one is not restricted to the bombarding time inequalities of methods 1) and 2). An important additional advantage is that the effective charge can be calculated for all of several activities which may be present in the data, without repeating the experiment.

An example of this technique arose when we were determining the (α,n) total cross section of ^{208}Pb and ^{209}Bi by α-activity measurements of the residual nuclei ^{211}Po and ^{212}At.[2] In the first use, ^{211}Po, only one activity is present with a half-life of 0.505 sec, and the program ACT was set up with a bombarding plus wait time of 2.56 sec, thus di-

gitizing the beam in 128 channels of 20 msec/channel. This was followed by 32 counting periods of the α-detectors of 100 msec, each recording 128 channels of energy information from the ADC. For the $^{209}Bi(\alpha,n)^{212}At$ reaction, however, two activities are formed, ^{212}At(0.30sec) and ^{212m}At (0.12sec) which have different α-decay spectra. By analyzing separately the different energy regions of the spectra and evaluating the effective charge for each activity, it is possible to measure simultaneously the (α,n) total cross section to the ground state and to the isomeric state of ^{212}At. This information is of direct relevance to the total reaction measurement of α's on ^{209}Bi at energies well below the Coulomb barrier.[2]

References

1. A.R. Barnett, R.W. Goodwin and W.D. Harrison, Annual Report, Williams Laboratory 1968, p. 168.

2. A.R. Barnett, J.S. Lilley and F. Chwieroth, This Report, Section 29.

45. 0° Measurements with the Split-Pole Magnetic Spectrometer

W. W. Dykoski and D. Dehnhard

The double focusing properties of the Enge split-pole magnetic spectrometer make it easy to do experiments at 0°. In many experiments, the measurement of the cross section at 0° is of considerable interest. We have performed several test experiments using the $^{29}Si(^{3}He,d)$ reaction at 25 MeV.

Between the target and spectrometer entrance aperture we placed a set of guard slits to prevent the beam from hitting that aperture. The size of the guard slits was such that they did not limit the solid angle given by the entrance aperture. A Faraday cup was placed in the focal plane of the spectrometer and a position-sensitive detector was placed at a larger ρ-value. The detector was covered with a polyethylene absorber foil of 30 mills thickness to stop any doubly scattered ^{3}He.

The position spectrum from the $^{29}Si(^{3}He,d)$ reaction to the 0.678 MeV and 0.709 MeV doublet in ^{30}P is shown in the Fig. 45-1 . We have not yet tried to detect particles at a ρ-value smaller than that of the particle beam because we expected considerable background due to slit edge scattering.

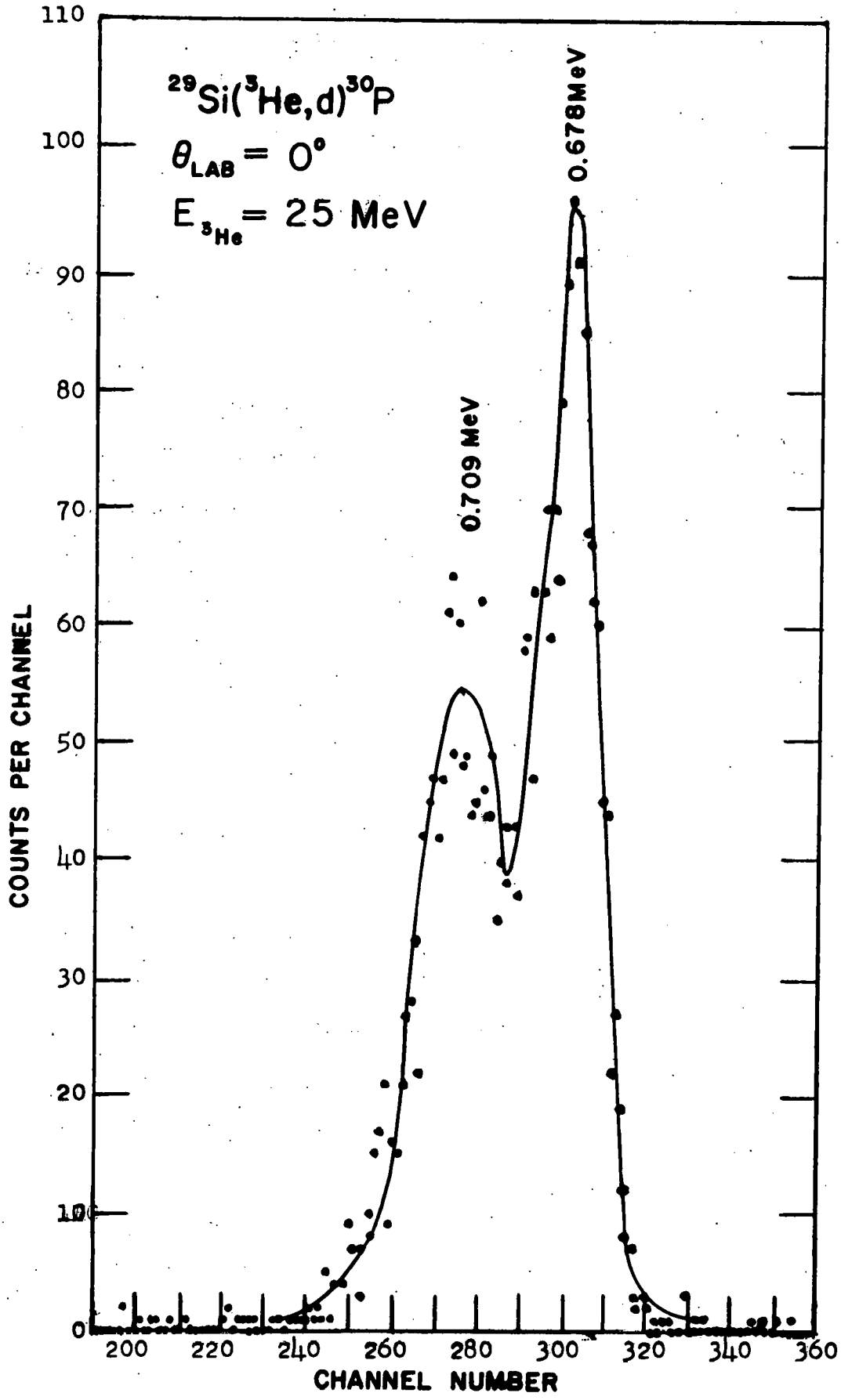
$^{29}Si(^{3}He,d)^{30}P$
$\theta_{LAB} = 0°$
$E_{^{3}He} = 25$ MeV
0.678MeV
0.709 MeV
COUNTS PER CHANNEL
CHANNEL NUMBER
0
10
20
30
40
50
60
70
80
90
100
110
200
220
240
260
280
300
320
340
360

Fig. 45-1

B. EXPERIMENTAL INSTRUMENTATION

46. Vacuum Target Transfer System

H. Ohnuma

In order to make contamination-free targets for materials which are easily oxydized or absorb humidity in the air, a new evaporation chamber, transfer box, and a storage chamber were designed. One can evaporate up to four targets in the chamber, put them in the transfer box, and attach it to the target chamber for the split-pole spectrometer, which is evacuated beforehand. One can store targets in a vacuum storage chamber when they are not used. This system has successfully been used for calcium targets so far.

---

47. Target Preparation Facilities

George Ott

The last year has seen a considerable expansion of the target preparation facility. A new vacuum system for evaporation and sputtering has been completed giving the laboratory a total of three vacuum systems available for target preparation. Two of the systems use oil diffusion pumps and the third is a turbo-molecular system. There has been put into operation a one-kilowatt continuous duty R.F. generator that provides power for sputtering.

The chemical steps in target preparation have been made more efficient by the establishment of a chemical laboratory in a room having a fume hood which is adjacent to the target preparation room.

The target laboratory processed and completed over 150 requests for targets making a total of nearly 500 individual targets from the following elements:

Aluminum, Antimony, Barium, Bismuth, Beryllium, Boron, Cadmium, Calcium, Carbon, Chromium, Cobalt, Copper, Erbium, Fluorine, Gadolinium, Germanium, Gold, Indium, Iridium, Iron, Lanthanum, Lead, Lithium, Magnesium, Nickel, Nitrogen, Palladium, Phosphorus, Samarium, Scandium, Selenium, Silicon, Silver, Tellurium, Terbium, Tin, Titanium, Vanadium, Ytterbium, and Zirconium.

Samarium targets, which had previously been troublesome when using Lanthanum for reducing the oxide of Samarium, have now been made with great success using Titanium as the reducing agent. It was found that Lead, which is furnished in isotopic form as the nitrate by Oak Ridge, made target preparation easier if it was first heated in a test tube over a Bunsen burner thereby reducing it to the oxide before it was placed in the vacuum evaporator to make the target.

---

48. High Resolution Proton Spectrometer (HRS) for the Los Alamos Meson Physics Facility (LAMPF)

N. M. Hintz

For the past several years the author has been a member of the HRS design committee at Los Alamos. The group has been responsible for establishing specifications and weighing design trade-offs for a spectrometer to be used primarily for proton-nucleus experiments near 800 MeV. Also the HRS group considered a number of problems associated with beam background, targeting, and detection systems.

The LAMPF beam is to have a maximum energy of 800 MeV, energy spread ± 3.5 MeV and emittance of 0.075 π cm·mrad. Currents of up to 100 μa unpolarized or 600 na polarized should be available in the HRS area. Early in the game it was realized that little useful nuclear structure information could be obtained unless the overall energy resolution were considerably better than the ~7 MeV beam spread. A figure of 100 keV, FWHM, for $p+Mg^{24}$ at 45° was originally chosen, but this has recently been reduced somewhat and it is now expected that the overall resolution will be better than 50 keV, especially for heavier targets where kinematic energy variations with lab angles are less serious.

Various simple schemes were studied in first order by the committee, after which detailed calculations were made by H. Enge (MIT) and K. Brown (SLAC) on fancier systems. The nearly final proposal which has emerged is as follows: An H^- beam from the linac is stripped, bent, dispersed (horizontally) and then "twisted" ($x \rightarrow y$, $y \rightarrow x$) to give a vertically dispersed beam 1 cm wide by 13 cm high on the target. The spectrometer, whose dispersion is matched by the beam analysis system, is to consist of a quadrupole followed by two 75° uniform field sections (QDD) with shaped entrance and exit boundaries to correct aberrations. The bending radius will probably be in the vicinity of 4 meters to give higher dispersion and to allow ground state (p,t) reactions to be studied (~18 kG at R=4m). An acceptance solid angle of 2-3 msr should be anticipated. The entire system, magnets, mount, and shielding will weigh around 1000 tons and stand over 50 feet tall.

Because of the dispersion matching, the overall system will be achromatic from linac output to magnet focal plane. Thus, only energy loss in the target will be measured.

Final calculations (by Enge and Brown) are now underway in second

order and by ray tracing. Our schedule calls for final magnet and beam handling optics to be completed by September 1969 so then engineering design can proceed.

---

49. Magnetic Pair Spectrometer

R. A. Wallen and N. M. Hintz

Work on this project was discontinued in the fall of 1968 because of lack of the funds required to complete the needed electronics and computer interfacing.

C. ACCELERATOR PERFORMANCE AND DEVELOPMENT

50. Linear Accelerator Machine Operation

Peter Stasz

The Linear Accelerator was officially shut-down at 4:23 p.m. on January 7, 1969. During the final months of operation only necessary repairs were done to the machine to keep it operational so as to make available maximum experimental time. The ratio of 40 MeV to 10 MeV experimental time was roughly 55% to 45%.

During the period from September 1968 until shutdown the time available was divided as follows:

Experimental	2340 hours	78.5%
Trouble	382 hours	12.8%
Maintenance and Warm-up	159 hours	5.4%
Surplus	97 hours	3.3%
	2978 hours	100%

Distribution of experimental time:

10 MeV Unpolarized	8 hours	0.4%
10 MeV Polarized	1062 hours	45.4%
40 MeV Unpolarized	1008 hours	43.1%
40 MeV Polarized	262 hours	11.1%
	2340 hours	100%

The resnatrons operated well during the last year with resnatron 1 having logged 15,894 hours without repair.

Resnatron	Nominal Power Level	Hours Run	Openings
1	0.6 MW	2815.5	None
2	2.4 MW	1850	1
3	3.2 MW	0	None
4 (driver)	0.8 MW	2815.5	1

51. General Operation of the Tandem Van de Graaff

C. H. Poppe and P. Stasz

As in previous years, the Tandem was scheduled for 24-hour a day operation, seven days a week, with the exception that Monday morning is reserved for regular maintenance. In February it was decided to make the first Monday of every month an extended maintenance so that jobs too long to be completed during the regular half-day maintenance could be completed at monthly intervals.

From August to December, 1969 the machine ran extremely well and it was not necessary to enter the tank, By December, however, a large backlog of major maintenance and repair items had accumulated, so it was decided to schedule a shutdown and enter the tank. No unusual problems were encountered and after checking resistors, screens, etc. and installing replacements when necessary, the tank inside was cleaned and closed again. At this time a home-made einzel lens was installed in the source, replacing the original HVEC unit on the duoplasmatron source assembly. The glass in the HVEC einzel lens was attacked by Li vapor from the Li charge exchange canal and had developed a leak. The new design used a porcelain insulator instead of glass and is designed to that it is difficult for Li to deposit on the insulator.

After this scheduled shutdown, the machine again ran well until April 29 at which time the charging belt broke after 7394 hours of running time. Inspection of the belt tunnel showed that the breaking of the belt had caused no damage to the belt guides. The belt had apparently

worn through in one spot and the subsequent tear developed from that point. A new belt was installed and an attempt was made to align the belt tunnels. At this time it was discovered that the support brackets to which the belt guides are attached were cast in such a way that each belt guide would be slightly bowed downward. This bowing could be as much as 0.070 in. at the center and was highly variable. Furthermore, in the dead sections between accelerating columns, the belt guides were supported by a different kind of bracket which did not impart such a bowing to the guides. Hence, there would be a discontinuity in the belt tunnel at each dead section. It was suggested that this would be a major contributor to belt wear and an attempt to improve the situation was made by shimming the belt guides at the dead sections in such a way that they would be bowed approximately the same as the others.

During the belt change a careful inspection of the accelerating column was made, looking for sections which showed heavy tracks between electrodes. On the suggestion of the High Voltage Engineering Company, the worst of these sections were shorted out. A computer program which calculated beam trajectories through inclined-field accelerating tubes was used to insure that the shorting of sections was done in such a way so as to cause little or no change in the position and angle of the beam leaving the accelerator. In all, more than 10% of the accelerating column was shorted out.

After the belt change, terminal voltage did not reach the former maximum even after considerable conditioning. The columns appeared to

condition well, but whenever the terminal was pushed beyond 7 MV, sparks to the tank wall would occur every 5 to 10 minutes. Consequently, on June 9 the tank was again entered. It was discovered that a great deal of belt material in the form of dust and flakes was deposited in many places. The material was apparently coming from wearing of the inside of the belt on the bottom belt guides of the upper belt tunnel. It was decided to realign the upper belt tunnel in order to decrease belt wear. All of the upper belt guides and belt guide brackets were removed and the brackets were machined so that the horizontal surface which supports the belt guide will transmit little if any torque to the guide. Hence, the bowing of the guides mentioned above disappeared and the entire belt tunnel could be aligned accurately with respect to a piano wire stretched over the motor and alternator.

After this tank opening the machine operation was complicated by a series of minor problems, including low source output and trouble with the 300 kV isolation transformer. These problems were overcome and the machine ran well at 9.5 MV on the terminal. (The experimental program did not require any higher voltages.)

In order to check belt wear and to see if the realignment of the belt tunnel was successful, the tank was opened again on July 28. The inside was found to be unusually clean, so that after the usual resistor check and a thorough clean-out of the false floor under the terminal, the tank was closed up. By the next day a terminal potential of 8.8 MV had been easily reached and machine operation has been satisfactory since that time.

Beams of ^{1}H, ^{2}H, ^{3}He, ^{4}He, and ^{16}O have been used this year. ^{1}H and ^{2}H were used about two-thirds of the time, while ^{3}He and ^{4}He the remaining third. Only one run using ^{16}O was made this year.

The operation of the accelerator is summarized as follows:

Used for experimental work	4,422 hours	50.4%
Scheduled maintenance	821 hours	9.4%
Machine conditioning and operator training	1,217 hours	13.9%
Experiment set-up time	184 hours	2.1%
Machine development	88 hours	1.1%
Trouble time	1,736 hours	19.8%
Surplus	36 hours	.4%
Miscellaneous	256 hours	2.9%
	8,760 hours	100.0%

Experimental time is up from last year by 10%. Much of this has come from more efficient setting up of experiments and using only 1% of available accelerator time for machine development (most development has been done with the accelerator running). The small amount of surplus time indicates the degree to which time on the machine is requested.

52. The Enge Split-Pole Magnetic Spectrometer

D. Dehnhard

The magnetic spectrometer of the Enge-split-pole type[1] has been used quite extensively during the whole year. Because of the obvious advantage of having experimental data available for analysis on-line, many experiments were performed with an array of three position-sensitive detectors. In particular, when particle separation between deuterons and tritons was required, position-sensitive detectors were preferred over nuclear emulsion plates. Nevertheless, in many experiments photoplates were used successfully taking advantage of the broad range of the spectrometer. In no experiment was the full energy range of the magnet ($E_{max}/E_{min}=8$) used.

In most experiments resolution was limited by target thickness and not by spectrometer aberrations, detector noise, etc.

In an early test run an array of six detectors was set up and XE and E signals from three detectors were fed into two pairs of ADC's using an existing routing unit. It turned out that "cross talk" between various detectors in one pair of ADC's could not be completely eliminated and later experiments were therefore done with the use of three detectors whose signals were fed into three pairs of ADC's. A high quality routing system is presently under construction (J.H. Broadhurst) to be used for the six detector array in the spectrometer and for an array of $\Delta E/\Delta X \cdot E$ systems in the 8' scattering chamber or the ORTEC-chamber.

The variable (width and height) spectrometer entrance slit system--provided by the manufacturer--was found to be very unreliable. It was replaced by a slit system that allows use of five fixed size apertures without breaking vacuum. To determine the maximum vertical opening $2Z_1'$ for the spectrometer entrance aperture (see. Ref. 1), when a beam spot height of 2 mm is used, we have measured the counting rate as a function of the vertical opening for a set of five slits, 8.3 mm wide and 4, 6, 8, 10, and 12 mm high at a distance of 24.3 cm from the target. The beam was slightly defocused to assure uniform illumination of the target. We found (see Fig. 53-1) that at the high energy end of the focal plane ($\rho=\rho max$) the counting rate will be limited by the magnet pole faces at a vertical opening of $2Z_1' = 0.037 rad$. This is just slightly smaller than the 0.04 rad. opening recommended by H.E. Enge.[1] The difference is probably related to the finite target spot size. At smaller ρ-values, larger vertical openings can be used. They were determined by measuring the counting rate as a function of ρ with a fixed vertical aperture.

The position accuracy and reproducibility of the existing chain driven position detector mount was found to be too poor for experiments in which the detector position was to be changed. A new array mount and drive using a lathe screw was designed (W.W. Dykoski) and construction has begun. The detector position is designed to be reproducible to better than 0.05 mm corresponding to about 1 keV at 20 MeV at the high energy end. Fortunately, in most experiments detectors are kept at a fixed position and calibration is done by sweeping a peak of known energy across the detector by varying

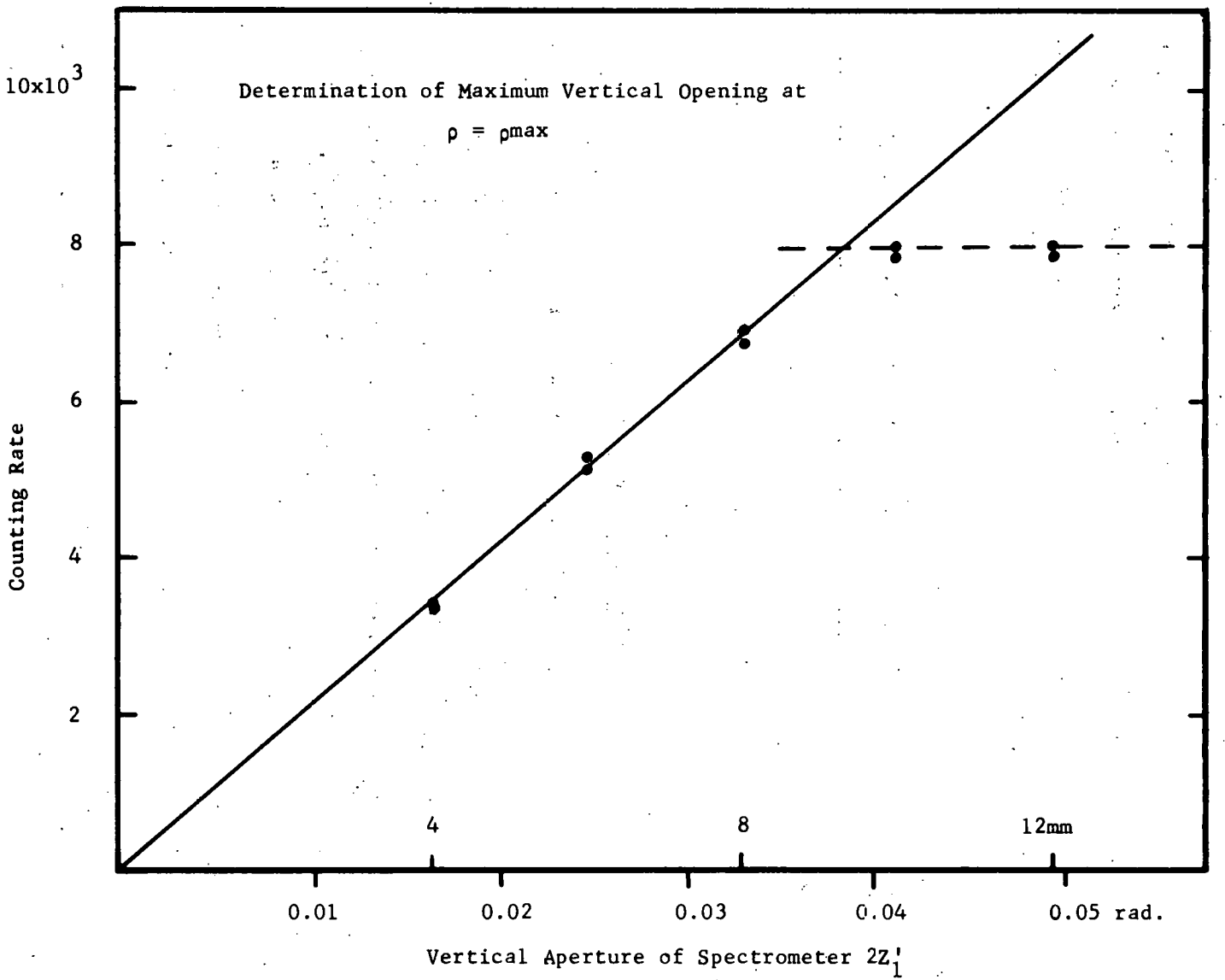
Determination of Maximum Vertical Opening at
ρ = ρmax
10x10^3
8
6
4
2
Counting Rate
4
8
12mm
0.01
0.02
0.03
0.04
0.05 rad.
Vertical Aperture of Spectrometer 2Z'1

Fig. 53-1

the magnetic field. This can be done to very high accuracy and excitation energies have been determined to better than 2 keV up to about 2 MeV.

Existing computer programs for use with the spectrometer have been improved and new codes have been written. They are described in Section 42 of this report.

References

1. J.E. Spencer and H.E. Enge, Nucl. Instr. and Meth. 49, 181 (1967).

---

53. On-Line Computer System

R. K. Hobbie, J. H. Broadhurst, R. Goodwin and B. Brown

The CDC-3100 computer in the Tandem Laboratory operated 8000 hours during the past year, or 160 hours per week. As in the past, the heavy demand for computer time for off-line analyses has been met only during occasional failure of the accelerator. The new disk/display system, mentioned in last year's progress report, is 90% complete. Funds for components for this unit have been provided by the Graduate School. Programming for this new system is in the planning stage.

---

54. Linear Accelerator Polarized Ion Source Operation

D. Watson and C. H. Poppe

During the period from August 1, 1968 until January 7, 1969, when the linear accelerator was shut down, the polarized ion source was scheduled for experiments for 1334 hours. This was approximately 57% of the available experimental time. There were 1062 hours of operation at 10 MeV compared to 262 hours at 40 MeV.

The continued use of silicone based oils in the diffusion pumps maintained the relatively long period between shutdowns due to oil contamination The time between major shut downs due to all causes, filament breaks, mirror wire breaks, diffusion pump failure, etc. was of the order of 400hours.

Because of the impending closedown of the linear accelerator, no major modifications or improvements to the source were carried out during these final months of operation. The ionizer and sixpole magnet from this source, with minor modifications, are to be used in the polarized negative ion source now being built for the MP Tandem.

55. Polarized Negative-Ion Source for the MP Tandem

C. H. Poppe, V. Shkolnik, D. L. Watson, J. J. Turgeon, T. O. May, D. Tweeton and J. H. Broadhurst

A basic description of the polarized negative-ion source now under construction was given in the 1968 Progress Report. At this writing, construction and assembly have been completed on the atomic beam system and differential pumping column. Tests on the atomic beam will begin after modifications to the sextupole magnet return yoke are completed.

Design of most of the remaining components has been completed and construction is under way. The tandem injector cage has already been enlarged to accommodate the source and construction of the insulating platform which is to support the source at the injector potential will start soon.

Fig. 55-1 shows an elevation of the polarized source assembly. Four vacuum boxes are supported from an I beam framework. The right-hand box houses the three-stage differential pumping column for formation of the atomic beam. The first stage is pumped by a 850 cfm Roots blower backed by a 140 cfm Stokes mechanical pump. The next two stages are pumped by two 6-in. oil diffusion pumps on each stage. After testing a number of pumps, the NRC VHS-6 with a measured speed of 2300 ℓ/sec was chosen.

Attached to the atomic-beam box is the box housing the sextupole magnet and the low-field r.f. transition unit. The next two boxes house the ionizer and charge exchange system, respectively. The ionizer box

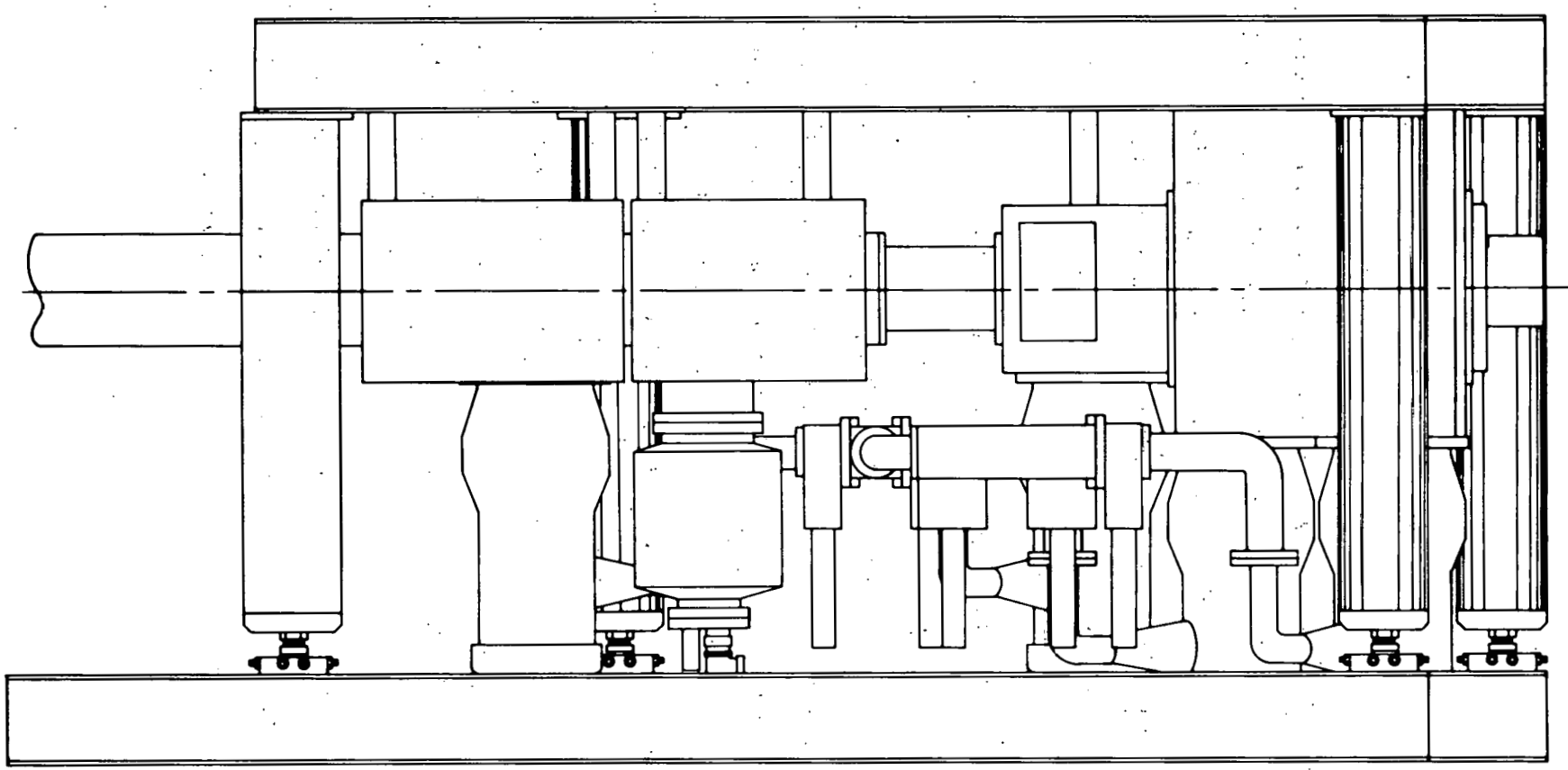

Polarized Source

Fig. 55-1

will be pumped by a Granville-Phillips Electro-Ion pump, while an oil diffusion pump will be used on the charge-exchange box.

Details of the beam transport system between the charge exchange region and the tandem have been completed and the design of the foil stripper assembly for installation in the tandem terminal has been submitted to the shop. Tests on the production of negative ions by charge exchange in Cs vapor have continued throughout the year using the facilities described in the 1968 Report.[2]

The following sections detail progress made in certain areas:

1. Charge Exchange Tests with Cesium Vapor.

Tests of our alkali vapor charge exchange system as described in last year's Progress Report[2] have continued intermittently throughout the past year. However, with this system it was not possible to make any quantitative measurements because the component of the negative beam due to H^- produced from H_1^+ could not be separated from the H^- produced from H_2^+ or H_3^+ and other negative components of the beam. To overcome this difficulty the equipment has been rebuilt with a mass spectrometer as the detecting unit. In conjunction with this an einzel lens has been placed after the charge exchange canal to focus the negative beam into the mass spectrometer.

Measurements with this new system have been underway for about 6 weeks. The investigations being carried out at present are:

(a) Variation of the overall charge exchange efficiency with vapor thickness.

(b) Variation of the exchange efficiency as a function of incident beam energy.

Preliminary indications show that an incident energy of 2-2.5 keV and a canal temperature of 180°-200° C (i.e. cesium thickness of 15-20 μ-cm in the canal) will yield the highest charge exchange efficiency. The ionizer, charge exchange and beam transport systems are being designed to operate in this energy region.

2. The Foil Stripper.

The proposed foil stripper is to be mounted in the first access opening downstream from the gas stripper canal in the high voltage terminal of the tandem Van de Graaff. When the foil stripper is in use, the gas canal now being used for stripping will be lifted 1.75 in. and out of the way of the beam by two air cylinders activated by a two-way valve with gas pressure from a nitrogen bottle inside the terminal. (The two-way valve is to be controlled from the ground end by the usual Lucite rod.) Each cylinder is attached to the flange carrying the existing adjustable cradle with the lift points close to the cradle and the restraining spring. When the cylinder retracts to the down position the spring returns the canal tube to the cradle and the canal's alignment is left unchanged. The mechanical connection between cylinders and the canal tube incorporates metal bellows rated more than 180 PSI, eliminating sliding seals between the tank atmosphere and the accelerating tube.

The stripper consists of 72 frames with 1/2 inch dia. 10 $\mu g/cm^2$ carbon foils backed by Formvar, mounted on a 35SS Boston Gear chain with A-1

attachments. Fig. 55-2 shows details of the mechanism.

1. Foil in position
2. 8-tooth chain sprocket
3. 5:1 gear reduction
4. 8-point Geneva drive
5. Shaft coupling
6. The driven Alnico magnet
7. The driving Alnico magnet
8. Alignment bolts
9. Chain tensioning shims and bolts
10. Foil guard plates
11. Mounted foils

The outside magnet is driven from the ground end by a reversible geared-down motor via another long rod, with a Theta Instrument Co. 3-digit shaft encoder attached to it (through another 10:1 gear reduction). The display unit at the operator console gives information concerning the position of the driving magnet. The two features of the Geneva mechanism, intermittent motion and self-locking, require (for an 8-point device and 5:1 reduction) that the driven magnet mistracks for more than three turns in either direction before this starts to affect the position of the chain. The mistracking is not expected to exceed a few degrees. The shaft friction will be reduced by incorporating several miniature bearings (not shown on Fig. 55-2)and by applying high-vacuum lubrication grease.

In order to insure the ease of mounting of a loaded stripper in place, a full-sized model was built and positioned without touching any part of the terminal structure.

3. The Beam Transport.

The version of the beam transport which is to be built first is intended to produce only transverse vector polarization. Its elements are

Foil Stripper Assembly

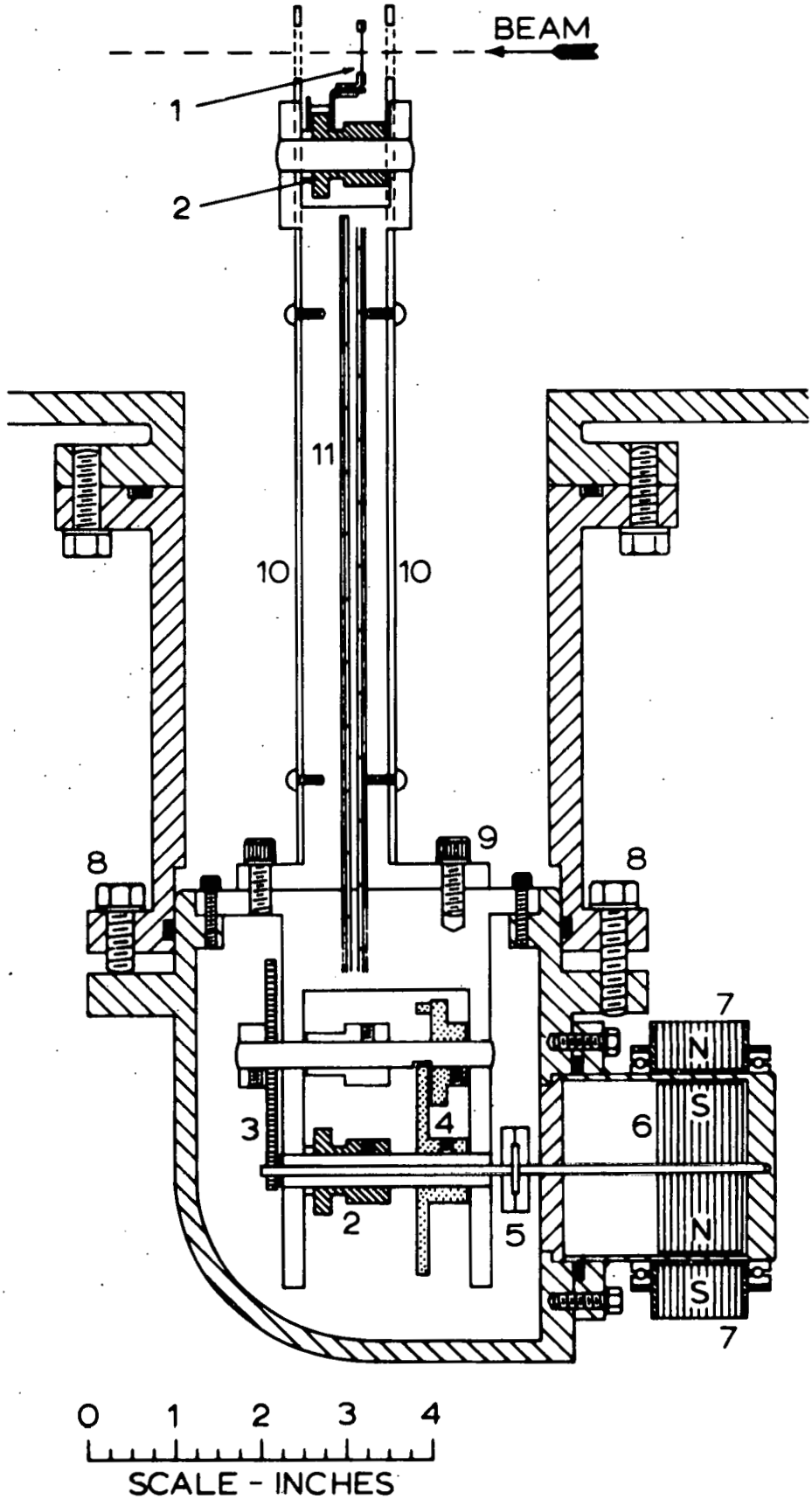

Fig. 55-2

shown on Fig. 55-3 and are all designed except for the 45° inflection magnet.

A valve (1) separates the charge exchange box from the first gridded Einzel Lens (2) which focuses an incident parallel beam in the plane of the figure at exactly the middle of the spin-rotating solenoid (5). Before entering the solenoid, however, the beam passes through an electrostatic mirror housing (3) and an electrostatic mirror (4). The latter changes the spin orientation of the beam from axial to transverse and its relatively large effective depth of 1 inch separates spatially the unwanted component

$$H_2^+ \longrightarrow 2H_1^+ \longrightarrow 2H_1^-$$

generated by scattering inside the charge exchange. This component has only half the energy of the polarized beam and they emerge from the mirror 0.5 in. apart, which is more than the beam diameter at this point. A baffle at the mirror exit stops the unpolarized component after which it is pumped out. At the same time the mirror removes the positive (unexchanged) beam and an attempt will be made to use this beam for continuous monitoring of the intensity and position of the polarized component. It is also recognized that the mirror introduces an axial asymmetry in the plane perpendicular to the drawing, as follows from the matrix elements pertaining to this mirror

$$M_{hor} = \begin{pmatrix} -1 & 0 \\ 0 & -1 \end{pmatrix}, \qquad M_{vert} = \begin{pmatrix} 1 & 5.66 \\ 0 & 1 \end{pmatrix}$$

Beam Transport for Negative Polarized Ions

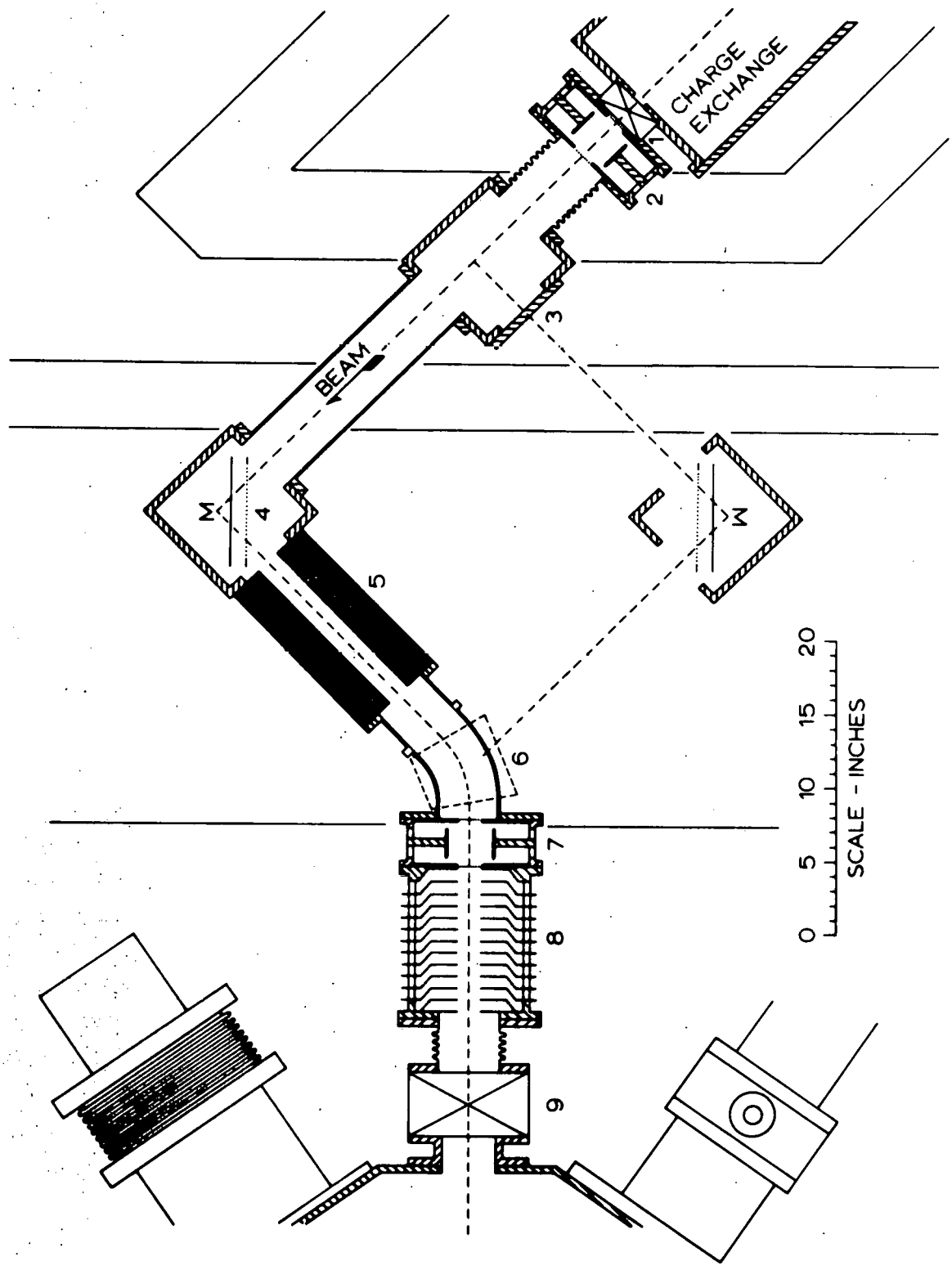

Fig. 55-3

If the beam is focused to have the crossover at the point M, this asymmetry disappears. For fine adjustments of the beam position the mirror can be inclined remotely with respect of the plane of the drawing and rotated about the axis perpendicular to this plane and passing through M.

The spin-rotating solenoid is of the sheathed design and capable of producing 53 k-gauss-cm of magnetomotive force needed to rotate spins of 5.0 keV deuterons by 180°. It is wound with square wire and water cooled.

The 45° inflection magnet (6) will be designed either with variable shim angles (in order to compensate for the axial asymmetry) or with fixed shim angles computed to preserve the axial symmetry for a beam with the crossover in the middle of the preceding solenoid.

The second gridded Einzel lens (7) and the accelerating column (8) accelerate the beam to about 20 to 40 keV and focus it onto the first fixed aperture of 0.170 in. diameter and 50 inches away. The accelerating column has twelve electrodes of spun stainless steel separated by 0.750 in. porcelain rings 8.0 in. O.D. The rings and the electrodes are aligned and glued together in the same fashion as the Einzel lenses. For polarized beam, the inflection magnet in the injector proper will be well degaussed. A second valve (9) separates the beam transport from the injector's pumping manifold.

The beam transport system will be pumped through its own manifold by an oil diffusion pump with a freon-cooled baffle. The manifold connects onto the system at the two mirror housings and between the inflection magnet and the solenoid.

In order to provide longitudinal polarization for the deuteron beam, the transport system will be rearranged permanently by mirror imaging the electrostatic mirror (4), the solenoid (5), the inflection magnet (6), by adding a mirror to the housing (3) and another identical solenoid between the two mirrors. The first Einzel lens will then be adjusted to produce the beam crossover at the symmetry point M of the second mirror.

The transmission of the described beam transport will depend mostly on the beam emittance determined by the ionizer and the charge exchange. An estimate based on the emittance of the Glavish strong-field ionizer, neglecting scattering in the charge exchange canal, suggests a transmission of roughly 50%.

4. Electronics.

The negative polarized-ion source is designed to operate at a negative potential of up to 380 kV. The power for the source (approximately 50 kw will be required) will be provided by a 65 kw generator situated on the high voltage platform. The generator will be belt-driven by a 100 h.p. motor fixed to the ceiling of the injector basement.

To make the most efficient use of the ion-source on the tandem, the source is being designed so that it can be tuned for optimum output while the tandem is being used for experiments requiring non-polarized beams. This requires that the source be essentially independent of the present injector with regard to such equipment as power supplies and controls and that these be remotely operable from outside the accelerator hall. To

facilitate this type of operation it has been decided that wherever feasible, the remote programming of the power supplies, etc., will use a ± 1V full scale reference voltage. This reference voltage will be used in conjunction with a reversible motor-driven 10-turn Helipot to control the power supplies. Fig. 55-4 is a schematic diagram of one component of the proposed control system. The "raise"|"lower" function is provided by a spring-loaded rocker switch which returns to the neutral position when not in use. Both the "raise" and "lower" parts of the system are identical except for the connections to the helipot motor. The signal from the rocker switch (at the remote location) is used to drive a neon bulb optically coupled to the ground end of a lucite light pipe. This light signal is detected by a photo-transistor at the high potential end and is converted into the drive voltage for the helipot.

A system of this type has been built and tested over a period of several weeks and its performance has been found to be very satisfactory. Sixteen of these dual light pipe systems will be assembled inside an insulating tube approximately 4 in. in diameter and 8 ft. long. The values of the parameters set by these systems will be read from meters viewed by closed circuit television. A voltage-to-frequency converter will be used to measure the more critical parameters.

Most of the power supplies to be used for the source are standard commercial units. However, in order to make the best use of the available space, the large high current supplies (350A at 35v) for the six-pole magnet and the various solenoids will be built to our own design.

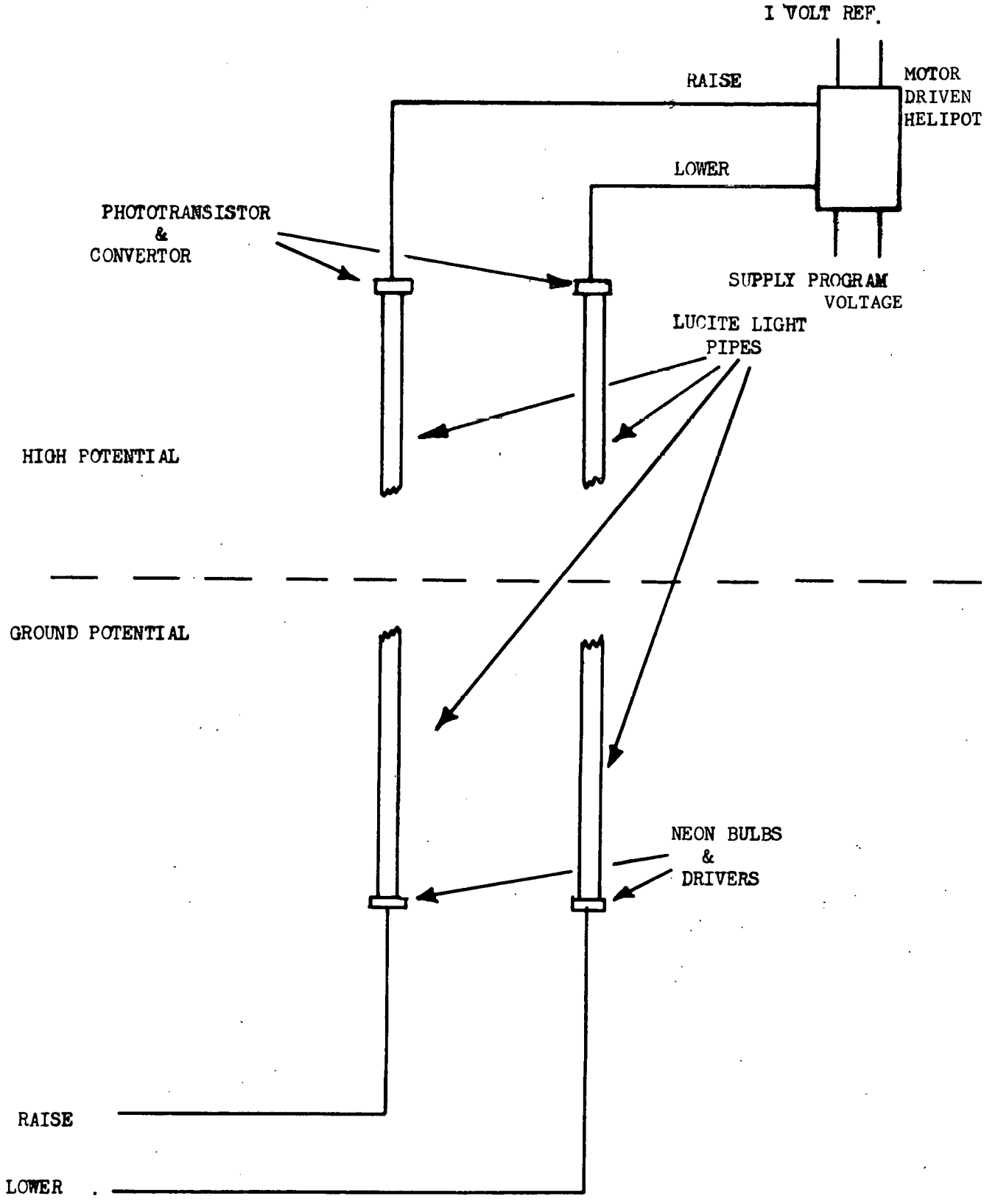

Schematic diagram of the light pipe system for controlling the polarized negative-ion source.

Fig. 55-4

For the dissociator section of the atomic beam, a 2 kw 27 MHz self-excited oscillator will be used. The use of this type of oscillator avoids problems due to mismatching that can be caused by changes in the dissociator pressure and temperature.

To avoid having to shut the polarized source down completely when it is not in use, an automatic interlock and protection logic system is being developed.

References

1. Williams Laboratory of Nuclear Physics Annual Report, (1968) p. 204.

2. Ibid., p. 209.

APPENDIX

56. Laboratory Personnel

Research

Faculty

J. Morris Blair
George W. Greenlees
Norton M. Hintz
John H. Broadhurst
Ronald E. Brown
Russell K. Hobbie
Carl H. Poppe
William R. Phillips[1]
Dietrich Dehnhard
John S. Lilley

Research Associates

A. Ross Barnett
William Makofske
Hajime Ohnuma
Vladimir Shkolnik
Poul Vedelsby[2]
Douglas L. Watson

Research Assistants

Frederick Becchetti, Jr.
Clark Bergman[3]
Jones Chien
Robert Cornett[4]
Frank Chwieroth[4]
Philip Debenham
Ralph De Long
William Dykoski
Daniel Fitzgerald
Lyle Johnson[4]
Ting Chen Kan[3]
Albert Kuhfeld
Dennis Leavitt
Henry Liers[3]
Nanjappa Lingappa[3]
David Madland
Peter Mailandt
James Morgan[3]

Research Assistants (Continued)

David Olsen
Michael Oothoudt
Arimilli Padmanabham
Phillip Pooley[4]
Pedro Ruenes
Jerry Sievers
Robert Snyder
Allen Sourkes
Daryl Tweeton
Richard Wallen
David Weisser[3]

Engineering

Electrical Design and Manufacture and Accelerator Operation

Donald Bauman[5] (Tandem Engineer)
Barry Brown[6] (Computer)
Robert Featherstone[7] (Linac Engineer)
Robert Goodwin[2] (Computer)
Michael Lamatsch[5] (Tandem Engineer)
Peter Stasz (Tandem Engineer)
David Freeman[5]
James Heinen
Frank Lang
Curtis Lehrke
Russel Lund[8]
Thomas May
Dennis Olson
Warren Rauch
James Turgeon

Mechanical Design and Manufacture

Richard Hendricks[9] (Design Engineer)
DeWayne Varnes (Tandem Shop Foreman)
Victor Christianson
Jon Dalrymple
Ray Johnson
Milan Kalish[10]
William Mann[8]
Chester Peske
James Pilgram

Others

Nancy Strebe (Secretary)

Marjorie Maloney (Nuclear Plate Scanning, part-time)

Mary Evanson (Nuclear Plate Scanning, part-time)

George Ott (Target Preparation)

Gordon Schissel (Principal Stores Clerk)

12 part-time student technicians

1. Visiting Associate Professor, terminated December 1968.
2. Terminated, July 1969.
3. Terminated.
4. Summer only.
5. Terminated, March 1969.
6. Joined project June 1969.
7. Terminated, September 1968.
8. Terminated, January 1969.
9. Terminated, June 1969.
10. Terminated, February 1969.

57. Advanced Degrees Granted, Academic Year 1968-9

T. C. Kan, M.S. "Sources of Error in Cross Section Measurements with a Gas-cell Target"

David G. Madland, M.S. "A One-dimensional Spark Chamber for Energy Analyzing Magnets"

D. C. Weisser, Ph.D. "A Search for an Excited State in He^4 Near 30 MeV and an Optical Model Analysis of Alpha Particle Scattering"

J. F. Morgan, Ph.D. "Elastic Scattering of Alpha Particles by C^{12} Between 19 and 30 MeV"

Clark Bergman, Ph.D. "The Scattering of Alpha Particles by O^{16} Between 18.9 and 30 MeV"

Henry Liers, Ph.D. "The Elastic Scattering of 39.6 MeV Protons by the Nickel Isotopes"

Nanjappa Lingappa, Ph.D. "Inelastic Scattering of 40 MeV Protons by Ni^{58} and Ni^{60} and Coupled Channel Analysis"

58. Reports and Publications

(a) Internal Laboratory Reports

Control System for 90° Analyzing Magnet
C. Bergman and R.K. Hobbie
COO-1265-70.

Computer Subroutines for Quadrupole Calculations
C. H. Poppe
UMWL 34, May 22, 1969.

(b) List of Publications

Experimental Study of the (d,He^3) Reaction on Even-A Isotopes of Mo
H. Ohnuma and J.L. Yntema
Phys. Rev. 176, 1416 (1968).

Study of the $Ca^{48}(He^3,p)Sc^{50}$ Reaction
H. Ohnuma, J.R. Erskine, J.A. Nolen, Jr., J.P. Schiffer, and P.G. Roos
Phys. Rev. 177, 1695 (1968).

Study of the J Dependence in the (d,He^3) Reaction
H. Ohnuma and J.L. Yntema
Phys. Rev. 178, 1654 (1968).

Experimental Study of the (d,t) Reaction on Even-Mass Mo Isotopes
H. Ohnuma and J.L. Yntema
Phys. Rev. 178, 1855 (1968).

Study of the $Zr^{94}(He^3,d)Nb^{95}$ Reaction
H. Ohnuma and J.L. Yntema
Phys. Rev. 179, 1211 (1968).

Computer Control of the Analyzing Magnet of an MP Tandem Van de Graaff Accelerator
C. Bergman and R.K. Hobbie
Rev. Sci. Inst. 40, 1079 (1969).

Search for Unbound States in He^3 Through $Li^6(p,\alpha)$
D.K. Olsen and R.E. Brown
Phys. Rev. 176, 1192 (1968), COO-1265-65.

Study of He^3+He^4 and H^3+He^4 Systems with the Resonating-Group Method
R.E. Brown and Y.C. Tang
Phys. Rev. 176, 1235 (1968), COO-1265-63

^{16}O Analogue States in the $^{15}N(p,n)^{15}O$ Reaction
A.R. Barnett
Nucl. Phys. A120, 342 (1968).

The University of Minnesota Polarized Proton Source
R.N. Boyd, C.G. Hoot, C.H. Poppe, J.A. Sievers and J.H. Williams
Nucl. Instr. and Meth. 63, 210 (1968).

A Beam Bunching System for a Tandem Electrostatic Accelerator Using Solid State Circuitry
H. Fanska, N.G. Ward, J.S. Lilley and C.G. Williamson
Nuc. Instr. and Meth. 63, 93 (1968).

Elastic and Inelastic Proton Scattering from Even Isotopes of Ca, Sn, and Te
W. Makofske, W. Savin, H. Ogata and T.H. Kruse
Phys. Rev. 174, No. 4, 1429 (1968).

Thin Lithium Targets Sealed in Nickel for Low Oxygen Contamination
D.C. Weisser and R.K. Hobbie
Rev. Sci. Inst. 40, 683 (1969).

The Determination of Nuclear Matter Sizes in the Tin Isotopic Sequence
R.N. Boyd and G.W. Greenlees
Phys. Rev. 176, 1394 (1968).

An Analysis of Quasi-Elastic (p,n) Reactions Using a Reformulated Optical Model
C.J. Batty, E. Friedman and G.W. Greenlees
Nuc. Phys. A127, 368 (1969).

Nuclear-Matter Radii from Analysis of 14.5 MeV Proton and Neutron Scattering
G.J. Pyle and G.W. Greenlees
Phys. Rev. 181, 1444 (1969).

$B^{11}(He^3,\alpha)$ Reaction at 33 MeV
D. Dehnhard, N. Williams and J.L. Yntema
Phys. Rev. 180 (4), 967-70 (1969).

The Use of an On-Line Computer to Divide Signals from a Position-Sensitive Detector
P.H. Debenham, D. Dehnhard, and R.W. Goodwin
Nucl. Instr. and Meth. 67, 288 (1969).

(c) Papers in Press or Submitted for Publication

Study of the $Al^{27}(He^3,p)Si^{29}$ and $Al^{27}(He^3,p\gamma)Si^{29}$ Reactions
L. Meyer-Schutzmeister, D.S. Gemmell, R.E. Holland, F.T. Kuchnir, H. Ohnuma, and N.G. Puttaswamy
submitted to Phys. Rev.

Coulomb Excitation and Reorientation of the Octupole State in ^{208}Pb
A.R. Barnett and W.R. Phillips
to appear in Phys. Rev.

Energy Levels in ^{33}P
G. Hardie, R.E. Holland, L. Meyer-Schutzmeister, F.T. Kuchnir, and H. Ohnuma
submitted to Nucl. Phys.

Quadrupole and Octupole Transitions in F^{19} from Deuteron Scattering
D. Dehnhard and N. Hintz
submitted to Phys. Rev.

Coulomb Excitation of Bismuth and the Weak Coupling Model
R.A. Broglia, J.S. Lilley, R. Perazzo and W.R. Phillips
submitted to Phys. Rev.

Nucleon-nucleus Optical Model Parameters, $A>40$, $E<50$ MeV
F.D. Becchetti and G.W. Greenlees
to appear in Phys. Rev. (C00-1265-59).

Proton and Neutron Distributions Calculated Using an Effective Single Particle Potential
C.J. Batty and G.W. Greenlees
to be published in Nuc. Phys.

The Elastic Scattering of Protons by O^{16} in the Energy Range 16-30 MeV
O. Karban, P.D. Greaves, V. Hnizdo, J. Lowe, N. Berovic, H. Wojciechowski, and G.W. Greenlees
to be published in Nuc. Phys.

Elastic and Inelastic Scattering of 15 MeV Deuterons by F^{19}
D. Dehnhard and N.M. Hintz
submitted to Phys. Rev.

The Elastic Scattering of 39.6 MeV Protons by Even Isotopes of Ni and Zn
H.S. Liers, R.N. Boyd, C.H. Poppe, J.A. Sievers, and D.L. Watson
submitted to Phys. Rev.

(d) Papers Presented at Meetings and Conferences

Coulomb Excitation of ^{209}Bi
J.S. Lilley and W.R. Phillips
Bull. Am. Phys. Soc. 13, 1471 (1968).

Complex Particle Scattering on Even Isotopes of Sn and Te
W. Savin, W. Makofske, H. Ogata and T.H. Kruse
Bull. Am. Phys. Soc., 14, 4, 491 (1969).

Physically Related Spin-Orbit and Isospin Form Factors in the Optical Model
G.J. Pyle, W. Makofske, G.W. Greenlees
Bull. Am. Phys. Soc. 14, 4, 573 (1969).

Evidence for Splitting of a Bound Isobaric Analog State in Co^{58}
F.D. Becchetti, Jr., D. Dehnhard, and T.G. Dzubay
Presented at the Second Conference on Nuclear Isospin, Asilomar, California, 13-15 March 1969.

Gamma Decay of the 8.31-MeV Analog State ($J^{\pi}=5/2^{+}$, T=3/2) in Si^{29}
F.T. Kuchnir, L. Meyer-Schutzmeister, N.G. Puttaswamy, H. Ohnuma, R.E. Holland and D.S. Gemmell
Bull. Am. Phys. Soc. 13, 1371 (1968).

$Sc^{45}(d,t)Sc^{44}$ Reaction
H. Ohnuma, A.M. Sourkes, and N.M. Hintz
Bull. Am. Phys. Soc. 14, 601 (1969).

States in Odd-Odd Sc Nuclei from (d,α) Reactions on Ti
R.A. Wallen, H. Ohnuma, and N.M. Hintz
Bull. Am. Phys. Soc. 14, 601 (1969).

Experience with the Williams Laboratory On-Line Computer System
R.K. Hobbie and R.W. Goodwin
Presented at the Conference on Computer Systems in Experimental Nuclear Physics, Skytop, Pennsylvania (COO-1265-76).

Experience with Williams Laboratory Users Programs
R.W. Goodwin and R.K. Hobbie
Presented at the Conference on Computer Systems in Experimental Nuclear Physics, Skytop, Pennsylvania (COO-1265-77).

Differential Cross Sections and Polarization for 40 MeV Protons Elastically Scattered from Zn Isotopes
R.N. Boyd, H.S. Liers, C.H. Poppe, J.A. Sievers, and D.L. Watson
Bull. Am. Phys. Soc. 13, 1446 (1968).

Proton Elastic Scattering Cross Section and Polarization Measurements on the Ni Isotopes at 39.6 MeV
H.S. Liers, R.N. Boyd, C.H. Poppe, D.L. Watson, and J.A. Sievers
Bull. Am. Phys. Soc. 14, 623 (1969).

New K=0 Rotational Bands of Yb^{174} from the $Yb^{176}(p,t)$ Reaction
M. Oothoudt, P. Vedelsby, N.M. Hintz
Bull. Am. Phys. Soc. 14, 509 (1969).

States in Sm^{150} from the $Sm^{152}(p,t)Sm^{150}$ Reaction
P. Debenham and N.M. Hintz
Bull. Am. Phys. Soc. 14, 509 (1969).

$Sc^{45}(d,t)Sc^{44}$ Reaction
H. Ohnuma, A.M. Sourkes, and N.M. Hintz
Bull. Am. Phys. Soc. 14, 601 (1969).

States in Odd-Odd Sc Nuclei from (d,α) Reactions on Ti
R.W. Wallen, H. Ohnuma, and N.M. Hintz
Bull. Am. Phys. Soc. 14, 601 (1969).

States in Ti^{44} and Cr^{48} from the (p,t) Reaction
D.G. Madland and N.M. Hintz
Bull. Am. Phys. Soc. 14, 602 (1969).

Optical Model Analysis
G.W. Greenlees
Gordon Conference on Nuclear Structure, 1969.

Study of (α,t) Reactions on 1p-Shell Nuclei
H.T. Fortune, D. Dehnhard, R.H. Siemssen, and B. Zeidman
Bull. Am. Phys. Soc. 14, 487 (1969).

Isotope Shift of Coulomb Displacement Energies in Ti, Cr, and Fe
T.G. Dzubay, R. Sherr, D. Dehnhard, and F.D. Becchetti, Jr.
Bull. Am. Phys. Soc. 13, 1403 (1968).

Neutron and Proton Tunnelling Reactions with ^{208}Pb
W.R. Phillips and A.R. Barnett
Proc. Heavy Ion Conference, Heidelberg, July 1969.

Reorientation Effects in the Electric Octupole Coulomb Excitation of ^{208}Pb
A.R. Barnett and W.R. Phillips
Proc. Heavy Ion Conference, Heidelberg, July 1969.

A Search for the First T=2 State in ^{8}Be
W.D. Harrison, A.R. Barnett, C. Bergman and D. Weisser
Bull. Am. Phys. Soc. 13, 1587 (1968).

18.02 MeV Resonance in ^{16}O
J.F. Morgan and A.R. Barnett
Bull. Am. Phys. Soc. 13, 1426 (1968).

Quadrupole Moment of 3^- State in ^{208}Pb
A.R. Barnett and W.R. Phillips
Bull. Am. Phys. Soc. 13, 1470 (1968).

Total Reaction Cross Section of α's on ^{208}Pb and ^{209}Bi Below the Barrier
A.R. Barnett and J.S. Lilley
Proc. International Conference on Nuclear Structure, Montreal, August 1969.